

ACOUSTICS OF DUCTS WITH FLOW AND ITS RELATION
TO ACOUSTICALLY INDUCED VALVE-PIPE INSTABILITIES

by

VIJAY KUMAR SJNGHAL

Submitted to the Department of Aeronautics and Astronautics on December 9, 1975 in partial fulfillment of the requirements for the degree of Doctor of Philosophy.

ABSTRACT

Experimental and analytical studies are presented for various aspects of the acoustics of hard walled ducts carrying uniform flow. The upstream and downstream emission of sound from a stationary source into a moving fluid in a duct is studied for plane waves and higher order modes. The sound waves are attenuated by their interaction with turbulence in the duct. Due to convective effects this attenuation is larger when the wave travels against the flow than when it travels with the flow. Reflection coefficients measured at the upstream and downstream ends of the duct reveal that three times more acoustic energy is lost at the downstream end than at the upstream end. The flow induced contribution to the termination resistance at the exit end is found to be proportional to the Mach number. When the flow Mach number is greater than 0.4 typically, the losses in the duct and at the ends of the duct are so large that its acoustic resonances are suppressed.

These results in the aeroacoustics of ducts are applied to the problem of acoustically induced axial instabilities in valve-pipe systems. It is shown that the acoustic reaction force on the valve due to the fluctuating mass flow rate in the duct can act as a negative damping. If this negative damping is greater than the inherent mechanical "resistance" in the valve and in the duct, the system is unstable. An instability parameter is defined in terms of the mass flow characteristics of the valve and the acoustical characteristics of the duct. Duct lengths equal to odd multiples of quarter wavelength corresponding to the natural frequency of the valve are found to be the most unstable. Half wavelength ducts or multiples thereof are the most stable but stability cannot be guaranteed by changing the length alone. Neutral stability curves and the

frequency of excitation on the verge of instability are determined from numerical solution of the equations of motion. Regions of moderate and violent instability are identified. Experimental results on a very simple idealized model give excellent qualitative agreement.

Some observations are made on the lateral and torsional modes of excitation and on the flow-excitation of side branch cavities in ducts. With increasing flow speed the modes of a side branch cavity are excited successively. Nonlinear interactions of these modes lead to sum and difference tones. If the Mach number is less than 0.4 (approximately) and if the side-branch cavity is in the center of the duct, additional excitation of duct modes occurs. Design of quiet cavities is also outlined.

Thesis Supervisor: Uno Ingard
Title: Professor of Physics and of
Aeronautics and Astronautics

Thesis Supervisor: Jack L. Kerrebrock
Title: Professor of Aeronautics and
Astronautics and Director of
Gas Turbine Laboratory

Thesis Supervisor: John Dugundji
Title: Professor of Aeronautics and
Astronautics

ACKNOWLEDGEMENTS

I am grateful to everyone who helped me in any way in my research efforts. I owe my knowledge of aeroacoustics to my thesis supervisor Professor Uno Ingard whose ingenuity, depth of knowledge, creative thinking and interest in me and my work made this thesis possible. Professor Jack Kerrebrock and Professor John Dugundji assisted me whenever I needed help. It is not possible to list the name of everyone who has contributed either directly or indirectly to this effort but special mention must be made of assistance received from Professor Richard Lyon and Professor Patrick Leehey; Professor and Mrs. Ingard, Professor and Mrs. Kerrebrock; T. Christensen, Roy Andrews and Ken Griffiths of the Gas Turbine Laboratory workshop; Fred Merlis and Allan Shaw of the Experimental Projects Laboratory; my colleagues Ara Demirjian, George Succi, Bill Patrick, Tony Galaitsis, H. Lakshmi Kantha, Jeff Tarvin, Hisashi Kobayashi, John Bertschy and Y. C. Cho; my friends Perla Figa, Paula Mann, Lily Singh, Shirley Schwebach, Nur Dolay, Marissa Ortega, Betsy Ohsol, Cathy Simmons, Wendy Zoehfeld and Kathy Thomas; my roommates Mike Christie, Ed Meyer, Martin Hellwig, Barry Goldman and Ted Postol; my friends Tara and Madhu Singhal, Bhag and Sarla Jain, Peter and Anita Bromley, Douglas and Lora McQueen, Bob and Reiko Anderson, Kaplesh Kumar, Manjit Kalra, Lajpat Utreja, Hisashi and Miyako Kobayashi, Ramesh Agarwal and Sudhir Jain; Mrs. Gayle Ivey who ran the Gas Turbine Laboratory and

Miss Clare Smith for running superbly the physical acoustics laboratory; employees of the Research Laboratory of Electronics; Dennis Speliotis, Ken Harte, Ted Lewis and Nate Curland of Micro-Bit Corporation; my parents, my brothers and my sister.

Two very special friends and co-workers Angelo Moretta and Peter Bromley built most of the equipment in such versatile and ingenious ways that variety of bench-top experiments can be performed readily. The credit for making the final typed version goes to Lee Beth Smith of Micro-Bit Corporation.

This research was supported in part by ONR grant N00014-67-A-0204-0019, in part by a one semester fellowship from the Research Laboratory of Electronics and in part by a summer job from Micro-Bit Corporation.

TABLE OF CONTENTS

<u>Chapter No.</u>		<u>Page No.</u>
1	Introduction	8
2	Acoustics of Ducts with Flow	13
3	Theoretical Analysis of Valve Instability	18
4	Discussion of Experimental Results on Valve Instability	32
5	Acoustically Induced Flow Instability in Side Branch Cavities	37
6	Concluding Remarks	41

Appendices

A	Upstream and Downstream Sound Radiation Into a Moving Fluid	44
B	Emission of Higher-Order Acoustic Modes Into a Moving Fluid in a Duct	48
C	Sound Attenuation in Turbulent Pipe Flow	52
D	Effect of Flow on the Acoustic Resonances of an Open-Ended Duct	55

Figures

1	Schematic drawing of the experimental setup.	62
2-9	Stability contours obtained analytically.	65
10-11	Mass flow characteristics of the valve.	73
12	Experimentally observed stability contours.	76
13	Experimentally observed frequency of excitation.	79
14	Screeching frequency for a side branch cavity.	82
15	Nonlinear coupling between the cavity modes.	83
16	Coupling between cavity modes and the axial duct modes.	85

17 An inclined cavity can be as quiet as a duct
without cavity.

86

References

87

CHAPTER 1

INTRODUCTION

The parameters responsible for the instability induced by acoustic feedback force acting as a negative damping have never been clearly established. We show that a stable "control valve" regulating the flow of fluid through a duct can be made violently unstable simply by changing the length of the discharge duct when all other geometric and flow parameters are kept constant. This is the clearest example of self-excitation in which the acoustic reaction forces couple with the structural resonances to generate unstable modes of vibration. The experimental evidence supports essential aspects of the theory. This work is applicable not only to valve-pipe systems but also to the excitation of orchestral reed instruments like the clarinet, oboe and bassoon.

The simplest model for all these systems consists of a valve plug which controls the flow of fluid through a discharge duct (Fig. 1). Other design features found in actual systems are secondary for the understanding of the excitation mechanism though they may be necessary for their usefulness. Such a valve has three basic degrees of freedom: (a) translation in the y direction, called the axial mode since it causes a velocity perturbation along the axis of the duct, (b) the lateral mode i.e. translation in the z direction since it excites the cross modes of the duct, and (c) the torsional mode which constitutes

rotational oscillations about x axis. The lateral and torsional mode excitation by acoustic feedback has never been studied.

To study the axial oscillations we must isolate them from the lateral and torsional modes. Surprisingly, we found that the torsional vibrations are the easiest to excite, but they can be suppressed by torsionally stiffening the end of the cantilever beam as shown in figure 1. These torsional modes were not acoustically coupled but were most probably excited by vortices shed alternately from the opposite edges of the valve plug. Even with this modification, at large flow velocities torsional modes were sometimes excited when the duct lengths were such that the system was stable for axial oscillations.

Maeda¹ studied the lateral instability of a poppet valve where the rate of change of momentum of the fluid acted as a negative damping. Maeda's arguments are based on the formulation by Lee and Blackburn² for the axial oscillations.

Our preliminary theoretical investigations for the acoustically induced lateral instability reveal that lateral instabilities can occur only when the structural resonance frequency of the valve is less than the first acoustic cross-mode frequency of the duct. The most unstable region is in the vicinity of the first cut-off frequency of the duct but with the valve frequency slightly lower than the duct frequency. Even in this frequency range the valve can be stabilized by stiffening it in relation to the acoustic destabilizing force

due to the modulation of the flow. Though lateral instability was experimentally observed, it was not acoustically coupled. Study of lateral and torsional modes is continuing and will be reported later.

Acoustically induced axial instability was first studied by Ainsworth³ and Ezekiel⁴. The same problem was later investigated by Tominari⁵, Saito⁶, Funk⁷, Ito⁸⁻⁹, Kasai¹⁰, Ichikawa and Nakamura¹¹, and Wandling and Johnson¹². The later papers consider different types of valves, additional fluid lines, extra springs or more accumulators. All of these studies involved actual hydraulic valves. Because of the presence of extra springs and accumulators, sharp bends and sudden changes in the cross-sectional areas of the conduits, these real-life devices are too complicated to reveal the basic destabilizing mechanism. High viscosity of the oil, large viscous and static friction in the valve, misalignments in the various parts, trapped air bubbles in oil, changes in oil temperature and spurious cavities (formed because of the need to attach pressure gages in the valve chambers) are responsible for some of the experimental difficulties encountered. Air bubbles trapped in oil can alter the performance so drastically that the valve can not be made unstable⁴. Ezekiel⁴ echoed a general feeling of hopelessness when he said that every time any part was changed, no matter how insignificant, it seemed the entire stability picture may change. They found

it extremely difficult to make consistent experiments, therefore the experimental data reported is very meager and is in a very narrow range of duct lengths. The theory is also unnecessarily complicated mainly because of their unwillingness to model the problem. The physical mechanism responsible for the instability is therefore masked by complex nonlinear differential equations or analog simulation techniques. They do show correctly that the most unstable pipe lengths are the odd multiples of the quarter wavelength corresponding to the natural frequencies of the valve whereas multiples of half wavelength are the most stable.

A similar reasoning was used by Wilson and Beavers¹³ to explain the excitation of the clarinet modes. They expanded on the ideas of Backus¹⁴ who had neglected the inertial term in comparison to the spring and the damping forces. Their experimental set up is also quite complicated but they report the most extensive experimental results.

St. Hilaire, Wilson and Beavers¹⁵ have shown through long involved mathematical analysis that unsteady Bernoulli pressure term is responsible for the excitation of the reed instruments. Our analysis indicates that unsteady Bernoulli pressure cannot destabilize a reed. The growth rate of the instability was measured by St. Hilaire¹⁵ et al to be proportional to $V\omega_m^3$ where V is the velocity through the slit opening and ω_m is the natural frequency of the reed. For reed excitation we propose the acoustic feedback mechanism.



Since very little was known about the acoustical characteristics of ducts with flow, all of the investigators mentioned above used less important acoustical parameters in their analyses and ignored the more important effects. They talked about including the viscosity and heat conduction losses in the duct without being aware that turbulent flow gives larger sound attenuation¹⁶⁻¹⁷ even at fairly low flow velocities. The radiation losses from the end of the duct¹⁸ were either completely left out^{3-12,15} or the effect of flow on the radiation losses¹³⁻¹⁴ was ignored. Therefore they came up with stability parameters which are only partially correct. Their major conclusions are qualitatively correct because the resonance frequency of the duct for small flow rates is only weakly dependent on flow. But at moderate flow rates when the flow begins to assert its influence on the acoustical characteristics of ducts, their conclusions will most likely not hold ground.

All aspects of the acoustics of ducts with flow are not yet fully understood. Mechel, Schilz and Dietz¹⁹, Athrens and Ronneberger¹⁶, Ronneberger and Schilz¹⁶ and Ronneberger²⁰ have made significant contributions to the acoustics of ducts with flow. We have extended their work and have succeeded in building a stronger theoretical base for some of their findings.

CHAPTER 2

ACOUSTICS OF DUCTS WITH FLOW

The generation of sound at discrete frequencies as from orifices, side branch resonators, valves, human whistling, orchestral reed instruments and orifices coupled to ducts is poorly understood and the acoustic feedback theory outlined in the next chapter can be helpful in understanding these phenomena if we know enough about the acoustical characteristics of a duct with flow.

The question of upstream and downstream energy division from a sound source placed in a duct with flow still remains to be resolved (at least experimentally). We explored the influence of fluid motion on sound emission from a stationary source in a duct^{21,22}. The ratio of upstream to downstream pressure was found to be intimately linked to the nature of the flow boundary conditions in the source region. For plane sound waves emitted by a compact source, whose characteristic length is small compared to the wavelength of sound, we found that the ratio of the amplitude of the upstream to downstream pressure $|P_-/P_+|$ is $(1+M)^2/(1-M)^2$ when the flow in the source region is streamlined. Here M is the Mach number of the mean flow in the duct. The same pressure ratio is $(1+M)/(1-M)$ if the boundary flow in the source region is turbulent. Similar results were obtained for a source emitting higher order modes.²² The results of these investigations have been published and

reprints of these papers are included with this thesis as appendices A and B.

Propagation of sound through the duct is another major aspect of this study. A simple quasistatic modulation of the pressure drop in the duct gives rise to an oscillatory friction drag. Thus there is an added attenuation of sound waves due to the turbulence in the flow.¹⁷ This attenuation is higher in the downstream direction (by a factor of three at a flow velocity equal to half the speed of sound). The attenuation per diameter of travel distance, can be expressed as

$$\alpha = 8.7\psi M / \{2(1 \pm M)\} \text{ decibels} \quad (2.1)$$

where ψ is the turbulent flow friction factor, the positive sign is for downstream propagation whereas the minus sign is for upstream propagation. The turbulent attenuation exceeds the viscothermal attenuation when $M > 2.86 \times 10^{-3} f^{0.5}$. At 450 Hz, if M is greater than 0.06, the turbulent attenuation is larger than that due to viscothermal losses. The results of this investigation have also been published and a reprint of the paper is included with this thesis as appendix C.

In addition to the acoustic losses in the turbulent flow within the duct, there are similar aeroacoustic interactions and losses in the entrance and the exit flows.¹⁸ The effect of these interactions can be determined from measurements of the acoustic pressure reflection coefficients at the ends of the duct. We have carried out a detailed experimental study of this

problem and have published the results. A reprint of this paper is included with this thesis (appendix D). For this reason we shall here give only a brief review of this work. For further details the reader is referred to appendix D. For small ka and up to moderate Mach numbers, i.e. $ka < 0.5$ and $M < 0.5$, the magnitude of the pressure reflection coefficient R_1 at the downstream end was measured to be approximately unity. The reflection coefficient of unity (actually slightly greater than unity) does not mean that the acoustic end loss is zero. At a Mach number of 0.4, the absorption coefficient at the exit is about 0.82. Also this flow induced loss at the exit end of the duct is equivalent to a normalized specific acoustic termination resistance $\theta_t \approx M$. As we shall see in the next section, θ_t is one of the most important acoustic parameters needed for verification of the theory. Our determination of termination resistance is indirect and at best approximate. It constitutes the weakest link in the quantitative comparison of the theoretical formulation with the experimental results.

In the absence of flow $\theta_t \approx (ka)^2/2$. Therefore for even a modest flow in the duct, $M > (ka)^2/2$, the flow induced end losses are far greater than the radiation losses in the absence of flow. These flow losses have been completely ignored by all previous investigators.³⁻¹⁵

At the upstream end, on the other hand, the magnitude of the reflection coefficient R_2 is less than unity and decreases

monotonically with increasing Mach number, $|R_2| \approx (1-M)^j / (1+M)^j$ where $j \approx 1.33$. Using the measured values of the reflection coefficients at the two ends, it is easily shown that the sound absorption at the exit is about three times larger than at the inlet.

Because of the radiation loss from the ends of the duct, a duct of length L acts as if it is lengthened by a small amount ϕ at each end. At the exit end our measurements of the end correction ϕ gave $\phi \approx 0.6a(1-M^2)$ where a is the hydraulic radius of the duct.

The end losses dominate the turbulent attenuation in a duct of hydraulic diameter d if

$$\frac{(1-M^2)}{M} \ln \left(\frac{1+M}{1-M} \right) > \frac{\psi L}{nd} \quad (2.2)$$

where $d=2a$. For $0 < M < 0.5$ the internal flow induced acoustic losses in the duct play a minor role compared with the end losses if L/d is less than 200. Interesting cases of acoustically induced instability occur for small length to diameter ratios. Therefore in almost all cases the end losses induced by flow are dominant.

The acoustic losses increase the width of the resonances (i.e. they decrease the Q value) and reduce the intensity of the resonant peaks. Above a flow Mach number of about 0.4 the losses become so large that the axial resonances of the duct are practically "washed out" by the flow. This implies that for Mach numbers greater than 0.4 in the duct it will be

practically impossible to excite acoustically induced instabilities (if unsteady shock effects are excluded from the analysis).

In the absence of a valve plug we found that at sufficiently low flow speeds, corresponding approximately to the Mach number range $0.1 < M < 0.3$, the axial modes of the open-ended duct are excited by the flow. In this range the power emitted from the duct, in both the upstream and downstream directions, is proportional to the fourth power of velocity. It is this ability of the duct to filter and amplify selectively the turbulent pressure fluctuations near its resonance frequencies, which is responsible for the acoustically induced instabilities.

CHAPTER 3

THEORETICAL ANALYSIS OF VALVE INSTABILITY

Qualitative description of the instability mechanism

The valve-pipe system under consideration is shown in Figure 2. If the piston is disturbed from its equilibrium position, in the absence of any feedback it will return to its equilibrium position after executing damped oscillatory motion. However, the oscillation of the piston makes the mass flow through the valve time dependent and gives rise to a velocity fluctuation at the entrance of the pipe connected to the valve. This, in turn, causes acoustic pressure fluctuations and hence an acoustic reaction force on the valve.

For certain pipe lengths, this sound wave after reflection from the end of the duct may give rise to an acoustic reaction force which is in phase with the velocity of the piston. In that case this acoustic feedback force acts as a negative damping in the system. If this negative resistance force exceeds the small but positive inherent mechanical damping, an initial perturbation of the valve from its equilibrium position will grow exponentially in time until nonlinearity or other constraints (including mechanical failure) limit further growth. The magnitude of this reaction force is obviously dependent on the acoustical characteristics of the termination of the duct and the length of the duct.

The acoustic reaction force can also be out of phase with the piston velocity, thus adding to the friction in the system.

The valve is then unconditionally stable even if the mechanical damping is zero.

In this study we will determine the conditions for stability in terms of an instability parameter η which is a function of the mechanical properties of the piston and the acoustical characteristics of the duct. The relevant duct parameters are the effective duct length L_1 , the cross-sectional area A and the acoustical damping of the duct. The effective duct length $L_1 = L + 0.3d + \phi_1$ where L is the actual duct length, d the duct diameter and ϕ_1 is the end correction at the valve end.

Equation of Motion

A perturbation y in the axial position of the valve away from the equilibrium location h results in a perturbation in the mass flow rate given by $(\dot{m}/dh)y$. The mass flow rate \dot{m} is also a function of the pressure drop ΔP but the effect of the term $(\partial \dot{m} / \partial \Delta P)_h$ is small in comparison to $(\partial \dot{m} / \partial h)_{\Delta P}$. If $U_v = dy/dt$ is the velocity of the valve plug and u the fluctuation in axial flow velocity at the entrance to the pipe, then the conservation of mass requires that

$$\frac{d\dot{m}}{dh}y(t) = \rho(A_v U_v + Au) \quad (3.1)$$

Here ρ is the mean density of the fluid and A_v is the cross-sectional area of the valve.

Normally an axial valve instability results in a growing oscillation at a frequency close to one of the characteristic

axial frequencies of free oscillations of the valve. In the vicinity of such a "resonance" the valve can be described dynamically as a mass-spring oscillator with a characteristic mass W , a spring constant K and a natural frequency $\omega_m = \sqrt{K/W}$.

In the linear range we can write the pressure fluctuation at the entrance of the pipe and at the valve piston as

$$P = U_v Z_m / A_v \quad (3.2)$$

$$P = \rho c \zeta u \quad (3.3)$$

Where Z_m , the mechanical impedance of the valve is given by

$$Z_m = -i\omega W + R + i \frac{K}{\omega} = R - i\omega W \left[1 - \left(\frac{\omega_m}{\omega} \right)^2 \right] \quad (3.4)$$

Incidentally, this is another way of writing the well-known equation of motion

$$W \frac{d^2 y}{dt^2} + R \frac{dy}{dt} + Ky = \text{FORCE} = P A_v$$

for a damped spring-mass system. Here R , the mechanical resistance of the oscillator is responsible for the friction force $R U_v$ on the valve. The specific acoustic input impedance $\zeta = \theta - i\chi$ is a function of frequency $\omega = 2\pi f$, the length L and the acoustic termination resistance θ_t of the duct.³⁰

$$\theta = \theta_t (1 + \tan^2 kL) / (1 + \theta_t^2 \tan^2 kL) \quad (3.5)$$

$$\chi = (1 - \theta_t^2) \tan kL / (1 + \theta_t^2 \tan^2 kL) \quad (3.6)$$

where k is the wave number = ω/c and c the sound speed

The equation of motion of the valve is obtained by combining equations (3.1) to (3.4) as

$$\left[R + \left(\frac{A_v}{A} \right)^2 A \rho c \theta - \frac{A_v}{A} \frac{dm}{dh} \frac{c \chi}{\omega} \right] - i\omega \left[W + \left(\frac{A_v}{A} \right)^2 A \rho c \frac{\chi}{\omega} \right] + \frac{i}{\omega} \left[K - \frac{A_v}{A} \frac{dm}{dh} c \theta \right] = 0 \quad (3.7)$$

This has the form of a harmonic oscillator equation in which the effect of the acoustic reaction force on the valve is expressed as contributions to resistance, the mass and the stiffness of the valve.

The acoustic effect on the spring constant is a reduction of K and this causes the frequency of oscillation to be always less than the frequency of free oscillations of the valve.

The additional mass due to acoustic load on the piston is proportional to the acoustic input reactance χ of the duct and is small ordinarily. For small duct lengths this additional mass is proportional to the mass of air ρAL in the duct. When the reactance is negative, this additional mass term acts effectively as a stiffness.

The most important acoustic effect is its contribution to resistance. It consists of two parts, one being the acoustic radiation loss which is always positive and thus provides additional damping of the valve. The second acoustic contribution to the resistance $-(A_v/A)(d\dot{m}/dh)c\chi/w$ is proportional to the acoustic input reactance χ and to the slope $d\dot{m}/dh$ at the operating point of the valve characteristic relating the mass flow rate \dot{m} and the valve displacement h . This is a negative contribution to resistance in the range of duct lengths where χ is positive. It is this negative resistance

which is responsible for the instability of the valve. If the magnitude of this quantity is larger than the sum of the intrinsic mechanical resistance R of the valve and the small contribution from the acoustic resistance θ , the system will be unstable.

The slope dm/dh being approximately proportional to the diameter of the valve, is an important parameter in the stability analysis; the larger it is, the more likely is the occurrence of an instability.

Equivalent termination resistance, θ_t

The acoustic termination resistance θ_t accounts not only for the acoustic radiation loss from the end of the duct but also for the acoustic losses in the fluid within the pipe. The latter, in turn, has two causes: viscosity-heat conduction and the interaction of sound with turbulent flow in the duct.

The various mechanisms and their contributions to θ_t are:

$\theta_t^{(1)}$ due to the acoustic radiation from the end of the duct³⁰,
 $\theta_t^{(2)}$ due to the interaction of sound with the exit jet from the duct¹⁸, $\theta_t^{(3)}$ caused by acoustic losses due to viscosity and heat conduction³⁰ and $\theta_t^{(4)}$ arising from the sound-turbulence interaction in the duct¹⁷.

$$\theta_t^{(1)} \approx \frac{1}{4} (d/\lambda)^2 \quad (3.8)$$

$$\theta_t^{(2)} \approx \beta M \quad (3.9)$$

$$\theta_t^{(3)} = \frac{L}{d} \frac{\omega}{c} \left[\sqrt{\frac{2\mu}{\omega \rho}} + (\gamma-1) \sqrt{\frac{2K}{\omega \rho C_p}} \right] \quad (3.10)$$

$$\approx 5.8 \times 10^{-5} \frac{L}{d} \sqrt{f}$$

$$\theta_t^{(4)} \approx \psi M \frac{2L}{d} \quad (3.11)$$

Here C_p is the specific heat at constant pressure, γ the ratio of specific heats, K the heat conduction coefficient, μ the coefficient of viscosity, λ the wavelength and β is a numerical constant ≈ 0.5 to 1 .

At the comparatively low frequencies of interest (wavelength much larger than the pipe diameter), the sound-turbulence interaction is usually dominant for flow Mach numbers larger than 0.1 .

$$\theta_t \approx \theta_t^{(2)} + \theta_t^{(4)} = \left(\beta + \frac{2L}{d} \psi \right) M \quad (3.12)$$

With $\beta \approx 0.5-1.0$ and $2\psi L/d \approx 0.5$, we see that for $M \approx 0.1$, the equivalent resistance θ_t will be approximately 0.1 to 0.15 . The understanding of sound-turbulence interaction is still far from complete and the determination of θ_t is therefore only approximate.

θ_t can also be determined experimentally from measurement of the frequency dependence of the magnitude of the acoustic input impedance $|Z|$ at the entrance of the pipe. In a frequency range in the vicinity of a frequency ω_n , at which the pipe length is an odd number of quarter wavelengths $L = (2n+1)(\lambda/4)$, $|Z|$ has a maximum at ω_n and the "sharpness" of the response

curve for $|Z|$ in this region is

$$Q_n = \frac{\omega_n}{\Delta\omega_n} = \frac{(2n+1)(\pi/2)}{\theta_t} \quad (3.13)$$

where $\Delta\omega_n$ is the width of the curve at which the value of $|Z|$ is $1/\sqrt{2}$ of the maximum value.

Definitions

For the following development, it is convenient to define a system instability parameter η , a frequency ratio x , a non-dimensional length y and the logarithmic decrement of the oscillator δ .

$$\eta = \frac{A_v}{A} \frac{dm}{dh} \frac{c}{K\theta_t} \quad (3.14)$$

$$x \equiv \omega/\omega_m \quad \text{AND} \quad y \equiv L/\lambda_m \quad (3.15)$$

$$\delta \equiv \pi \frac{R}{W\omega_m} \equiv \pi \frac{R\omega_m}{K} \quad (3.16)$$

The Q value of the oscillator is then

$$Q \equiv \frac{\omega_m W}{R} \equiv \frac{K}{R\omega_m} \quad (3.17)$$

In terms of x and y ,

$$kL = 2\pi \frac{L}{\lambda} = 2\pi \frac{\omega}{\omega_m} \frac{L}{\lambda_m} = 2\pi x y \quad (3.18)$$

Here λ_m is the wavelength of sound at the frequency $f_m = \omega_m/2\pi$.

The stability conditions can now be obtained from equation (3.7) in terms of the parameters defined above.

Sufficient condition for stability

In order to obtain a sufficient condition for stability, we shall consider the worst possible situation which corresponds to the largest possible value of the negative resistance. If the resistance of the valve exceeds this maximum value of the negative resistance, the valve will be stable under all operating conditions. Actually, even if the intrinsic resistance of the valve is zero, it is still possible for the valve to be stable if the losses due to acoustic radiation exceed the negative resistance. This rather unlikely possibility corresponds to the condition

$$\left(\frac{A_v}{A}\right)^2 A \rho c \theta > \frac{A_w}{A} \frac{dm}{dh} \frac{c \chi}{\omega} \quad (3.19)$$

which can be expressed as

$$\eta < \left(\frac{A_v}{A}\right)^2 \frac{A \rho L}{W} \frac{x}{\pi y} \quad (3.20)$$

where we have made use of the fact that the maximum value of χ_t/θ is 0.5. The factor $A \rho L/W$ is the ratio between the total mass of the fluid in the pipe and the mass of the valve. This is usually quite small and the condition (3.20) generally cannot be fulfilled in practice and we must rely upon factors other than acoustical damping to achieve stability. One possibility is, of course, the use of mechanical damping of the

valve.

If R is not zero, it is reasonable to neglect the second term in the resistive part of equation (3.7), and the sufficient condition for stability for all operating conditions and all pipe lengths requires that mechanical resistance coefficient be larger than a critical value such that

$$R > \frac{1}{2} \frac{A_v}{A} \frac{c}{\theta_t} \frac{dm}{dh} \frac{1}{\omega} \quad (3.21)$$

which can be expressed in dimensionless form as

$$\eta < \frac{2x}{Q} = \frac{2}{\pi} x \delta \quad (3.22)$$

Since x in most cases of interest is close to unity, we may express this sufficient condition for stability approximately by the rule that the instability parameter η of the system should be less than twice the inverse of the Q value or less than 1.6 times the logarithmic decrement of the valve. On closer examination one finds that x depends somewhat on θ_t and if this dependence is accounted for (equation 3.28) the sufficient condition for stability in equation (3.22) takes the form shown in figure 2. This condition, however, corresponds to the worst of the operating parameters. Much less stringent requirements for stability result if this worst operating point is avoided.

Stability diagrams

If the sufficient condition in equation (3.22) is not satisfied, the question whether the system is stable or unstable

involves more detailed studies based on the actual value of the acoustical equivalent resistance and not on the maximum value. To find the actual value, we should solve equation (3.7). The general solution, however, leading to a determination of the real and imaginary parts of $\omega = \omega_r + i\omega_i$, is quite involved and has not as yet been carried out. But if we are concerned mainly about the conditions for stability and not the growth or decay rates of the oscillations, it is sufficient to solve the equation when we restrict ourselves to the case $\omega_i = 0$. The solution thus obtained defines the relationship between the parameters involved that leads to the stability contours which represent the border between unstable and stable regions. Thus if we let ω be real in equation (3.7), we obtain the following relations for the determination of $\omega = \omega_r$ and the relationship between the parameters that yield neutral stability.

$$R - \frac{A_v}{A} \frac{dm}{dh} - \frac{c \chi}{\omega} = 0 \quad (3.23)$$

$$\omega W - \frac{1}{\omega} \left(K - \frac{A_v}{A} \frac{dm}{dh} - c \theta \right) = 0 \quad (3.24)$$

We have in these equations neglected the mass load and the second term in the resistive part of equation (3.7). Equation (3.23) simply says that the effective resistance force on the piston, including the effect of the acoustic reaction force, is zero when the system is on the verge of self-oscillation. In terms of the system parameters η , y , Q , x and θ_t , equations

(3.23) and (3.24) can be expressed as

$$\frac{x}{\eta Q} = \frac{(1 - \theta_t^2) \theta_t e}{1 + \theta_t^2 e^2} \quad (3.25)$$

and

$$\frac{1}{\eta} (1 - x^2) = \frac{\theta_t^2 (1 + e^2)}{1 + \theta_t^2 e^2} \quad \text{OR} \quad 1 - \frac{1 - x^2}{\eta} = \frac{1 - \theta_t^2}{1 + \theta_t^2 e^2} \quad (3.26)$$

where we have made use of equations (3.5) and (3.6) to express θ and x in terms of the system parameters. Here, $e = \tan kL$.

From equation (3.26) it is clear that x is always less than unity i.e. the frequency of oscillation of the valve is less than the natural frequency. This has been verified experimentally^{4,13} and is due to the negative contribution to spring constant from the acoustic feedback.

From equations (3.25) and (3.26) follow

$$y = \frac{1}{2\pi x} \arctan \left[\frac{1}{\theta_t Q} \frac{x}{\eta - (1 - x^2)} \right] \quad (3.27)$$

and

$$1 - x^2 = \frac{1}{2} S \left[1 \pm \sqrt{1 - \frac{4(\epsilon^2 + \theta_t^2 \eta^2)}{S^2}} \right] \quad (3.28)$$

where $S = \eta(1 + \theta_t^2) + \epsilon^2$ and $\epsilon = 1/Q$

For a prescribed value of Q , θ_t and η we first obtain the frequency ratio x from equation (3.28). Then the stability contour, i.e. the relation between η and y representing neutral stability is given by equation (3.27). The function $\eta = \eta(y)$ for given values of the parameters Q and θ_t has several branches.

Having obtained the first branch $\eta_1 = \eta_1(y)$, we find the others simply by displacing the variable y so that the n th branch is

$$\eta_n = \eta_1 \left(y + \frac{n\pi}{2\pi x} \right) \quad (3.29)$$

These branches represent the stability contours for the different modes of motion of the system. The qualitative behavior of the first few branches is shown in Figure 3. Each branch approaches $\eta=1$ asymptotically as $y \rightarrow \infty$. Below each contour the corresponding mode is stable, and above the contour it is unstable. In order for the system to be stable for all possible modes of oscillation, the operating point, i.e. the values of η and y , must lie below all the contours.

Stability contours obtained in this manner are shown in figures 4 to 6. The corresponding contours for the frequency ratio x (i.e. the frequency of oscillation corresponding to neutral stability) are shown in figures 7 to 9.

Once the instability parameter is defined to be inversely proportional to θ_t , the remaining effect of θ_t on the stability contours is seen to be negligible; increasing θ_t then has the effect of increasing the end correction to the duct (Figures 4 and 5). The Q value of the valve has a more pronounced effect on the stability contours as shown in Figures 4 and 6. Larger Q is reflected mainly by a downward translation of the stability boundary and a small increase in the end correction. Larger Q implies smaller damping and therefore a system that

can be made unstable more readily.

Even though we have not presented curves for the growth rates, using qualitative arguments it is very easy to show that the magnitude of the negative damping is large in the immediate vicinity to the left of the stable regions and small in the immediate vicinity to the right thereof.

The flow velocity in the pipe affects the acoustical damping of the duct and thus is indirectly reflected in the instability parameter. Its influence on the resonance frequencies of the duct is usually negligible since it involves the factor $(1-M^2)$.

As an example of the use of stability diagrams, consider a valve with $Q=20$ and a duct with $\theta_t=0.1$ (Figure 4). An operating point corresponding to $\eta=0.2$, $y=0.5$ then corresponds to stable operation whereas for $\eta=0.2$, $y=0.25$ it is unstable. Actually, in this particular example, with an instability parameter $\eta=0.2$ and a Q value of 20, the values of the duct length parameter $y=L/\lambda_m$ yielding stability, correspond to the intervals $y=0$ to 0.2, 0.27-0.7, 0.83-1.2, 1.39-1.7, 1.93-2.2 etc. As η increases, these regions diminish until for $\eta > 0.82$ the system becomes unstable for all lengths $L > 0.08 \lambda_m$. On the other hand, for $\eta < 0.1$ the system is stable for all values of L . This latter result is consistent with the sufficient condition $\eta < 2x/Q$.

Stabilizing an unstable valve

To stabilize a given system we have several options involving among others, an increase in the acoustical or mechanical damping in the system, an increase in the stiffness of the valve (and a corresponding increase in the resonance frequency of the valve) or a change in the length of the pipe so that the acoustic reaction force acts as a stabilizing positive damping. An orifice located at the end of the duct will introduce both acoustical and mechanical damping.

CHAPTER 4

DISCUSSION OF EXPERIMENTAL RESULTS ON VALVE INSTABILITY

It is essential to keep the experimental system for studying valve instability as simple as possible to avoid the difficulties that other investigators⁴ have faced. The simplest system seems to be a straight uniform duct with a cantilever beam acting as a valve. A beam machined from a large chunk of metal is also the easiest way to get the smallest damping in the system. The roots of the beam are curved to avoid sharp turns which cause stress concentration and result in cracks. Such a valve has many modes but we were able to excite only the first bending and the first torsional mode. All attempts to excite the second bending mode were unsuccessful though torsional modes are almost nonexistent when the modification shown in figure 1 is used. Attempts to eliminate the torsional vibrations by rounding the edges were unsuccessful.

The natural frequency of the beam is obtained by hitting the beam with a small hammer and Fourier analyzing the impact sound as received on a microphone placed nearby.

The "valve" is mounted on a milling machine bed thus making it possible to move the valve along three independent directions relative to the duct. The duct is held in a big chamber filled with glass wool to avoid reflections of sound from the chamber and the end of the duct is unflanged. Thus the valve can be positioned independently of the duct and its

separation distance from the duct or their relative alignment can be varied.

A suction system is used so that the fluid flow is as "clean" as possible without any interference from unnecessary piping that is associated with blowing air systems. The flow is provided by a steam ejector which is acoustically isolated from the "valve-pipe" system by the almost "anechoic" chamber. The steam ejector is essentially a constant flow device and therefore in the experiments we adjust the flow rate to a desired value, then change the gap between the "valve" and the duct until the system is on the verge of self-oscillation.

The valve is expected to behave like an orifice so that the volume flow rate is directly proportional to the opening h and the square root of the pressure drop ΔP across the valve where ΔP is the difference of the atmospheric pressure from the pressure in the chamber. We expect the pressure recovery in the duct or in the chamber to be almost negligible. At constant pressure drop the flow rate is measured to be directly proportional to h (Figure 10) and the slopes are approximately proportional to $\sqrt{\Delta P}$ (Figure 11). At small ΔP and large h this relationship has to be modified since then a larger fraction of the pressure drop occurs in the duct instead of the valve orifice.

Having chosen the beam and the pipe cross-section, $d\dot{m}/dh$ and θ_t are the only controls we have on the instability parameter.

Since the equivalent termination resistance θ_t is proportional to the Mach number in the duct (equation 3.12), we can simplify the experiment by holding the flow rate constant. Here the constant flow characteristic of the steam ejector is a big plus. The length of the duct is easily changed by changing the duct that is attached to the chamber. The instability parameter is now directly proportional to the square root of the pressure drop. The beam is now brought closer and closer to the duct until it just begins to vibrate. The pressure drop ΔP that is required for a given flow rate through the valve and the gap size h determine $d\dot{m}/dh$. Results obtained in this manner are shown in Figure 12. The qualitative resemblance with Figure 4 is very encouraging.

It is difficult to compare the theoretical predictions with the experimental results because in the analysis we neglected the effect of flow on the Q value of the beam. The dependence of Q on flow is now being studied experimentally. At values of L/λ_m (e.g. $L/\lambda_m \approx 0.9$) where large pressure drop is required to destabilize the valve, the flow velocity through the opening is so large and consequently the Q value of the valve so low that it is almost impossible to get the beam to oscillate in bending mode though it was still possible to excite the torsional modes of the beam, either because the negative damping arising from the reaction forces is larger or because the mechanical damping is lower for the torsional modes when

compared with the bending modes.

Four strain gages are mounted on the root of the cantilever beam to measure its bending modes. The Fourier analysis of the output from strain gages and the output from a microphone placed nearby give the same frequency of excitation. The oscillation frequency for various duct lengths at the verge of instability is shown in Figure 13.

It is observed that when a duct of a certain length is being tested to determine the boundary between stable and unstable regions, the vibrations grow very violently--to the point of breaking the beam or to the point where the beam starts hitting the duct--when the pressure drop is increased by a very small amount (like 5 to 10 mms of mercury) if the duct length is in the immediate vicinity to the left of the stable region e.g. $L/\lambda_m \approx 0.25$ or 0.7 . On the other hand, when the length of the duct is in the immediate vicinity to the right of the stable region, e.g. $L/\lambda_m \approx 1.0$ or 1.5 , the instability parameter η can be increased by large amounts without any significant increase in noise or vibrations. Incidentally the unwanted collisions between the "valve" and the duct hindered our attempts to measure growth rates but effort is continuing in that direction.

When the experimental neutral stability curve (Figure 12) is compared with a typical stability curve predicted analytically, a leftward shift along the L/λ_m axis is observed. The small

end correction to the duct is unable to explain this trend toward lower L/λ_m .

The data presented here is consistent with the data reported by Ezekiel⁴ and Wilson and Beavers¹³. The nondimensional parameters used by them are different from the ones we have used. They use $\Delta P/(Kw)$ as the instability parameter where w is some characteristic length. Ezekiel⁴ chooses w to be the width of the valve port whereas in the work of Wilson and Beavers¹³ w represents the steady state gap opening h . Our parameter η is much better because it involves the flow characteristics of the valve and the acoustical characteristics of the duct. Their parameters also have the disadvantage of including the spring constant K in several of the nondimensional parameters necessary for the theoretical analysis. Direct comparison of the result is meaningless because the experimental systems used in the three sets of experiments are quite different. It should be noted that the theory of Wilson and Beavers¹³ predicts that in the second stable region centered around $L=\lambda$ the maximum pressure drop up to which the system is stable is larger than the corresponding maximum in the stable region around $L=\lambda/2$. Their experiments show the reverse to be true. Our theory and experiments (Figures 4 and 12) confirm their experimental findings.

CHAPTER 5

ACOUSTICALLY INDUCED FLOW INSTABILITY IN SIDE BRANCH CAVITIES

Often the ducts carrying flow have side branch cavities. These cavities are sometimes associated with the control valve regulating the fluid flow but their presence is not necessarily linked to valves. At times, they are deliberately included to damp the hydraulic surges or to act as sound absorbers. It is well-known that they can be set in violent acoustic oscillations by the flow. The screeching of side branch resonators has been the subject of numerous studies²⁴⁻²⁹. The fluid dynamic models²⁵⁻²⁷ are based on excitation of the shear layer, are somewhat empirical and have only been partially successful. Here we describe some experiments which show that the duct and the location of the resonator along the duct have significant effects on the excitation characteristics.

A cavity 3 inches deep and 3/4 inch square cross-section is cut from commercial tubing with 1/8 inch thick walls and is attached to a duct of 3/4 inch square cross-section. The cavity can be joined easily to the duct with plasticine when a 1 inch square is shaved off on a milling machine from the top surface of the duct. The duct is mounted on the flow facility in the manner described earlier for the valve-pipe system. Because we use a suction device, the flow is smooth and we can easily isolate the cavity acoustically from the flow device. The noise produced is Fourier analyzed on a real time spectrum

analyzer.

As indicated in Figure 14, screech occurs over a wide range of flow velocities. The intensity of this excitation can be surprisingly large. In our experiment with a single cavity, under special conditions (e.g. modification of the edges) levels exceeding 127 dB were observed at 1 foot from the entrance of the pipe. Qualitatively we can state that as the flow velocity is increased gradually through the pipe, we encounter flow regimes in which the various modes of the side branch cavity are excited. In Figure 14 we notice the concentration of points at frequencies which correspond to the depth being odd multiples of quarter wavelength (cavity depth = $(2n+1)\lambda/4$ where n is an integer). For deep cavities (width \ll depth), if we account for the gross flow modification of the end correction of the cavity, the peaks of the spectra can be identified as odd multiples of the quarter wave length resonance of the side branch cavity. The associated amplitude changes in the radiated noise level lead us to postulate a shear layer at the mouth of the cavity, whose characteristic frequency increases monotonically with the flow velocity. When a multiple or submultiple of this characteristic shear layer frequency is near a resonance frequency of the side branch resonator, a coupled resonance radiates intense sound. The strength of the excitation depends on how close the two frequencies are to each other, the strongest being at exact coincidence.

To explore the possible role of the degree of turbulence in the duct on the excitation, experiments were carried out with the side branch cavity located in the vicinity of the entrance of the duct, in the center of the duct and near the downstream end of the duct. It is found that when the cavity is very close to the ends, the distance to the end being typically less than 4 duct diameters, excitation is suppressed because the boundary layer is poorly established.

When the side branch cavity is moved farther from the ends as shown in Figure 15, several resonances are observed that cannot be identified as odd multiples of the quarter wavelength resonance. The motion of the shear layer provides the nonlinear coupling between the cavity modes, thus generating the sum and difference tones. The peaks labeled f_1 , f_3 and f_5 represent the one-quarter, three-quarter and five-quarter wavelength resonances of the side branch cavity. The remaining peaks are not related to the quarter wavelength resonances. However, upon closer examination we find that the peak labeled f_{3-1} represents a difference frequency of f_3 and f_1 , whereas the peak labeled f_{3+1} is the sum frequency of the two. Similarly we identify f_{1+1} as a peak at twice the first frequency and f_{3+3} as a peak at twice the third frequency. Other such combinations are also identified in the figure.

Another interesting coupling effect was observed when the side branch cavity was located at the center of the duct. A

typical result is shown in Figure 16. Here the spectral line representing the resonance of the side branch cavity has several "satellites". These "satellites" are found to occur at frequencies given by $f_1 \pm nf_d$, where f_1 is the cavity mode, f_d is the fundamental axial duct frequency and n is an integer. In other words, this resonance indicates nonlinear coupling between the side branch cavity and the axial resonances of the main duct. Again this coupling is undoubtedly provided through the modification of the shear layer by the axial motion in the duct.

It is most interesting to observe that the "satellites" disappear at sufficiently high flow speeds. This is actually to be expected¹⁸, since as a result of the flow induced damping, the axial modes are, in effect, eliminated by the flow at sufficiently high flow speeds.

It is puzzling to find that a cavity inclined as shown in Figure 17a is as quiet as a duct without any side branch cavity whereas a cavity inclined the other way (Figure 17b) whistles very violently, the noise level sometimes exceeding 125dB for a single cavity.

CHAPTER 6

CONCLUDING REMARKS

Significant progress has been made in our understanding of the emission and propagation of acoustic waves in uniform hard walled ducts carrying a uniform flow though a lot more still needs to be done. The upstream and downstream emission of sound from a stationary source into a moving fluid in a duct depends on the boundary conditions in the source region. A change in boundary conditions results in a transition from "laminar" to "turbulent" state but these boundary conditions need to be established rigorously. Of course, the important question of division of acoustic energy with or against the flow still remains to be resolved.

The attenuation of plane waves by the turbulence in the flow is explained by a simple quasistatic model. The analysis needs to be extended to higher order modes. Also the difference in experimental results obtained from the standing wave technique and the pulse excitation remains to be explained.

The end correction, the termination resistance and the reflection coefficients from the ends of the duct are measured for plane sound waves propagating in ducts carrying uniform flow. The contribution of flow to the equivalent termination resistance is approximately equal to the Mach number of the flow but this observation needs to be substantiated by further detailed experiments and mathematical analysis.

Since these investigations on duct acoustics have already been published in the Journal of the Acoustical Society of America, only a brief review is included in this thesis and the reprints can be found in the appendices.

This knowledge is used for a study of the acoustically induced instabilities in valve-pipe systems. The oscillations of the valve modulate the mass flow through the pipe. The resulting velocity perturbation leads to an acoustic reaction force on the valve. We determine the operating conditions for this acoustic reaction force to act as a negative damping. The length of the duct determines to a large extent whether the reaction force is stabilizing or destabilizing. An instability parameter is defined in terms of the mechanical properties of the valve and the acoustical characteristics of the duct. The stability contours show that for small values of the instability parameter, the valve is always stable regardless of duct length but for large values of the instability parameter all pipe lengths are unstable.

The salient features of the theory are verified experimentally except for a phase shift which cannot be explained by the small end correction to the pipe. Only the axial modes are studied in detail. Torsional modes are the easiest to excite but can be quenched almost completely by torsionally stiffening the end of the cantilever beam that is used for the investigations of axial valve oscillations. It is possible to excite the

lateral modes of a valve whose predominant degree of freedom is the lateral translatory motion of the valve stem. The lateral and torsional modes observed experimentally did not seem to be acoustically coupled. Preliminary analytical investigations reveal the existence of acoustically coupled lateral modes. The torsional and the lateral modes need further study.

Some remarks are included on the excitation of side branch cavities in ducts with flow. Coupling of cavity modes with the axial modes of the duct is demonstrated. A cavity inclined properly with respect to the duct axis is found to be as quiet as a duct without the cavity. The sound absorption characteristics of these inclined cavities need further study.

Appendix A

Reprinted from: The Journal of the Acoustical Society of America

Upstream and downstream sound radiation into a moving fluid

Uno Ingard

Departments of Physics and of Aeronautics and Astronautics and Research Laboratory of Electronics, Massachusetts Institute of Technology, Cambridge, Massachusetts 02139

Vijay K. Singhal

Department of Aeronautics and Astronautics and Research Laboratory of Electronics, Massachusetts Institute of Technology, Cambridge, Massachusetts 02139

(Received 1 June 1973)

An experimental demonstration of the influence of fluid motion in a duct on the sound pressure field radiated in the upstream and downstream directions from a stationary sound source is presented. The measured ratio between the upstream and downstream sound pressure amplitudes in the duct is presented as a function of the flow Mach number in the range $M = 0-0.5$. The results are discussed in the light of a mathematical analysis of the problem.

Subject Classification: 14.6; 1.6.

INTRODUCTION

The problem of sound radiation from a source in relative motion with respect to the surrounding fluid has become of considerable interest in recent years, particularly in connection with noise generation in aircraft and in various types of fluid machinery. Although the basic effects, as well as many details of the influence of fluid motion on sound radiation, have been identified by several investigators,¹⁻⁵ these studies have been limited to mathematical analysis of the idealized case of moving point sources. The problem of sound emission from real sources of finite dimensions has received much less attention. The purpose of this paper is to present an explicit experimental demonstration of the influence of relative fluid motion on sound radiation from a stationary source, with particular attention to the relation between the sound pressure fields radiated upstream and downstream.

I. EXPERIMENTAL ARRANGEMENT

The experimental arrangement is shown schematically in Fig. 1. A sound source is mounted in one of the side walls of a rectangular duct with inner dimensions $\frac{1}{2} \times \frac{1}{2}$ in. The duct is connected to a pump through a plenum chamber, and the flow speed in the tube can be varied between 0 and 170 m/sec, which corresponds to a Mach number range in air of about 0-0.5.

The loudspeaker is driven by means of a pulse generator and produces harmonic sound pressure wave trains in the duct. The carrier frequency of these waves is chosen to be considerably lower than the cutoff frequency for the first higher-order acoustic mode in the duct, so that at the carrier frequency only the plane-wave mode will be able to propagate. Pulse, rather than steady-state, excitation of the sound source was used so

that the problem of reflection from the ends of the duct did not have to be considered in the analysis of the data. The reflection problem will be discussed separately in a forthcoming paper.

The pressure pulses are detected by two identical pressure transducers mounted in the side walls of the duct on the upstream and downstream sides of the sound source at equal distances from it. In the absence of flow, $M=0$, the recorded pulses from these transducers are simultaneous and identical in shape, as demonstrated by the results shown in Fig. 1. Any difference in the sensitivity of the transducers is compensated for by gain adjustment of the transducer amplifiers, so that in the absence of flow the amplitudes of the recorded pulses from the transducers are equal.

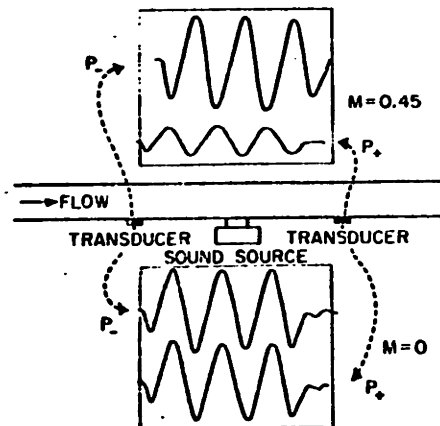


Fig. 1. Examples of recorded pressure pulses in the upstream (p_u) and the downstream (p_d) directions at flow Mach numbers $M=0$ and $M=0.45$.

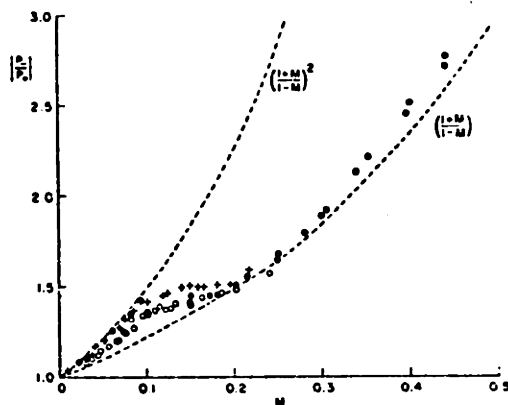


FIG. 2. Mach number dependence of the measured ratio $|p_-|/|p_+|$ between the pressure amplitudes radiated in the upstream and downstream directions. \bullet —1477 Hz. \circ —1000 Hz. $+$ —1050 Hz (different location in the duct).

When the air in the duct is moving, however, the pressure amplitudes are no longer equal; the amplitude in the upstream direction is larger than in the downstream direction, and the difference increases monotonically with the flow speed in the duct. An example of recorded upstream and downstream pressure waves at a flow Mach number M of 0.45 is shown in Fig. 1. In addition to the obvious difference in the pressure amplitudes, a difference in the time of arrival of the two pulses is also apparent in this figure. This time difference is governed by the average flow Mach number across the duct.⁶ From the measured value of this time difference and the distance between the sound source and the receivers the flow Mach number in the duct was determined.

The Mach number dependence of the ratio $|p_-|/|p_+|$ between the upstream and downstream pressure amplitudes obtained in this manner is illustrated in Fig. 2. Measurements were carried out at two frequencies, 1000 Hz and 1477 Hz. As can be seen, there is no marked difference in the amplitude ratio at these two frequencies. Furthermore, the results obtained did not depend on the strength of the source signal within the amplitude range available in our experiment.

Qualitatively, the observed higher sound pressure in the upstream direction is to be expected from the fact that the sound pressure about a moving source in a medium at rest is larger in the forward direction. In our case, with the sound source at rest, the "forward" direction corresponds to the upstream direction.

The monotonic increase of $|p_-|/|p_+|$ with M indicates an irregularity or "transition" in the vicinity of $M \approx 0.1$ which corresponds to a Reynolds number of 0.5×10^3 , based on the duct diameter. In the following mathematical analysis of the radiation problem it will be shown that the Mach number dependence of $|p_-|/|p_+|$ is intimately linked to the nature of the flow boundary conditions in the source region and that if a change in

these boundary conditions occurs at a certain Reynolds number, a corresponding change in $|p_-|/|p_+|$ is to be expected.

II. MATHEMATICAL ANALYSIS

In the mathematical analysis of this problem we start from the wave equation for the sound pressure field $p(x, y, z, t)$

$$(1-M^2) \frac{\partial^2 p}{\partial x^2} + \frac{\partial^2 p}{\partial y^2} + \frac{\partial^2 p}{\partial z^2} - \frac{2M}{c} \frac{\partial^2 p}{\partial x \partial t} - \frac{1}{c^2} \frac{\partial^2 p}{\partial t^2} = 0, \quad (1)$$

where c is the sound speed, and M the mean Mach number in the duct. The coordinates x, y, z refer to a stationary laboratory frame of reference with respect to which the unperturbed fluid is assumed to move with uniform speed Mc in the positive x direction. We wish to solve this equation subject to the boundary conditions peculiar to our experimental arrangement.

The duct walls, placed in the planes $y=0, y=a$ and $z=0, z=b$, are assumed to be rigid everywhere except in the source region, as indicated in Fig. 3. Consequently, the normal components of the fluid velocity and the corresponding pressure gradients are zero at the boundaries except at the source. If the source, located in the wall in the plane $y=0$, produces a velocity perturbation u_y in the fluid flow in the plane $y=0$, the effect of the source can be expressed as the boundary condition

$$u_y = u_0 f(x, z, t) \quad (y=0). \quad (2)$$

It is important to realize, however, that this velocity perturbation of the fluid in the duct is not necessarily the same as the velocity of the oscillating air column in the throat of the loudspeaker source

$$u_s = \frac{\partial \eta_s(x, z, t)}{\partial t}, \quad (3)$$

where $\eta_s(x, z, t)$ is the displacement of the air column. Although $u_y = u_s$ is valid when there is no mean flow in the duct, the situation is more complex when mean flow is present. For example, if the flow over the source region is streamlined, the transverse oscillatory motion of the air of the source will result in a displacement of the streamlines, and this displacement gives rise to a velocity perturbation in the fluid flow given by

$$u_y(x, z, t) = \left(\frac{\partial}{\partial t} + Mc \frac{\partial}{\partial x} \right) \eta_s(x, z, t). \quad (4)$$

This model of the flow perturbation produced by the source is unrealistic if the boundary flow is turbulent, in which case the contributions from the space derivative in Eq. 4 at different locations of the source are expected to be largely uncorrelated and the effect correspondingly reduced. In the absence of this contribution, the boundary condition in Eq. 4 reduces to $u_y = u_s$.

RADIATION INTO A MOVING FLUID

In our experiment, since only the plane-wave mode is transmitted along the duct, it is expedient to introduce the average sound pressure \bar{p} over the duct cross section,

$$\bar{p} = \frac{1}{A} \iint p dy dz. \quad (5)$$

We now obtain a wave equation for \bar{p} by integrating Eq. 1 over the transverse coordinates y, z . We make use of the fact that the duct walls are rigid, except in the source region, and note that the average of $\partial^2 p / \partial z^2$ is zero. Similarly, the average of $\partial^2 p / \partial y^2$ is

$$(1/A) \int (-\partial p / \partial y) y dz,$$

where $(\partial p / \partial y)_0$ is evaluated in the source region of the wall at $y=0$. We can express $(\partial p / \partial y)_0$ in terms of the velocity perturbation u_y from the momentum equation

$$\rho \left(\frac{\partial}{\partial t} + Mc \frac{\partial}{\partial x} \right) u_y = - \frac{\partial p}{\partial y}. \quad (6)$$

The wave equation for the average pressure \bar{p} can then be expressed as

$$(1-M^2) \frac{\partial^2 \bar{p}}{\partial x^2} - 2 \frac{M}{c} \frac{\partial^2 \bar{p}}{\partial x \partial t} + \frac{1}{c^2} \frac{\partial^2 \bar{p}}{\partial t^2} = s(x,t), \quad (7)$$

where

$$s(x,t) = - \frac{\rho}{A} \left(\frac{\partial}{\partial t} + Mc \frac{\partial}{\partial x} \right) \int_0^b u_y(x,z,t) dz. \quad (8)$$

In this inhomogeneous wave equation the right-hand side is considered to be a known source function $s(x,t)$ defined in the source plane $y=0$, where u_y is given by Eq. 4. To solve this equation, we introduce the Fourier transforms

$$\bar{p}(x,t) = \iint P(k,\omega) e^{ikx} e^{-i\omega t} dk d\omega, \quad (9)$$

$$s(x,t) = \iint S(k,\omega) e^{ikx} e^{-i\omega t} dk d\omega, \quad (10)$$

and from Eq. 7 obtain

$$P(k,\omega) = \frac{-S(k,\omega)}{(1-M^2)(k-k_+)(k-k_-)}, \quad (11)$$

where

$$k_+ = \frac{\omega}{c(1+M)} \quad k_- = \frac{\omega}{c(1-M)}. \quad (12)$$

If we let the source region be limited to $-L < x < L$, so that $s(x,t)$ is zero outside this region, we can express $S(k,\omega)$ as

$$S(k,\omega) = \frac{1}{2\pi} \int_{-L}^{+L} s(x_0,\omega) \exp(-ikx_0) dx_0, \quad (13)$$

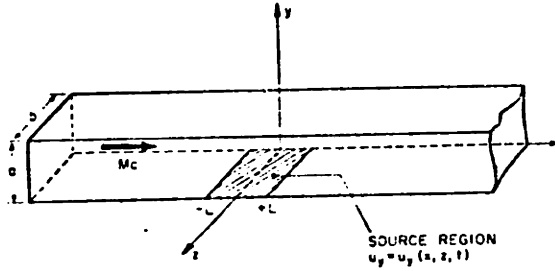


FIG. 3. The source region is in the plane $y=0$ of the duct and is defined by the perturbation of the fluid velocity u_y in the y direction.

where $s(x,\omega)$ is the temporal Fourier transform of $s(x,t)$. Then, from Eqs. 4 and 7, we have

$$S(k,\omega) = (i\omega) \left(\frac{A_s}{A} \right) \rho u_0 \left(1 - Mc \frac{k}{\omega} \right)^2 \eta_s(k,\omega), \quad (14)$$

where

$$\eta_s(k,\omega) = \frac{1}{2\pi\eta_0} \frac{1}{b2L} \int_0^b dz_0 \int_{-L}^{+L} \eta_s(x_0,z_0,\omega) \times \exp(-ikx_0) dx_0 \quad (15)$$

and $A_s = b2L$ is the source area, $u_0 = (-i\omega\eta_0)$ is the velocity amplitude of the source, and η_0 is the displacement amplitude. In the special case of a piston-like displacement such that $\eta_s(x_0,z_0,\omega) = \eta_0$ in the source region, we get

$$\eta_s(k,\omega) = \text{sinc} kL / kL. \quad (16)$$

Having obtained $S(k,\omega)$, we determine the pressure amplitude $p(x,\omega)$ from

$$p(x,\omega) = \int_{-\infty}^{+\infty} P(k,\omega) e^{ikx} dk = \int_{-\infty}^{+\infty} \frac{-S(k,\omega) e^{ikx}}{(1-M^2)(k-k_+)(k-k_-)} dk, \quad (17)$$

where $S(k,\omega)$ is given by Eqs. 14 and 15.

The poles $k = k_+$ and $k = k_-$, although located on the k axis in the present analysis, would contain a small positive and negative part, respectively, if some damping mechanism, such as viscosity or heat conduction, had been included in the analysis. Evaluating the integral by contour integration in the complex k plane, we can complete the contour in the upper k plane for $x > L$, and thus include the pole at $k = k_+$. The corresponding solution is then

$$p_+ = \frac{A_s}{A} \frac{1}{2} (\rho c u_0) \frac{1}{(1+M)^2} \eta_s(k_+,\omega) \exp \left[i \frac{\omega}{c(1+M)} x \right]. \quad (18)$$

INGARD AND SINGHAL

Similarly, by closing the path in the lower half-plane, we find, for $x < -L$,

$$p_- = \frac{A_+}{A_-} \frac{1}{2} (\rho c u_0) \frac{1}{(1-M)^2} \eta_+(k_-, \omega) \times \exp\left[-i \frac{\omega}{c(1-M)} x\right]. \quad (19)$$

These solutions represent the waves transmitted in the downstream and upstream directions traveling with the speeds $c(1+M)$ and $c(1-M)$, respectively, as expected. It is interesting to note that the amplitudes of these waves are different in the presence of flow in the duct. If the source region is acoustically compact, that is, if L is much smaller than the acoustic wavelength λ , the value of the source function η_+ is close to unity, as can be seen in the special example given in Eq. 16, and the ratio of the upstream and downstream pressure amplitudes becomes

$$\frac{|p_-|}{|p_+|} = \frac{(1+M)^2}{(1-M)^2} \left(\frac{\omega}{c} L \ll 1\right). \quad (20)$$

III. DISCUSSION

It should be emphasized that the Mach number dependence of the wave amplitudes, expressed by the factors $(1+M)^{-2}$ and $(1-M)^{-2}$ in Eqs. 18 and 19 and leading to the amplitude ratio in Eq. 20, depends intimately on the nature of the source and the velocity perturbation that it produces in the fluid. In the analysis carried out here the relationship between the (known) displacement of the air column in the loudspeaker throat and the corresponding velocity perturbation produced in the duct flow has been assumed to be described by Eq. 4, a relation based on the model of an oscillatory displacement of streamlined flow over the source region. In highly turbulent flow it may be more realistic to use as a boundary condition $u_y = u_s = \partial \eta_s / \partial t$ (obtained by neglecting $\partial / \partial x$ in Eq. 4), which means that the velocity perturbation in the duct flow equals the velocity in the loudspeaker throat. The amplitude ratio $|p_- / p_+|$ obtained in this case is $(1+M)/(1-M)$.

In Fig. 2, which shows the measured amplitude ratio $|p_- / p_+|$ as a function of the flow Mach number, we have also plotted the functions $F_1(M) = (1+M)^2 / (1-M)^2$ and $F_2(M) = (1+M)/(1-M)$, representing the theoretical results obtained on the basis of the two different boundary conditions that were considered. It is interesting to find that the experimental results fall between these theoretical curves. At Mach numbers less than ~ 0.1 , the data are in good agreement with the function F_1 , which indicates that the streamline model of the flow is meaningful. As the Mach number is increased, however, the data show a trend toward the function F_2 , which favors the boundary condition $u_y = u_s$.⁷

ACKNOWLEDGMENT

The experiments were carried out at the MIT Gas Turbine Laboratory, and we wish to thank Mr. Angelo Moretta for assistance in setting up the flow facility for the experiments. This work was supported by the U. S. Navy (Office of Naval Research) under Contract N00014-67-A-0204-0019.

¹D. I. Blokhintsev, "Acoustics of a Nonhomogeneous Moving Medium," NACA TM 1399 (Feb. 1956) (translation).
²H. G. Küssner, "Lösungen der klassischen Wellengleichung für bewegte Quellen," Z. Angew. Math. Mech. 24, 243-250 (1944).
³M. J. Lighthill, "On Sound Generated Aerodynamically: II. Turbulence as a Source of Sound," Proc. R. Soc. A 222, 1-32 (1954).
⁴P. M. Morse and K. U. Ingard, *Theoretical Acoustics* (McGraw-Hill, New York, 1968), pp. 682-689.
⁵R. Mani, "A Moving Source Problem Relevant to Jet Noise," J. Sound Vib. 25, 1-11 (1972).
⁶F. Mechel, W. Schilz, and J. Dietz, "Akustische Impedanz einer Luftdurchströmten Öffnung," Acustica 15, 199-206 (1965).
⁷Actually, if we account for the static pressure drop in the flow direction and the related difference in sound attenuation, for upstream and downstream propagation, the values for p_- / p_+ for $M > 0.2$ are reduced and the corresponding data points in Fig. 2 are brought to even better agreement with the $(1+M)/(1-M)$ curve than that shown in the figure.

Emission of higher-order acoustic modes into a moving fluid in a duct

Uno Ingard

Departments of Physics and of Aeronautics and Astronautics and Research Laboratory of Electronics,
Massachusetts Institute of Technology, Cambridge, Massachusetts 02139

Vijay K. Singhal

Department of Aeronautics and Astronautics and Research Laboratory of Electronics, Massachusetts
Institute of Technology, Cambridge, Massachusetts 02139

(Received 11 January 1974; revised 27 May 1974)

A study of the influence of fluid motion on the emission of higher-order acoustic modes from a stationary source in a duct is presented. In particular, the ratio between the upstream and downstream higher-order mode amplitudes is calculated. This ratio has been measured for the (1,0) mode in a rectangular duct at flow velocities from zero to 0.25 times the sound speed. The frequency dependence has also been measured at a fixed flow Mach number of 0.1.

Subject Classification: 28.60.

INTRODUCTION

Renewed interest in sound transmission through ducts has resulted in a large number of papers on the subject with particular emphasis on the effects of flow. In a recent review of the subject by Nayfeh, Kaiser, and Tellonis,¹ 114 references pertinent to duct acoustics are given.

Some of the effects of flow on the acoustic characteristics of lined ducts are related to the convection, refraction, and scattering of sound by the flow, and others involve the possible flow modification of the boundary impedance and the generation of noise by the flow.

This paper deals more with the influence of flow on the emission rather than the transmission of sound, as we discuss the flow dependence of the coupling between a stationary source and the duct modes. It represents an extension of a previous paper on the subject,² in which we determined the effect of flow on the ratio between the amplitudes of the plane waves emitted in the upstream and downstream directions from a stationary source in the wall of a rigid duct. In the present extension of this study we calculate the amplitude ratio also for higher-order duct modes and present experimental results for the (1,0) mode in a rectangular duct.

I. MATHEMATICAL ANALYSIS

If the mean flow velocity in the duct is V , the speed of sound c , and the corresponding mean Mach number $M = V/c$, the sound pressure field $p(x, y, z, t)$ satisfies the well-known wave equation

$$(1 - M^2) \frac{\partial^2 p}{\partial x^2} + \frac{\partial^2 p}{\partial y^2} + \frac{\partial^2 p}{\partial z^2} - \frac{2M}{c} \frac{\partial^2 p}{\partial x \partial t} - \frac{1}{c^2} \frac{\partial^2 p}{\partial t^2} = 0. \quad (1)$$

As indicated in Fig. 1(a), the source extends over a distance $2L$ along the axis of the duct and is confined to the two opposing side walls. In this region the source is specified by the time-dependent normal component of the displacement of the boundary. In general, the sound field produced by this source is composed of an infinite set of acoustic modes. If the walls of the duct are rigid,

some of these modes will propagate through the duct with undiminished amplitude (except for the small attenuation caused by turbulence, viscosity, and heat conduction) and some will decay exponentially with distance from the source region.

If the cross section of the duct is rectangular with dimensions a and b , the (m, n) mode in the duct can be written as

$$p_{mn}(x, t) \cos(m\pi y/a) \cos(n\pi z/b). \quad (2)$$

To obtain the equation for the amplitude function p_{mn} , we multiply Eq. 1 by $\cos(m\pi y/a) \cos(n\pi z/b)$ and integrate over the cross-sectional area of the duct. Then, accounting for the fact that the duct walls are rigid, except in the source region, we obtain the following equation for $p_{mn}(x, t)$:

$$\left\{ (1 - M^2) \frac{\partial^2}{\partial x^2} - \frac{2M}{c} \frac{\partial^2}{\partial x \partial t} - \frac{1}{c^2} \frac{\partial^2}{\partial t^2} - \left[\left(\frac{m\pi}{a} \right)^2 + \left(\frac{n\pi}{b} \right)^2 \right] \right\} p_{mn}(x, t) = s_{mn}(x, t), \quad (3)$$

where

$$s_{mn}(x, t) = -\frac{1}{ab} \int_0^b \left[\left(\frac{\partial p}{\partial y} \right)_{y=a} (-1)^n - \left(\frac{\partial p}{\partial y} \right)_{y=0} \right] \cos \left(\frac{n\pi z}{b} \right) dz. \quad (4)$$

The source term $s_{mn}(x, t)$ is determined by the normal component of the pressure gradient at the boundaries of the duct. We have assumed here a source limited to the walls $y=0$ and $y=a$. If the walls $z=0$ and $z=b$ also contain sources, a similar integral over these walls must be added.

The normal component of the pressure gradient is different from zero only in the source region, since the duct walls are rigid elsewhere. If in the source region the y and z components of the fluid velocity at the boundaries are u_y and u_z , the pressure gradients in the expression for s_{mn} are obtained from the momentum equation

$$-\frac{\partial p}{\partial y} = \rho \left(\frac{\partial}{\partial t} + V \frac{\partial}{\partial x} \right) u_y, \quad (5)$$

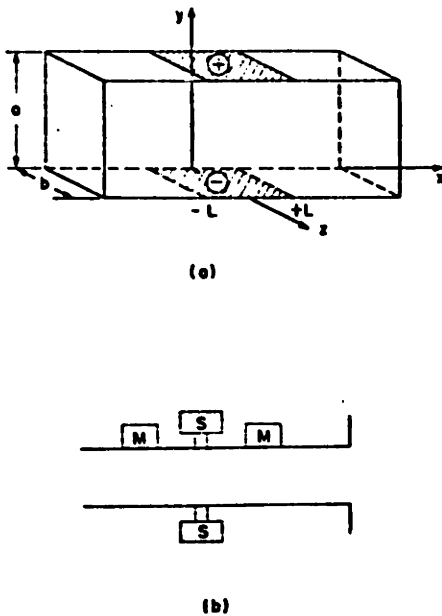


FIG. 1. (a) Source regions in the duct planes $y=0$ and $y=a$ (shaded). The two sources are operated in opposite phases, as shown by the plus and minus signs. (b) Schematic drawing of the experimental setup. S denotes the speakers and M the microphones.

with a similar expression for $\partial p/\partial z$ if there are sources in the planes $x=0$ and $x=b$.

If the flow is streamlined over the boundary in the source region and if the displacement of the boundary is η_n the normal component of the fluid velocity is

$$u_n = \left(\frac{\partial}{\partial t} + V \frac{\partial}{\partial x} \right) \eta_n, \quad (6)$$

which, to first order, is equivalent to continuity of velocity perpendicular to the deformed boundary. If, on the other hand, the flow is turbulent, the first-order contribution corresponding to $V \partial \eta_n / \partial x$ is expected to average to zero over the source so that $u_n \approx \partial \eta_n / \partial t$.

In any event, after having expressed the source function in terms of the known source characteristics, given either in terms of velocity or displacement, we can determine p_{mn} from Eq. 3 by means of a space-time Fourier transform and thus obtain the Fourier transform $P_{mn}(k, \omega)$ of the pressure amplitude in terms of the Fourier transform $S_{mn}(k, \omega)$ of the known source function. The quantity $S_{mn}(k, \omega)$ can be expressed as

$$S_{mn}(k, \omega) = (i\omega) \frac{A_s}{A} \rho c u_0 \left(1 - Mc \frac{k}{\omega} \right)^2 H_{mn}(k, \omega), \quad (7)$$

where

$$H_{mn}(k, \omega) = \frac{1}{2\pi\eta_0} \frac{1}{A_s} \int_0^b \cos\left(\frac{n\pi z_0}{b}\right) dz_0 \\ \times \int_{-L}^L \left[(-1)^m \eta(x_0, a, z_0, \omega) \right. \\ \left. - \eta(x_0, 0, z_0, \omega) \right] e^{-ikx_0} dx_0.$$

A_s is the "source" area $2bL$ and A is the duct area ab . The characteristic velocity amplitude u_0 is $\omega\eta_0$ and η/η_0 is the shape of the displacement function at the boundary in the source region. Quantity η_0 is used for normalization and will be taken to be the maximum displacement amplitude in the source region.

After some algebraic manipulation, we obtain the following expressions for the amplitudes p_{mn}^+ and p_{mn}^- of the (m, n) mode transmitted in the downstream and upstream directions, respectively:

$$p_{mn}^{\pm} = \frac{A_s}{A} \frac{1}{2} \rho c u_0 \frac{1}{\alpha_{mn}} \left[\frac{1 \pm M(1 - \beta_{mn}^{\pm})}{1 \pm M} \right]^2 H_{mn}(k_{mn}^{\pm}, \omega) e^{ik_{mn}^{\pm} x}, \quad (8)$$

where

$$k_{mn}^+ = \frac{\beta_{mn}^+ \omega}{1 + M} c, \quad k_{mn}^- = -\frac{\beta_{mn}^- \omega}{1 - M} c,$$

$$\beta_{mn}^{\pm} = \frac{\alpha_{mn} \mp M}{1 \mp M}, \quad \alpha_{mn} = [1 - (\omega_{mn}/\omega)^2]^{1/2},$$

$$(\omega_{mn}/c)^2 = (1 - M^2) \left\{ (n\pi/a)^2 + (m\pi/b)^2 \right\}.$$

The ratio between the upstream and downstream amplitudes is

$$F_1(M, \omega) = \left| \frac{p_{mn}^-}{p_{mn}^+} \right| = \left(\frac{1 + M}{1 - M} \right)^2 \left| \frac{1 - M(1 - \beta_{mn}^-)}{1 + M(1 - \beta_{mn}^+)} \right|^2 \frac{H_{mn}(k_{mn}^-, \omega)}{H_{mn}(k_{mn}^+, \omega)}. \quad (9)$$

Above the cutoff frequency, as ω goes from ω_{mn} to infinity, the quantity β_{mn}^- goes from $M/(1 + M)$ to 1 and β_{mn}^+ goes from $-M/(1 - M)$ to 1. If the frequency dependence of H_{mn} can be neglected, which is true for an acoustically compact source, the corresponding variation of the pressure ratio is from 1 to $(1 + M)^2/(1 - M)^2$.

Below the cutoff frequency, the quantity β_{mn}^{\pm} is complex,

$$\beta_{mn}^{\pm} = \frac{[1 - (\omega_{mn}/\omega)^2 - 1]^{1/2} \mp M}{1 \mp M}, \quad (10)$$

and as ω goes from zero to ω_{mn} , the ratio of the magnitudes of the pressure amplitudes p_{mn}^- and p_{mn}^+ remains the same, but the relative phase of p_{mn}^- and p_{mn}^+ changes.

It should be emphasized that the expression given in Eq. 9 for the pressure ratio corresponds to the assumption of streamlined flow, that is, when the fluid velocity and lateral displacement of the boundary in the source region are related as shown in Eq. 6. We have proposed² that this relation be modified to $u_n = \partial \eta_n / \partial t$ for a "turbulent" boundary layer. The corresponding modification of the expression for the pressure ratio involves replacing the function $F_1(M, \omega)$ in Eq. 9 by

$$F_2(M, \omega) = \left(\frac{1 + M}{1 - M} \right) \frac{1 - M(1 - \beta_{mn}^-)}{1 + M(1 - \beta_{mn}^+)} \frac{H_{mn}(k_{mn}^-, \omega)}{H_{mn}(k_{mn}^+, \omega)}. \quad (11)$$

In the case of a pistonlike source with a uniform displacement amplitude η_0 of the boundary in the source region, the quantity H_{mn} that enters into F_1 and F_2 becomes

$$H_{mn}(k_{mn}^{\pm}, \omega) = \sin(k_{mn}^{\pm} L) / k_{mn}^{\pm} L, \quad (12)$$

which for an acoustically compact source is close to unity.

II. EXPERIMENT

The experimental arrangement is shown schematically in Fig. 1(b). The duct has a rectangular cross section with the inner dimensions 3/4 in. \times 1 3/4 in. A sound source, a horn-type driver, is mounted in each of two opposite duct walls. The two sources are driven by harmonic pulse trains, 180° out of phase, and with the magnitude of the acoustic signals from the speakers adjusted to be the same, the (monopole) source strength of the source configuration will be zero, and no plane-wave component will be generated in the duct.

The cutoff frequency of the (1,0) mode is 3860 Hz. The next cutoff frequency is 7720 Hz, corresponding to the (2,0) mode. In our experiments the frequency was chosen to lie between these limits, so that only the (1,0) mode propagated through the duct. All other higher modes decayed exponentially with distance away from the source. To avoid propagational effects in our experiments such as attenuation of sound due to turbulence within the duct,³ the microphones were placed quite close to the source, in our case about 8.5 "diameters" away, but yet sufficiently far away to ensure that the exponentially decaying higher-order modes did not affect the results. To confirm the existence of only the (1,0) mode, the distribution of the sound pressure across the duct was measured and found to be in excellent agreement with the expected $\cos(\pi y/a)$ function. The sound pressure at the center of the duct, that is, at $y=a/2$, where the contribution from the (1,0) mode is zero, was found to be 30 dB lower than the amplitude of the (1,0) mode. The existence of such a "clean" (1,0) mode, even at a distance more than 50 diam from the source, was a clear indication that the wave-distorting propagational effects, such as refraction due to velocity gradients, were of little or no consequence in our experiment.

As indicated in Fig. 1(b), two microphones were used,

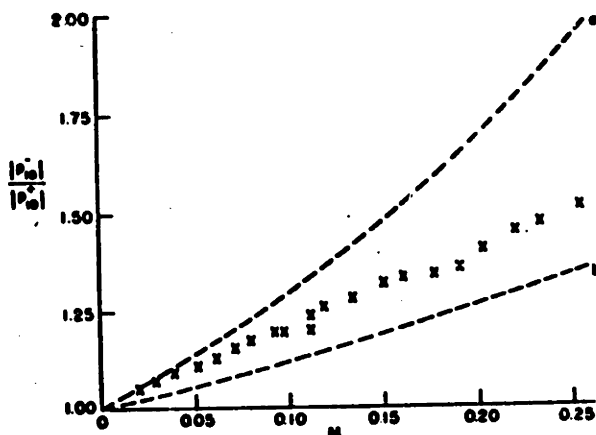


FIG. 2. Mach number dependence of the measured ratio $|p_{10}^-|/|p_{10}^+|$ between the pressure amplitudes radiated in the upstream and downstream directions at a frequency of 5500 Hz. The curve marked a corresponds to streamlined flow over the source boundary [function $F_1(M, \omega)$ in Eq. 9] and curve b is the proposed modification for a "turbulent" boundary layer [function $F_2(M, \omega)$ in Eq. 11].

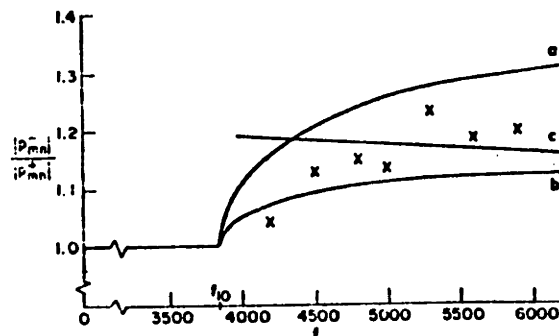


FIG. 3. The variation of $|p_{mn}^-|/|p_{mn}^+|$ with frequency f for a Mach number of 0.1, $m=1$, $n=0$. Curves a and b correspond to curves a and b in Fig. 2. The cutoff frequency for the (1,0) mode is f_{10} . Also shown for comparison is curve c which corresponds to the result for plane waves² generated by a finite size source in a "turbulent" medium.

one on the upstream and one on the downstream side of the sound source. Although the reflection from the end of the duct is much smaller for the (1,0) mode than for the plane wave, we used short pulse trains of the harmonic signal to the source, so that the incident and reflected wave trains in the duct could be separated readily.

As in our previous study of the plane-wave mode, we were interested here mainly in the ratio between upstream and downstream wave amplitudes. Figure 2 shows the measured value of $|p_{10}^-|/|p_{10}^+|$ as a function of the Mach number at a frequency of 5500 Hz. The experimental results fall between the functions $F_1(M, \omega)$ and $F_2(M, \omega)$ given in Eqs. 9 and 11, corresponding to the streamline flow model and the proposed modification for "turbulent" flow. At Mach numbers less than approximately 0.04, corresponding to a Reynolds number of 2.5×10^4 , the data are closer to the F_1 function. This result is, at least qualitatively, consistent with the results obtained for the plane wave, as described in our previous paper.²

The measured frequency dependence of $|p_{10}^-|/|p_{10}^+|$ at a fixed flow Mach number of 0.1 is shown in Fig. 3. Again, we find that the experimental results fall between $F_1(M, \omega)$ and $F_2(M, \omega)$. For comparison, the frequency dependence of the pressure ratio for the plane wave component is also shown. For an acoustically compact source this ratio is independent of frequency, but if we account for the finite source dimension, the frequency dependence is given by $(\text{sinc } L/kL)/(\text{sinc } L/kL)$. Although a similar factor enters in the frequency dependence for the higher mode, the dominant effect arises from the relationship between the wavelength and the duct dimension rather than from the wavelength compared with the source dimension, so that the net effect is an increase rather than a decrease with frequency in the investigated frequency range.

ACKNOWLEDGMENT

This work was supported by the U. S. Navy (Office of Naval Research) under Contract N00014-67-A-0204-0019.

¹A. H. Nayfeh, J. E. Kaiser, and D. P. Telfonis, "The Acoustics of Aircraft-Engine Duct Systems," AIAA paper 73-1153. (This paper contains an extensive set of references to earlier studies in duct acoustics.)

²U. Ingard and V. K. Singhal, "Upstream and Downstream

Sound Radiation into a Moving Fluid," J. Acoust. Soc. Am. 54, 1343-1346 (1973).

³U. Ingard and V. K. Singhal, "Sound Attenuation in Turbulent Pipe Flow," J. Acoust. Soc. Am. 55, 535-538 (1974).

Sound attenuation in turbulent pipe flow*

Uno Ingard and Vijay K. Singhal

Departments of Physics and of Aeronautics and Astronautics and Research Laboratory of Electronics,
Massachusetts Institute of Technology, Cambridge, Massachusetts 02139

Results of steady-state and pulse measurements of upstream and downstream attenuation of sound in turbulent pipe flow are presented and compared with calculated values obtained from a simple model in which the sound is treated as a quasistatic perturbation of the steady flow in the pipe.

Subject Classification: 28.60; 20.45.

INTRODUCTION

Under most conditions the attenuation of sound in a duct is basically the result of viscous and heat-conduction losses at the duct boundary. The corresponding losses in the bulk of the gas are small compared with the boundary losses, at least at sufficiently low frequencies. For a rigid smooth wall these viscothermal boundary losses account for the "classical attenuation" in a pipe, as was determined by Kirchhoff for the fundamental "plane" wave mode.¹ Actually, viscosity, and to a lesser extent heat conduction, are largely responsible for the acoustic losses even when the duct wall is irregular or is covered with an acoustic lining, although in such cases the attenuation is often expressed in terms of empirical material parameters, such as flow resistance, acoustic normal impedance, and the like, which are related only indirectly to the shear viscosity and heat conduction.

In the presence of mean flow, or at large acoustic amplitudes, additional losses can occur as a result of the generation of turbulence either by the large amplitude sound field itself or by the interaction of sound (at any amplitude) with the vorticity in the flow. This "nonlinear" contribution to sound absorption has been studied in several investigations during the past 40 years² and has recently been the subject of considerable attention in connection with the design of duct liners in aircraft.

In the light of these considerations, and in pursuance of our systematic study of sound propagation in ducts with flow, we have examined the propagation of sound in hard-walled pipes carrying turbulent flow.

I. QUASISTATIC APPROXIMATION

In this paper we report the results of measurements of sound attenuation in turbulent pipe flow and an attempt to understand these results in terms of a simple phenomenological theoretical analysis of the problem.³ In this analysis we consider the oscillatory flow in the sound field to represent a quasistatic modulation of the steady flow. This results in a modulation of the pressure drop in the pipe, which can be expressed as an equivalent turbulent friction acting on the oscillatory flow.

This approach does not deal explicitly with the detailed mechanism of the interaction of the sound wave with the turbulent flow, since this interaction is accounted for in

the empirical velocity dependence of the pressure drop per unit length in turbulent pipe flow. In a more detailed analysis we would have to consider not only the mean flow but also the turbulent spectrum, as well as the mean-flow profile in the duct.

If the mean velocity in the duct is V and the density is ρ , the steady-state pressure drop per unit length of the duct can be written as $(\psi/a)(\rho V^2/2)$, where a is the ratio between the area of the duct cross section and its perimeter ($a=d/4$ for a circular cross section of diameter d), and ψ is an empirically determined friction factor that depends on the Reynolds number R . The Reynolds number dependence of ψ has been studied experimentally by numerous investigators for pipes with varying degrees of wall roughness, and the results are summarized in most texts on fluid flow.⁴

In the presence of a fundamental acoustic mode in the pipe, the velocity and pressure fields will be perturbed. Accordingly, we express the velocity and the pressure as $V_0 + u(t)$ and $P_0 + p(t)$, where u is the oscillatory acoustic flow velocity and p the sound pressure. The quantities V_0 and P_0 are the unperturbed values of velocity and pressure. The time dependence of these quantities is neglected in the present analysis.

The corresponding perturbation of the turbulent friction in the pipe gives rise to an oscillating friction drag that affects the acoustic field with a contribution to the pressure gradient equal to

$$-\frac{\psi}{a} \rho_0 V_0 u - \frac{\rho_0 V_0^2}{2a} \frac{\partial \psi}{\partial V_0} u = -\frac{\psi}{a} \rho_0 V_0 u \left(1 + \frac{V_0}{2} \frac{\partial \ln \psi}{\partial V_0} \right).$$

The linearized momentum equation for the sound field is then

$$\rho_0 \left(\frac{\partial}{\partial t} + V_0 \frac{\partial}{\partial x} \right) u + \frac{\psi}{a} \rho_0 V_0 u \left(1 + \frac{V_0}{2} \frac{\partial \ln \psi}{\partial V_0} \right) + 2\zeta \rho_0 c u = -\frac{\partial p}{\partial x}, \quad (1)$$

in which we have expressed separately the viscothermal drag as an additional term $2\zeta \rho_0 c u$.

The continuity equation for the sound field is

$$\left(\frac{\partial}{\partial t} + V_0 \frac{\partial}{\partial x} \right) \rho + \rho_0 c^2 \frac{\partial u}{\partial x} = 0, \quad (2)$$

where we have introduced ρ/c^2 for the perturbation in density. For a wavelike perturbation, $\exp(ikx - i\omega t)$, Eqs. 1 and 2 reduce to

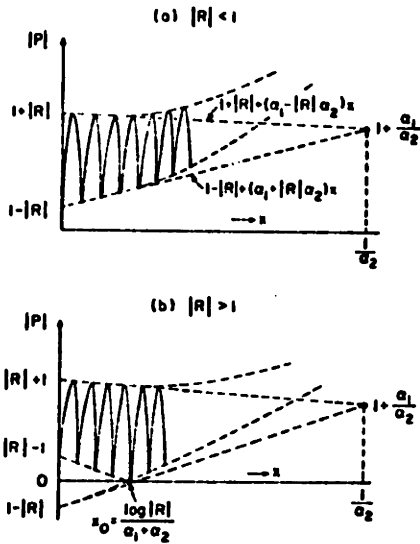


FIG. 1. Standing-wave patterns in a duct with flow. An acoustic wave $\exp(\alpha_1 x - ik_1 x - i\omega t)$ traveling in the negative x direction reflects from the end $x=0$ as $R \exp(-\alpha_2 x + ik_2 x - i\omega t)$, where $R = |R| \exp(i\phi)$. (a) With reflection coefficient $|R| < 1$; (b) With $|R| > 1$. The figures show the envelope of the pressure maxima and minima. From the tangents to these envelopes at the end of the duct, $x=0$, one can easily find from the information given on the figure the reflection coefficient $|R|$ and the attenuation coefficients α_1 and α_2 .

$$\left[-i \frac{\omega}{c} + ikM_0 + \frac{\psi}{a} M_0 + \left(\frac{\psi M_0 V_0}{2a} \right) \left(\frac{\partial \ln \psi}{\partial V_0} \right) + 2\beta_v \right] i + \frac{1}{\rho_0 c} ikp = 0$$

and

$$i\rho_0 cku + [-i(\omega/c) + ikM_0]p = 0, \tag{3}$$

where $M_0 = V_0/c$ is the Mach number of the flow in the pipe.

The corresponding dispersion relation $k(\omega)$ for the acoustic wave is then

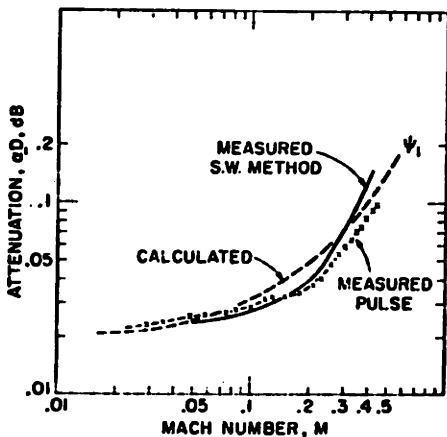


FIG. 2. Attenuation of a plane sound wave traveling against the direction of mean flow as a function of Mach number. The calculated curve ψ_1 is from theory with the published data⁴ on the friction factor ψ . Diameter $D = 4a$.

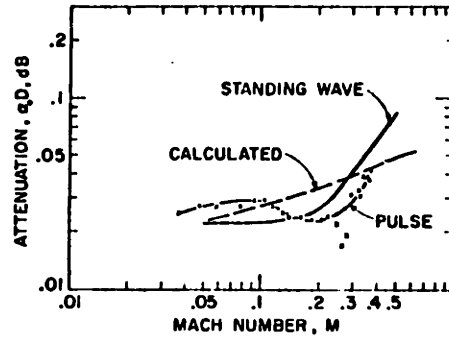


FIG. 3. Comparison of downstream attenuation measurements by the standing-wave and pulse techniques with the theoretical predictions.

$$\left[\frac{\omega}{c} - kM_0 + i \frac{\psi}{a} M_0 + \frac{i\psi M_0 V_0}{2a} \frac{\partial \ln \psi}{\partial V_0} + 2\beta_v i - \frac{1}{\rho_0 c} k \right] = 0. \tag{4}$$

Note that $V_0 \partial \ln \psi / \partial V_0$ is equal to $R \partial(\ln \psi) / \partial R$, where R is the Reynolds number, and that $\psi \partial(\ln \psi) / \partial V_0 = \partial \psi / \partial V_0$ is of first order in ψ . Then, neglecting the second-order product terms in ψ , $\partial \psi / \partial V_0$, and β_v , and with $(1+i\epsilon)^{1/2} \approx 1+i\epsilon/2$ ($\epsilon \ll 1$), we get the following expressions for the propagation constants k_+ and k_- for the acoustic waves traveling in the downstream and upstream directions of the turbulent flow

$$k_+ \approx \frac{\omega/c}{1+M_0} + i \left[\beta_v + \frac{\psi M_0}{2a} \left(1 + \frac{R}{2} \frac{\partial \ln \psi}{\partial R} \right) \right] \frac{1}{1+M_0}, \tag{5}$$

$$k_- \approx -\frac{\omega/c}{1-M_0} - i \left[\beta_v + \frac{\psi M_0}{2a} \left(1 + \frac{R}{2} \frac{\partial \ln \psi}{\partial R} \right) \right] \frac{1}{1-M_0}. \tag{6}$$

At zero flow and in the low-velocity laminar flow regime, the attenuation is caused solely by viscosity and heat conduction. As the Reynolds number increases, the flow becomes turbulent and the term $\psi M_0 / [2a(1 \pm M_0)]$ becomes the major contribution to the attenuation. It is larger in the upstream than in the downstream direction, the difference expressed by the factors $(1+M_0)^{-1}$ and $(1-M_0)^{-1}$. For example, at a Mach number of 0.5, neglecting viscothermal effects, we have $k_- = 3.0 k_+$. The term $(\psi M_0 / 4a) R \partial(\ln \psi) / \partial R$ is negative at low Reynolds numbers, but since it is only about 10% of the previous term, it is not very significant in most cases. It can be shown, however, that because of the rapid decrease of ψ with R at low Reynolds numbers the attenuation for downstream propagation actually can decrease with increasing velocity at very low flow speeds.

At high Reynolds numbers ψ becomes independent of R , and then only $\psi M_0 / [2a(1 \pm M_0)]$ contributes to the attenuation. By retaining only this term, the sound attenuation in a distance x of turbulent pipe flow can be expressed as

$$\text{Attenuation in decibels} \approx 8.7 \frac{\psi M_0}{2(1 \pm M_0)} \left(\frac{x}{a} \right). \tag{7}$$

For a square cross section, $d \times d$, we have $a = d/4$ and

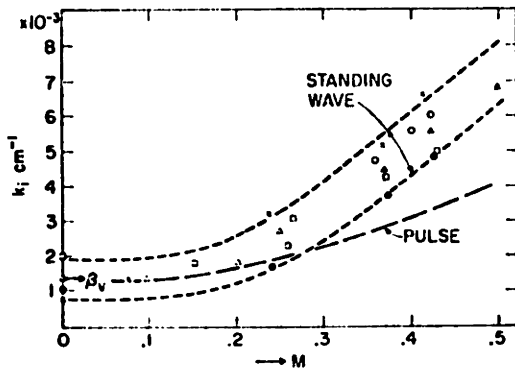


FIG. 4. Sound attenuation in turbulent pipe flow by standing-wave measurements at 1100 Hz with $p \sim p_0 \exp[-k_i x / (1 \pm M)]$, 3/4 in. by 7/8 in. rectangular cross section. Different points on the curve indicate the variability in the standing-wave procedure.

with a typical value $\psi \approx 10^{-2}$, we get

$$\text{Attenuation due to turbulence} \approx 0.17 \frac{M_0}{1 \pm M_0} \left(\frac{x}{d} \right) \text{ dB.} \quad (8)$$

As an example, for a travel distance $x = 100 d$ and $M_0 \approx 0.3$, the upstream attenuation is 7.5 dB and the downstream attenuation is 4 dB.

It is interesting to compare the viscothermal sound attenuation with that caused by turbulence alone. The viscothermal attenuation can be expressed⁵ as

$$\beta_v = \frac{1}{4a} \frac{\omega}{c} [d_v + (\gamma - 1)d_K],$$

where $d_v = [2\mu/(\rho_0\omega)]^{1/2}$ is the viscous acoustic boundary layer thickness, $d_K = [2K/(\rho_0\omega C_p)]^{1/2}$ is the thermal acoustic boundary layer thickness, $\gamma = C_p/C_v$ is the ratio of specific heats, μ the coefficient of shear viscosity, K the heat conduction coefficient, C_p the specific heat at

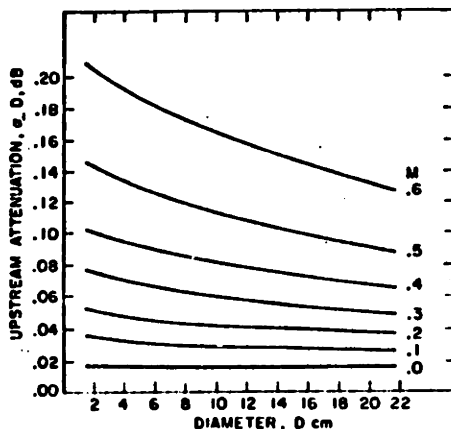


FIG. 5. Theoretically calculated upstream attenuation coefficients for "smooth" pipes as a function of the "diameter" of the pipe.

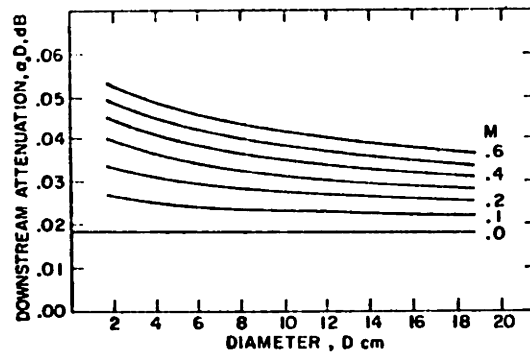


FIG. 6. Predicted downstream attenuation coefficients for "smooth" pipes.

constant pressure, and $f = \omega/2\pi$ the acoustic frequency.

The viscothermal attenuation is proportional to the square root of acoustic frequency, whereas the contribution caused by turbulence is (by the quasistatic approximation) independent of frequency. For air at standard conditions, $\beta_v \approx 1.43 \times 10^{-5} f^{1/2}/a$. This should be compared with the turbulent attenuation $\beta_t = 0.5\psi M_0/a$. With a typical value 10^{-2} for ψ , it follows that at $f = 100$ Hz we get $\beta_v = \beta_t$ when $M_0 \approx 0.03$ and at $f = 1000$ Hz, $\beta_v = \beta_t$, when $M_0 \approx 0.1$. In general, we see that β_t exceeds β_v if

$$M_0 > 2.86 \times 10^{-3} f^{1/2} \quad (9)$$

II. MEASUREMENTS

In experimental studies of the sound attenuation in turbulent pipe flow, we used a sound source mounted in one of the side walls, approximately midway between the open ends of a rectangular pipe with inner dimensions 3/4 in. by 3/4 in. or 3/4 in. by 7/8 in. One end of the duct was connected to a pump via a plenum chamber and the other end was open and unflanged. The flow velocity in the duct could be varied between 0 and 170 m/sec.

Two sets of experiments were undertaken, one with pulse excitation and the other with steady-state excitation of the sound source. In the pulse measurements, the sound source was driven by means of a pulse generator which produced harmonic sound pressure wave trains in the duct. The carrier frequency of these waves was chosen to be considerably lower than the cutoff frequency of the first higher-order mode in the duct, so that at the carrier frequency only the plane wave mode was able to propagate.

By mounting a pair of pressure transducers on either side of the sound source, the decay of upstream and downstream pulses in the known distance between the microphones in each pair was determined for a number of different flow velocities.

In the steady-state measurements the standing-wave field in the tube was recorded by means of a microphone probe, which was moved along the axis of the tube. The attenuation was then determined from the slope at the origin of the curve connecting the pressure minima in

the standing-wave pattern. Actually, a modification of the conventional procedure had to be made to accommodate the occurrence of a pressure reflection coefficient greater than unity at the downstream end of the pipe. This modification is summarized in Fig. 1.

III. DISCUSSION

Figures 2, 3, and 4 show that the attenuation is almost independent of the Mach number at low Mach numbers. For Mach numbers beyond 0.25, corresponding to Reynolds numbers (based on the pipe "diameter") larger than 1.1×10^5 , the flow dependence of the attenuation is quite pronounced in the upstream direction, less pronounced in the downstream direction.

The accuracy of measurements of this type is not particularly great, as can be seen from the spread in experimental data points shown in Fig. 4. Apart from the errors in purely acoustic measurements, there are several factors that influence the accuracy of these measurements. For example, there is a static pressure variation along the length of the pipe and a corresponding variation of the density and the flow velocity. This effect has been ignored in the analysis presented here, but a more detailed theoretical study revealed that these effects lead to additional terms, of second or higher order in M_0 , which in our case were always less than 10% of the leading terms considered here. At higher Mach numbers than those involved in our experiment ($M_0 < 0.45$), these correction terms must be accounted for.

Within the range of the accuracy of the measurements, the experimental and calculated attenuations are in fair agreement, particularly in the upstream direction. There appears to be a consistent pulse-measured attenuation somewhat lower than the steady-state measurements. Ahrens and Ronneberger⁶ found a strong frequency dependence, but our data show no such behavior in the range of frequencies investigated. At the partic-

ular frequency of our experiment, however, their data are in good agreement with ours.

On the basis of the analysis presented here, we have constructed the curves shown in Figs. 5 and 6, to be used as an aid in estimating the sound attenuation in turbulent pipe flow under some different conditions. In the preparation of these curves we used the empirical Reynolds number dependence of the friction coefficient ψ , as can be found in most texts on fluid dynamics.⁴

ACKNOWLEDGMENTS

This work was supported by the U. S. Navy (Office of Naval Research) under Contract N00014-67-A-0204-0019. Help from Mr. Jeffrey A. Tarvin, Department of Physics, MIT, in the initial stages of the experiments is gratefully acknowledged.

^{*}Presented at the Interagency Symposium on University Research in Transportation Noise, Stanford University, Stanford, California, 28-30 March 1973, and at the 85th Meeting of the Acoustical Society of America, Boston, Massachusetts, 10-13 April 1973.

¹G. Kirchhoff, *Pogg. Ann.*, Bd. 134 (1868).

²L. J. Sivian, *J. Acoust. Soc. Am.* 7, 94-101 (1935); P. J. Westervelt and P. W. Sieck, *J. Acoust. Soc. Am.* 22, 680(A) (1950). U. Ingard and H. Ising, *J. Acoust. Soc. Am.* 42, 6-17 (1967).

³At the Interagency Symposium at Stanford in March 1973, it was brought to our attention that an analysis similar to the one presented here had been carried out by T. E. Siddon and was to be reported at CANCAM '73, Montreal, Canada, 28 May-1 June 1973.

⁴For example, J. W. Dally and D. R. F. Harleman, *Fluid Dynamics* (Addison-Wesley, Reading, Mass., 1966), pp. 274-275.

⁵P. M. Morse and K. U. Ingard, *Theoretical Acoustics* (McGraw-Hill, New York, 1968), p. 519.

⁶C. Ahrens and D. Ronneberger, *Acustica* 25, 150-157 (1971).

Effect of flow on the acoustic resonances of an open-ended duct*

Uno Ingard

Departments of Physics and of Aeronautics and Astronautics and Research Laboratory of Electronics, Massachusetts Institute of Technology, Cambridge, Massachusetts 02139

Vijay K. Singhal

Department of Aeronautics and Astronautics and Research Laboratory of Electronics, Massachusetts Institute of Technology, Cambridge, Massachusetts 02139
(Received 6 June 1975)

The effect of flow on the acoustic resonances of an open-ended, hard-walled duct is analyzed. The flow produces acoustic losses both in the interior of the duct and at the ends. Unless the duct is very long, typically 100 times the diameter, the losses at the ends dominate. At flow Mach numbers in excess of 0.4 the losses are so large that axial duct resonances are almost completely suppressed. The plane-wave Green's function for the duct with flow is expressed in terms of the (experimentally determined) pressure reflection coefficients at the ends of the duct, and the flow dependence of the complex eigenfrequencies of the duct is obtained. Some observations concerning the noise produced by the flow in the duct are also reported.

Subject Classification: 28.60; 20.45.

INTRODUCTION

Some of the basic aspects of the acoustics of an open-ended duct without mean flow are discussed in general texts on sound.^{1,2} More technical details can be found in specialized treatises dealing, for example, with the acoustics of musical instruments³ and the vocal tract.⁴

In the most elementary treatment of the plane-wave eigenmodes of a straight uniform duct of length L with both ends open, it is assumed that the ends are pressure nodes, so that the wavelengths of the eigenmodes are $2L/n$, where n is an integer. The corresponding pressure reflection coefficient R at an open end of the duct is then $R = -1$. On this assumption no acoustic energy is radiated from the duct into the surrounding free space.

If the radiation is accounted for, the modes will be damped and the wavelengths of the eigenmodes are found to be somewhat longer than $2L/n$. The problem of reflection from the open end of the duct without mean flow but including the effect of radiation has been the subject of many studies of various degrees of sophistication.⁵⁻⁷

Viscothermal effects in the acoustical boundary layer, as well as in the bulk, also contribute to the damping,^{8,9} and at large amplitudes vorticity at the ends of the duct results in additional damping and a slight reduction of the wavelengths of the eigenmodes.

In many applications, the duct carries a mean flow and the acoustical characteristics of the duct are then altered; the damping of an eigenmode will be increased and its frequency decreased. One can identify several mechanisms that contribute to these effects, such as the convection of the sound by the mean flow, the interaction of sound with the turbulent flow within the duct, and the effect of flow on the reflection coefficients at the ends of the duct. The effect of turbulent flow on the attenuation of sound¹⁰⁻¹² and on the reflection of sound from an open end of a duct^{13,14} have been studied previously.

The main purpose of this paper is to investigate the effect of flow on the eigenmodes of a duct open at both ends, to account for these effects, and to investigate their relative significance. In addition, we wish to comment on the related problem of the noise produced by the flow in the duct.

I. A SIMPLE DEMONSTRATION

A simple experiment demonstrating the effect of flow on the acoustical response of an open-ended duct to an external sound field is shown in Fig. 1. Here the duct is attached to a suction plenum chamber so that flow can be drawn through the duct with speeds up to approximately half the speed of sound. The duct is excited by an external random noise field, and the response is determined by a microphone flush mounted in the wall of the duct at its center.

The upper trace in Fig. 1 shows the frequency spectrum of the microphone signal when there is no mean flow through the duct. The peaks in the spectrum signify the resonances of the duct. The absolute values of the peaks, or even their relative values, are of no particular interest in this context, since they include the response of the sound source. What is important in this demonstration is the influence of flow on the resonance peaks, and spectra were obtained for a wide range of flow speeds. Typical examples are shown in the middle and the lower traces in Fig. 1. The flow is seen to reduce the resonant peaks and to increase the width of the resonances, and at a flow Mach number of approximately 0.4 the resonances are practically eliminated. This experiment was carried out in a duct with a square cross section $\frac{1}{4}$ in. by $\frac{1}{4}$ in., but the results presented are applicable to ducts in general, as the discussion in the following sections indicates. In the experiments, the external sound field was always chosen large enough to exceed the flow noise (see Sec. V).

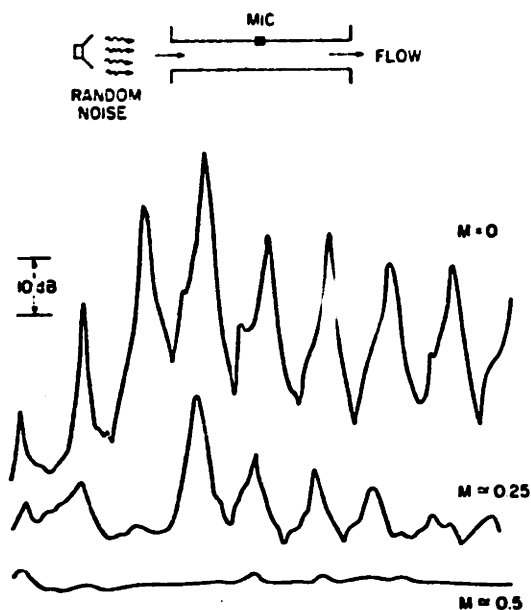


FIG. 1. Effect of flow on the frequency response of the axial modes of an open-ended duct to an external random noise field. Frequency scale 0-2000 Hz, linear. The flow produces acoustic losses and a downshift of the resonance frequencies. At Mach numbers above 0.4, the acoustic resonances are almost completely suppressed by the flow.

II. "INTERNAL" FLOW EFFECTS

In addition to the effect of convection of sound by the mean flow, which changes the phase velocity of the plane sound waves in the duct in the upstream and downstream directions by the factors $(1 - M)$ and $(1 + M)$, respectively (M =Mach number), there is also an effect of the turbulent flow on the sound attenuation in the duct. In a previous study,¹¹ we measured the attenuation of sound in turbulent duct flow with both steady-state and pulsed sound fields and attempted to explain the results obtained in terms of a quasistatic analysis of the problem. Although such an analysis, at best, can be expected to be meaningful only at low frequencies, the results obtained were found to be in relatively good agreement with the experiments. The corresponding propagation constants k_+ and k_- for upstream and downstream traveling plane waves $\exp(-ik_+x)$ and $\exp(ik_-x)$ are

$$\begin{aligned} k_+ &= \frac{\omega}{c} \frac{1}{1+M} + i \frac{A}{1+M}, \\ k_- &= \frac{\omega}{c} \frac{1}{1-M} + i \frac{A}{1-M}, \\ A &= \beta_0 + \frac{\phi M}{2d} \left(1 + \frac{R}{2} \frac{\partial \ln \phi}{\partial R} \right), \end{aligned} \quad (1)$$

where ϕ is the turbulent flow friction factor (defined by $\Delta p = (\rho V^2/2) \phi L/d$ = static pressure drop in a length L , V = mean flow velocity), M the mean flow Mach number in the duct, d the ratio between the cross-sectional area of the duct and its perimeter, and R the Reynolds number. The subscript plus refers to downstream and the subscript minus to upstream propagation.

III. END LOSSES

In addition to the acoustic losses in the turbulent flow within the duct, there are similar aeroacoustic interactions and losses in the entrance and the exit flows. The effect of these interactions can be determined from measurements of the acoustic pressure reflection coefficients at the ends of the duct. Such measurements have been carried out with the standing-wave method by Mechel *et al.*¹³ and by Ronneberger¹⁴ for Mach numbers up to 0.35 and over a comparatively wide range of frequencies. We have supplemented these measurements using both pulse and standing-wave techniques, arranged in such a way that the upstream and downstream reflection coefficients could be obtained simultaneously.

In the pulse measurements, harmonic wave trains were emitted from a sound source mounted in the side wall of the duct and the incident and reflected pulses were measured by means of microphones arranged as shown in Fig. 2. The use of two microphones made it possible to make appropriate corrections for the attenuation of the pulses within the duct.

In the steady-state experiments the sound source was mounted at the center of the duct and the sound-pressure amplitude distribution in the duct was measured by means of a probe microphone which could be moved along the duct. Examples of the measured pressure distribution in the duct, without flow and with flow, are shown in Figs. 3 and 4. It is interesting to note that in the presence of flow the sound field becomes asymmetrical with respect to the sound source location, with a higher sound-pressure amplitude on the upstream side of the source than on the downstream side. This is consistent with a previous study of acoustic pulses emitted in the upstream and downstream directions.¹⁵

From the sound-pressure distribution the reflection coefficients are determined as described in Refs. 11 and 13. The measured magnitudes of the reflection coefficients R_1 and R_2 at the downstream and upstream ends, respectively, are shown in Figs. 5 and 6. In the absence of flow, the magnitude of the reflection coefficient is approximately unity at sufficiently low frequencies, say, for $ka < 0.5$ ($k = \omega/c$, c = sound speed, a = duct radius). Our measurements were restricted to this frequency range and to flow Mach numbers up to 0.5. As can be seen from Fig. 5, the magnitude of the pressure reflection coefficient at the downstream end is approximately unity, or actually somewhat larger than unity in the velocity range considered. At the upstream end, on the other hand, the magnitude of R_2 is less than unity and decreases monotonically with the flow velocity.

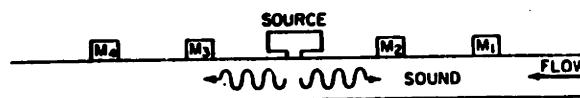


FIG. 2. Arrangement for pulse measurement of the pressure reflection coefficients at the ends of the duct. Two microphones are used as detectors of incident and reflected pulses on both sides of the sound source to make it possible easily to correct for the sound attenuation due to turbulent flow in the duct.

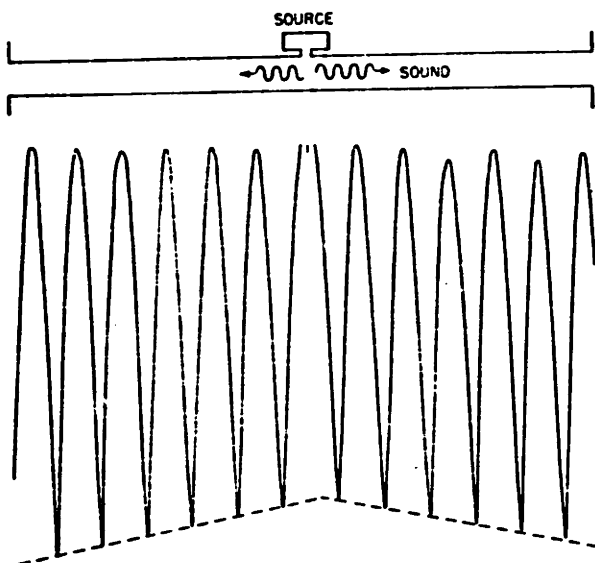


FIG. 3. Sound-pressure amplitude distribution in an open-ended duct without flow. The sound is generated by a source at the center of the duct. Frequency 1400 Hz. Duct cross section $\frac{3}{4}$ in. \times $\frac{3}{4}$ in.

These results are consistent with those reported by Mechel *et al.*¹³ and Ronneberger.¹⁴

In contrast to the no-flow case, a pressure reflection coefficient of unity in the presence of flow does not mean that the acoustic end loss is zero. Rather, if we use the expressions $I_+ = (1 + M)^2 (p_+^2 / \rho c)$ and $I_- = (1 - M)^2 (p_-^2 / \rho c)$ for the acoustic intensities in the downstream and upstream directions, the observed value of unity (approximately) of the magnitude of the pressure reflection coefficient R_1 at the downstream end corresponds to an acoustic absorption coefficient $\alpha_1 = 1 - (I_- / I_+)$ (due to sound-jet flow interaction) given by

$$\alpha_1 \approx \frac{4M}{(1+M)^2}. \quad (2)$$

In the absence of flow, the absorption coefficient at the end of the duct is due solely to sound radiation and can be expressed as

$$\alpha = 1 - |R|^2 = \frac{4\theta}{(\theta+1)^2 + \chi^2} \approx \frac{4\theta}{(1+\theta)^2}, \quad (3)$$

where $(\theta - i\chi) = (1 + R)/(1 - R)$ is the specific acoustic radiation impedance of the open end (normalized to ρc).

By comparison with Eq. 2 we note that the flow-induced losses at the exit end of the pipe are equivalent to a normalized specific acoustic termination resistance $\theta \approx M$.

In the long-wavelength limit $ka \ll 1$, the radiation resistance⁶ of an unflanged circular duct is $\theta \approx (ka)^2/2$, and it follows that in this case, for even a modest flow in the duct, $M > (ka)^2/2$, the flow-induced end losses are far greater than the radiation losses.

At the entrance of the duct the Mach number dependence of the experimentally determined pressure reflection

coefficient (Fig. 6) can be expressed approximately as

$$R_2(M) = R_2(0) \left(\frac{1-M}{1+M} \right)^\pi, \quad (M < 0.5), \quad (4)$$

where $\pi \approx 1.33$ for values of M less than 0.5. The corresponding absorption coefficient is then

$$\alpha_2 = 1 - R_2^2(0) \left(\frac{1-M}{1+M} \right)^{2\pi-2}, \quad (5)$$

which for small values of M reduces to

$$\alpha_2 \approx 1.33 M, \quad (M \ll 1). \quad (6)$$

By comparison with Eq. 2, which for $M \ll 1$ reduces to $\alpha_1 \approx 4M$, we note that the sound absorption at the exit is about three times larger than at the inlet.

The flow-induced sound absorption at the exit end is undoubtedly related to the interaction of acoustic waves with the jet discharge from the duct. At the inlet the flow losses generally are smaller, and the same also applies to the acoustic losses. At a Mach number of 0.4 we see from Eq. 2 that the absorption coefficient at the exit is about 0.82, and it is not surprising, then, that the acoustic resonances of the pipe will be practically "washed" out by the flow at higher flow speeds.

In the absence of flow and in a frequency range given by $ka < 0.5$ the phase of the reflection coefficient can be expressed approximately as $\phi = \pi + 2k\delta$, where δ is the "end correction" of the duct. The theoretical value of the end correction for an unflanged circular duct⁶ is $\delta \approx 0.61a$. In the presence of flow, we define the end correction δ by

$$\phi = \pi + \frac{2k\delta}{1-M^2}. \quad (7)$$

The measured values of ϕ at the downstream end were found to be almost independent of the flow velocity and the corresponding value of δ was found to be $\delta \approx 0.6a(1 - M^2)$. An analysis of the data of Mechel *et al.*¹³ also yielded results consistent with Eq. 7, though with a somewhat larger value of the end correction, $\delta \approx 0.66a \times (1 - M^2)$. For the purpose of the present paper such a difference in the end correction is not significant.

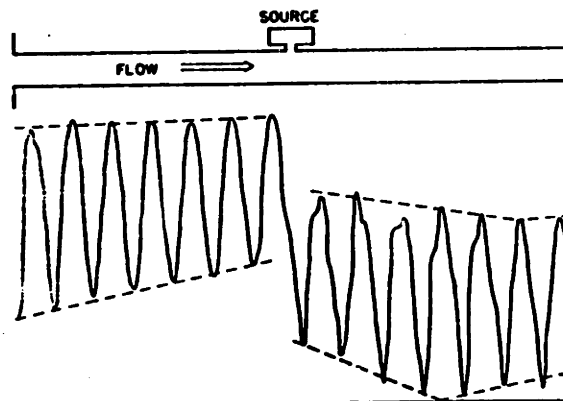


FIG. 4. Sound-pressure amplitude distribution in the open-ended duct (see Fig. 3) when the flow Mach number is 0.2.

May 15, 1991

by

John R. Hauser

May 15, 1991

John Hauser

Professor of Marketing Science

Thesis Advisor

by

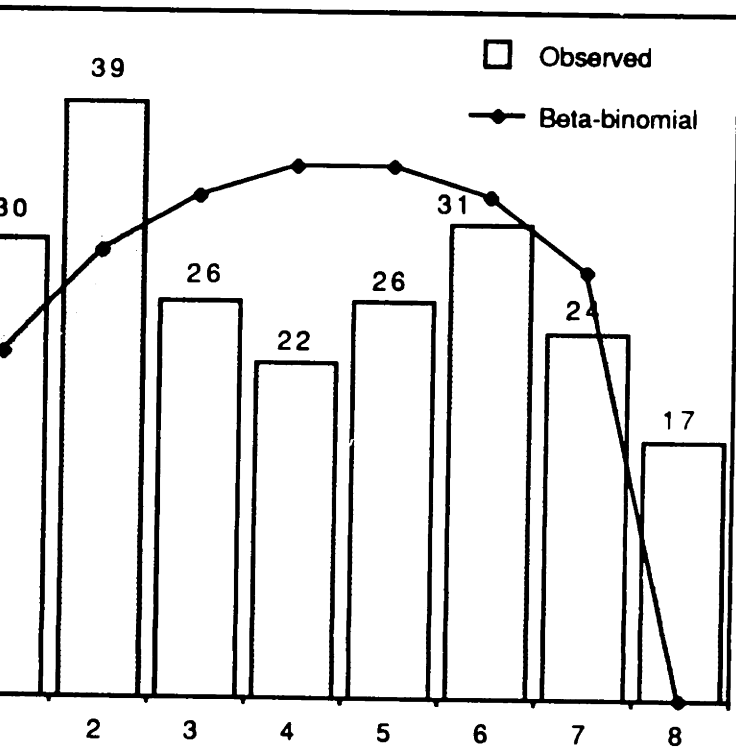
J. A. Barks

Jeffrey A Barks

Associate Dean, Master's and Bachelor's Programs



DATA FROM FOCUS GROUP INTERVIEWS
(BETA-BINOMIAL VERSUS SURVEY DATA)



Number of customers revealing need

alpha = 1.45, beta = 1.34

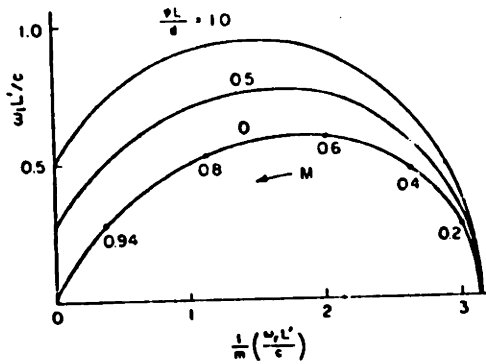


FIG. 7. Mach number dependence of the (complex) eigenfrequency of the m th axial acoustic mode of an open-ended duct of effective length L' . (ν is the friction factor, d the "hydraulic diameter," L the length of the pipe, and M the Mach number. See Eqs. 1 and 14.) The experimental basis for this result refers to the Mach number range 0–0.5. Therefore, at higher Mach numbers the curve in this figure may be regarded as an extrapolation.

In Fig. 7 we have illustrated in the complex ω plane the Mach number dependence of the eigenfrequencies $\omega_m = \omega_r - i\omega_i$. The bandwidth of the response curve is determined by (ω_i/ω_r) , which increases monotonically with M as shown in Fig. 8.

V. FLOW NOISE

In our response experiments it was important, of course, to make certain that the effect of the flow noise was insignificant compared with the source signal. Although the main purpose of this paper is a study of the influence of flow on the eigenfrequencies and acoustic response of an open duct to a sound source, we shall in-

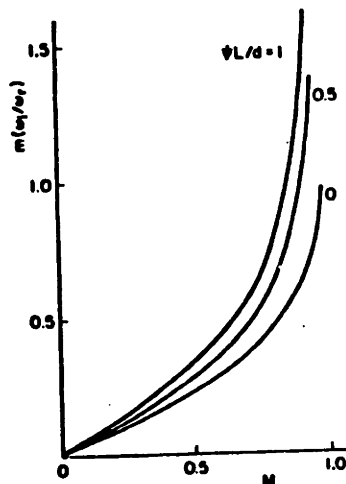


FIG. 8. Mach number dependence of the ratio between the imaginary and real parts of the complex frequency of the m th axial eigenmode of an open-ended duct. Only flow-induced acoustic losses are accounted for. The experimental basis for this result refers to the Mach number range 0–0.5. Therefore, at higher Mach numbers the curve in this figure may be regarded as an extrapolation.

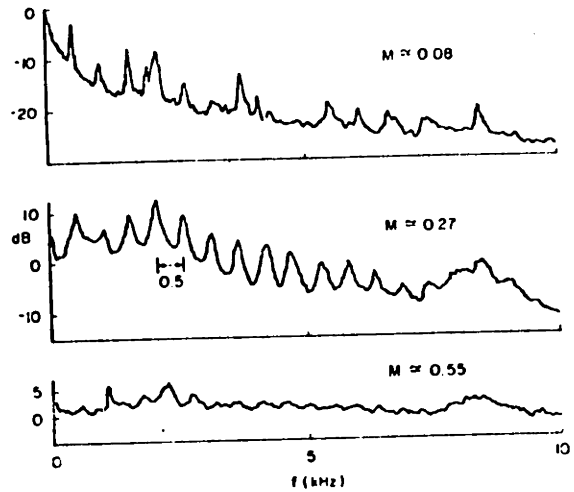


FIG. 9. Noise spectra produced by flow through a sharp-edged, smooth circular duct 12 in. long, with an inner diameter of $\frac{3}{4}$ in. and a wall thickness of $\frac{1}{16}$ in. The entrance end is unflanged, the exit end flanged. Frequency scale 0–10 kHz, linear. Upper trace $M \approx 0.08$; middle trace $M \approx 0.27$; lower trace $M \approx 0.55$. The middle trace indicates pronounced excitation of the axial modes of the duct.

clude here some observations about the noise produced by the flow.

Results of measurements of flow noise in ducts have been reported¹⁵ which suggest that the total acoustic power increases as V^n with values of n between 5 and 6. It has also been pointed out¹⁷ that in a finite frequency band (octave band), the exponent n in the velocity dependence of the acoustic power can vary considerably (typically between $n \approx 5$ and $n \approx 8$) from one octave band to another. It should be noted that unless special precautions are taken, it is difficult to differentiate between the flow noise within the duct and the noise generated in the immediate vicinity of the entrance and the exit of the duct. In many experiments these latter contributions are dominant, with the high-frequency noise originating mainly at the inlet and the low-frequency noise at the exit.

In experiments of this kind we observed that at sufficiently low flow speeds, corresponding approximately to the Mach number range $0.1 < M < 0.3$, the axial modes of the open-ended duct were excited by the flow, and that in this range the power emitted from the duct, in both the upstream and downstream directions, was proportional to V^n with $n \approx 4$.

Examples of observed noise spectra produced by the flow in a circular duct 12 in. long, with an inner diameter of $\frac{3}{4}$ in., are shown in Fig. 9. The microphone was located on the axis in front of the duct inlet. The axial modes are clearly noticeable in the spectrum for $M \approx 0.27$. At higher flow speeds such an excitation does not occur, which is consistent with our analysis of the flow dependence of the acoustic resonances of the duct. In this flow regime the velocity dependence of the acous-

tic power emitted from the duct in the downstream direction approaches that of a subsonic jet (eighth-power law) as the flow speed is increased, whereas in the upstream direction the velocity dependence was found to be markedly weaker, indicating that the bulk of the noise was not caused by the interior flow of the duct.

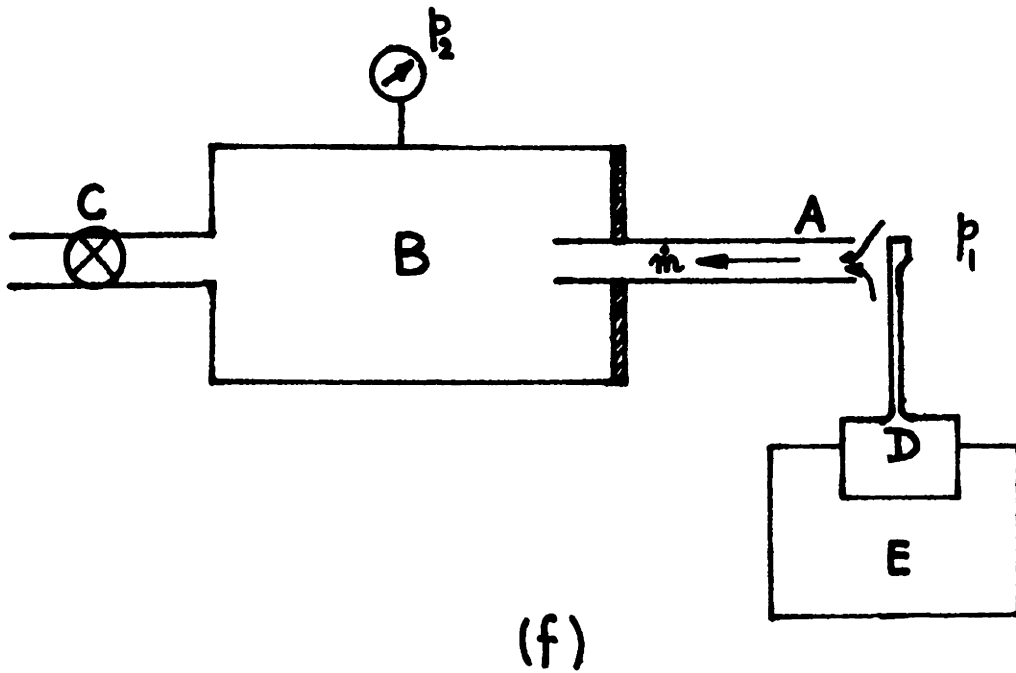
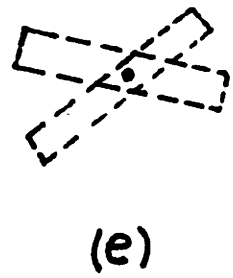
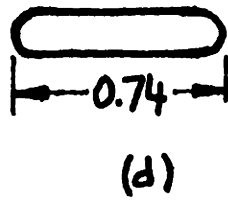
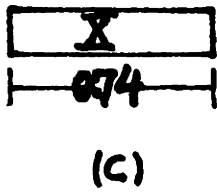
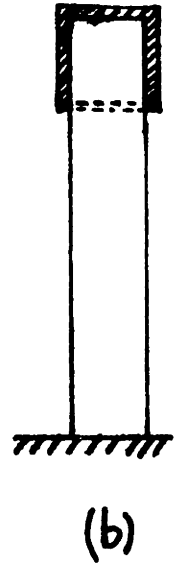
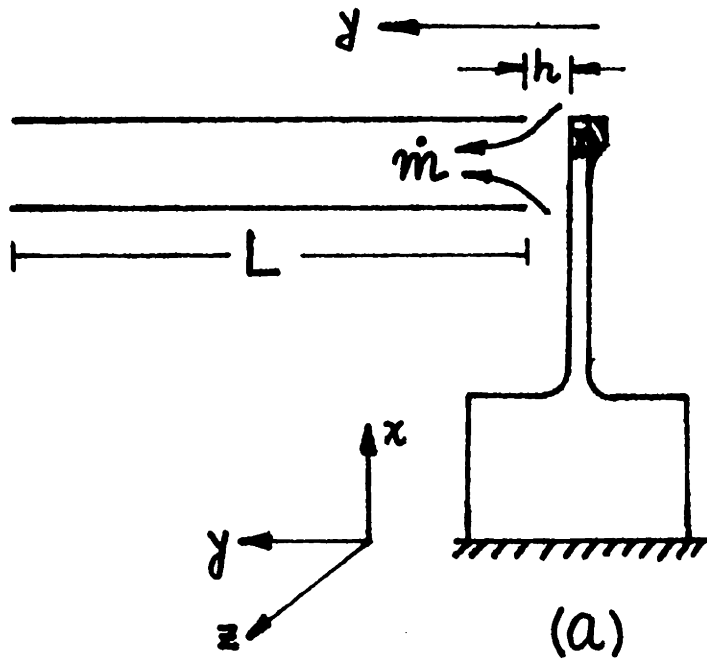
ACKNOWLEDGMENTS

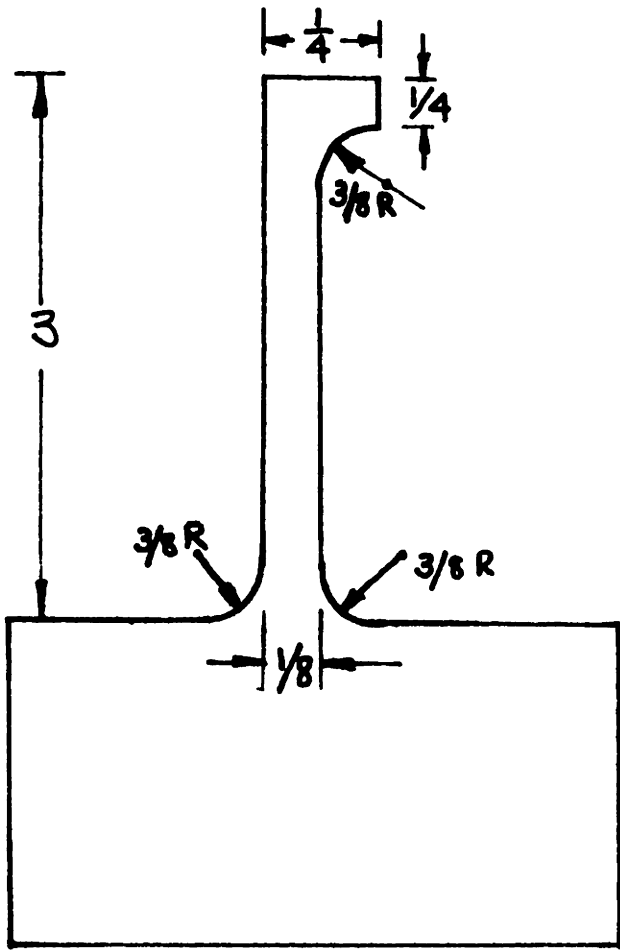
This work was supported in part by the U. S. Navy (Office of Naval Research) under Contract N00014-67-A-0204-0019 and in part by Research Grant NGR 22-009-805 with NASA Lewis Research Center.

*Sections I-IV were presented as paper T4 (U. Ingard, "Acoustical Characteristics of an Open-Ended Duct with Flow") at the 86th Meeting of the Acoustical Society of America in Los Angeles, California, on 31 October 1973. Section V was a part of the paper T6 (V. K. Singhal, "Flow Noise and Self-Excitation of Pipes") presented at the 89th Meeting of the Acoustical Society of America in Austin, Texas, on 10 April 1975.

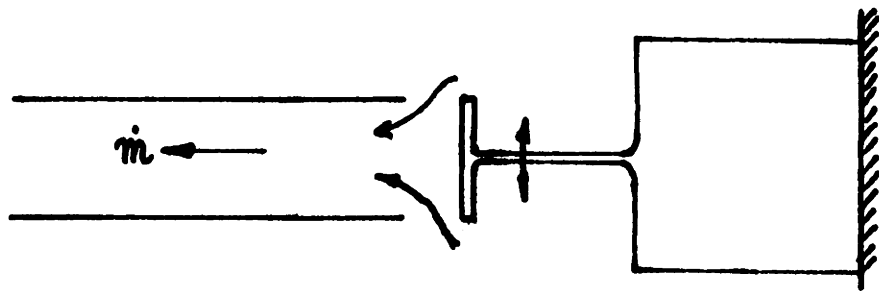
- ¹P. M. Morse, *Vibration and Sound* (McGraw-Hill, New York, 1948), 2nd ed.
²R. W. B. Stephens and A. E. Bate, *Acoustics and Vibrational Physics* (Edward Arnold, London, 1966), 2nd ed.
³J. Backus, *The Acoustical Foundations of Music* (John Murray, London, 1970); C. J. Nederveen, *Acoustical Aspects of Woodwind Instruments* (Frits Knuf, Amsterdam, 1969).
⁴J. L. Flanagan, *Speech Analysis, Synthesis and Perception* (Academic, New York, 1965); C. G. M. Fant, *Acoustic Theory of Speech Production* (Mouton, The Hague, 1970).
⁵J. W. Strutt, Lord Rayleigh, *Theory of Sound* (Dover, New York, 1945).

- ⁶H. Levine and J. Schwinger, *Phys. Rev.* **73**, 383-406 (1948).
⁷L. A. Vajnshtejn, *Zh. Tekh. Fiz.* [Sov. Phys.—Tech. Phys.] **19**, 911-930 (1949). English translation in "Propagation in Semi-Infinite Wave Guides," Research Report EM 63, Institute of Mathematical Sciences, New York University, January 1954, pp. 87-116. Similar studies for a duct with isentropic flow have been reported by D. L. Lansing, J. A. Drischler, and C. G. Pusey, *J. Acoust. Soc. Am.* **48**, 75(A) (1970), and by S. M. Candel, *J. Sound Vib.* **28**, 1-13 (1973).
⁸G. Kirchhoff, *Pogg. Ann.*, Bd. 134 (1868).
⁹P. M. Morse and K. U. Ingard, *Theoretical Acoustics* (McGraw-Hill, New York, 1968), pp. 519 ff.
¹⁰C. Ahrens and D. Ronneberger, *Acustica* **25**, 150-157 (1971); also, D. Ronneberger and W. Schilz, *Acustica* **17**, 168-175 (1966).
¹¹U. Ingard and V. K. Singhal, *J. Acoust. Soc. Am.* **55**, 535-538 (1974).
¹²T. E. Siddon, paper presented at CANCAM'73, Montreal, Canada, 29 May-1 June 1973.
¹³F. Mechel, W. Schilz, and J. Dietz, *Acustica* **15**, 199-206 (1965). The results presented here were obtained for a circular duct of 8.5-cm diameter, whereas our experiment was conducted in a $\frac{3}{4}$ in. by $\frac{3}{4}$ in. square-cross-section duct. For given ka the agreement is good when the results are plotted versus Mach number. Thus the Mach number is the proper parameter instead of the Reynolds number.
¹⁴D. Ronneberger, *Acustica* **19**, 222-235 (1967/68). (Reflection from downstream end only.) Also, E. Meyer and E. G. Neumann, *Physical and Applied Acoustics* (Academic, New York, 1972), Chap. 11.
¹⁵U. Ingard and V. K. Singhal, *J. Acoust. Soc. Am.* **54**, 1343-1346 (1973).
¹⁶E. Ia. Iudin, *Sov. Phys.—Acoust.* **1**, 383-398 (1955).
¹⁷U. Ingard, A. Oppenheim, and M. Hirschorn, *American Society of Heating, Refrigerating and Air-Conditioning Engineers (ASHRAE)*, Preprint No. 2068, RP-37 (1968).





(g)



(h)

Fig. 1: (a) Valve-pipe arrangement used for the experiments. Duct cross-section, $3/4$ inch x $1\ 3/4$ inch rectangular, is shown shaded in (b). The rectangular cantilever beam used as a valve is 0.74 inch wide. The valve is aligned almost 'perfectly' with respect to the pipe as shown in the side view in (b). The small end mass shown shaded in (a) quenched the torsional modes. Attempts to eliminate the torsional modes in preference to bending modes by rounding off the cross-section of the cantilever beam as shown in (d) were only partially successful. Cross-section 0.74 in x $1/8$ inch without the end mass is shown in (c), rounded cross-section in (d). Rounded cross-section was not used for the experiments reported here. Torsional modes about the x axis are shown in (e). In (f), flow through the pipe A is generated by a suction device (steam ejector) controlled by a valve C. Anechoic chamber B decouples acoustically the flow device from the duct. The valve D is bolted firmly to a milling machine bed E making possible the alignment of the valve with respect to the duct in x, y and z directions. The valve shown in (g) has first natural bending mode at 435 Hz and first natural torsional mode at 3250 Hz. Dimensions of the valve are in inches. A cantilever beam with an end plate covering the cross-section of the duct (h) is used for preliminary studies of torsional modes.

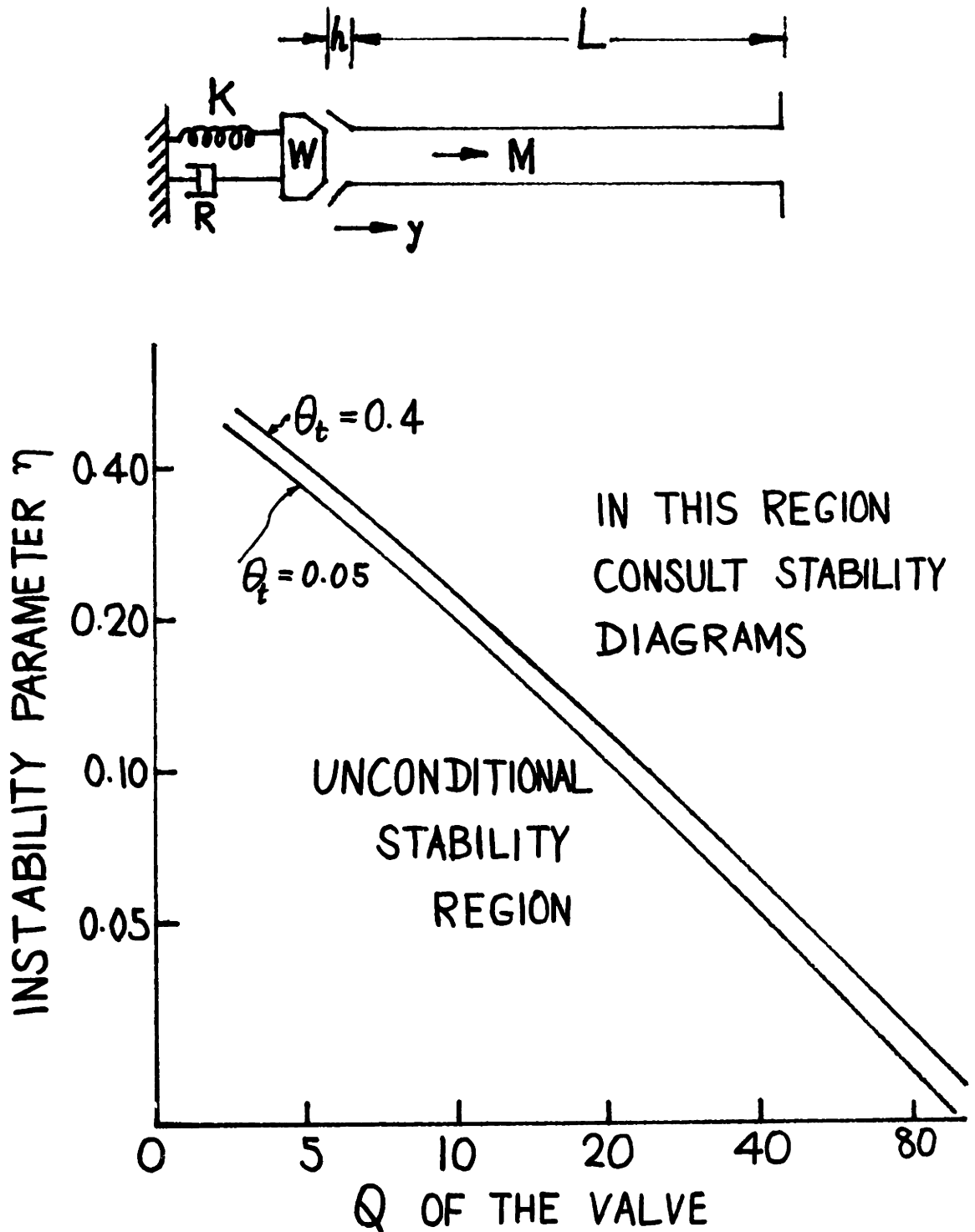


Fig. 2. The valve-pipe arrangement is modeled as a damped spring-mass oscillator with mass W , spring K and a mechanical damping coefficient R . The unconditional stability region as a function of the duct termination resistance θ_t is also shown.

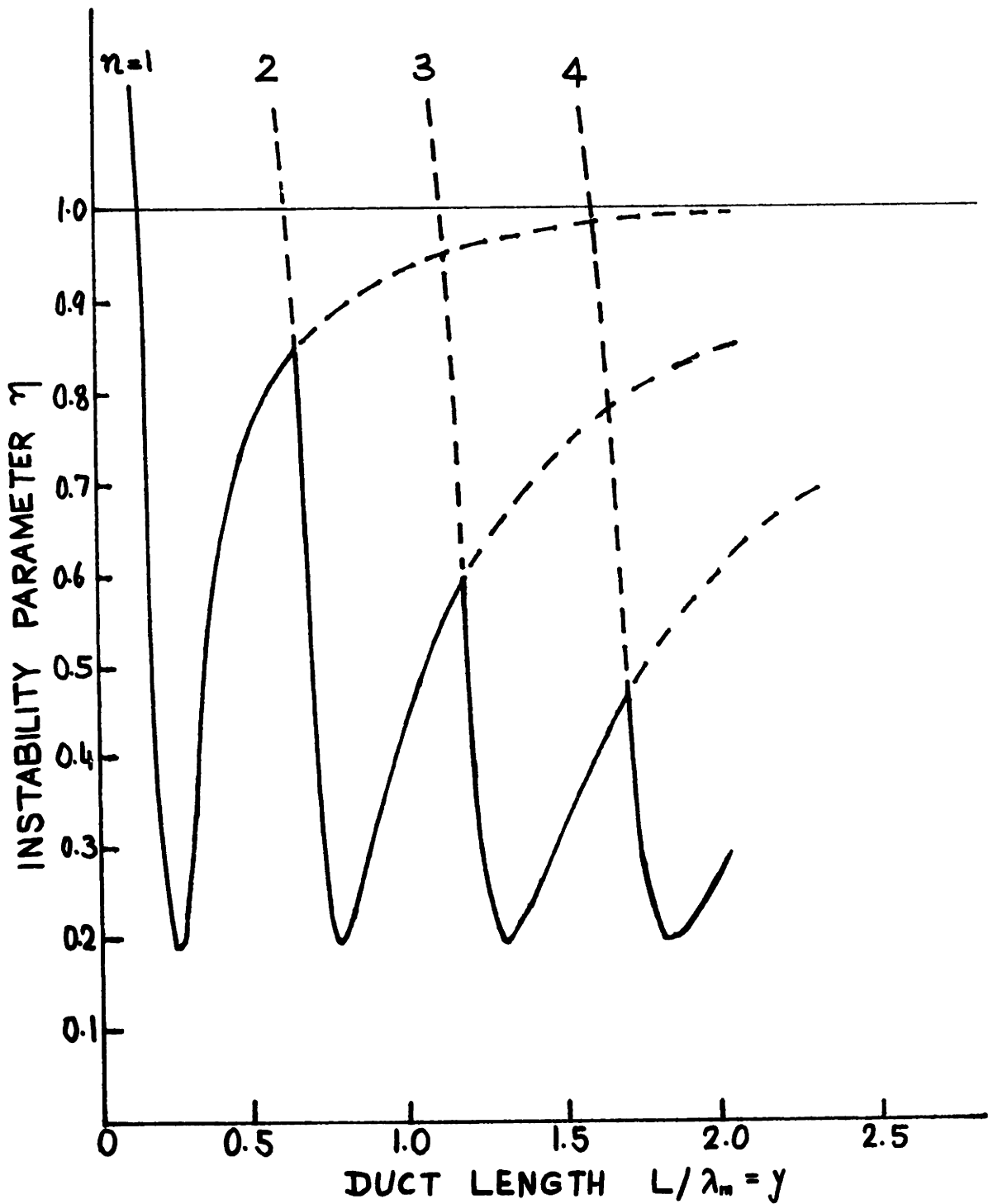


Fig. 3. Determination of the stability-contours for modes $n=1,2,3,4$ etc. All modes are stable below the solid contours. Various modes correspond to different number of wavelengths in the pipe.

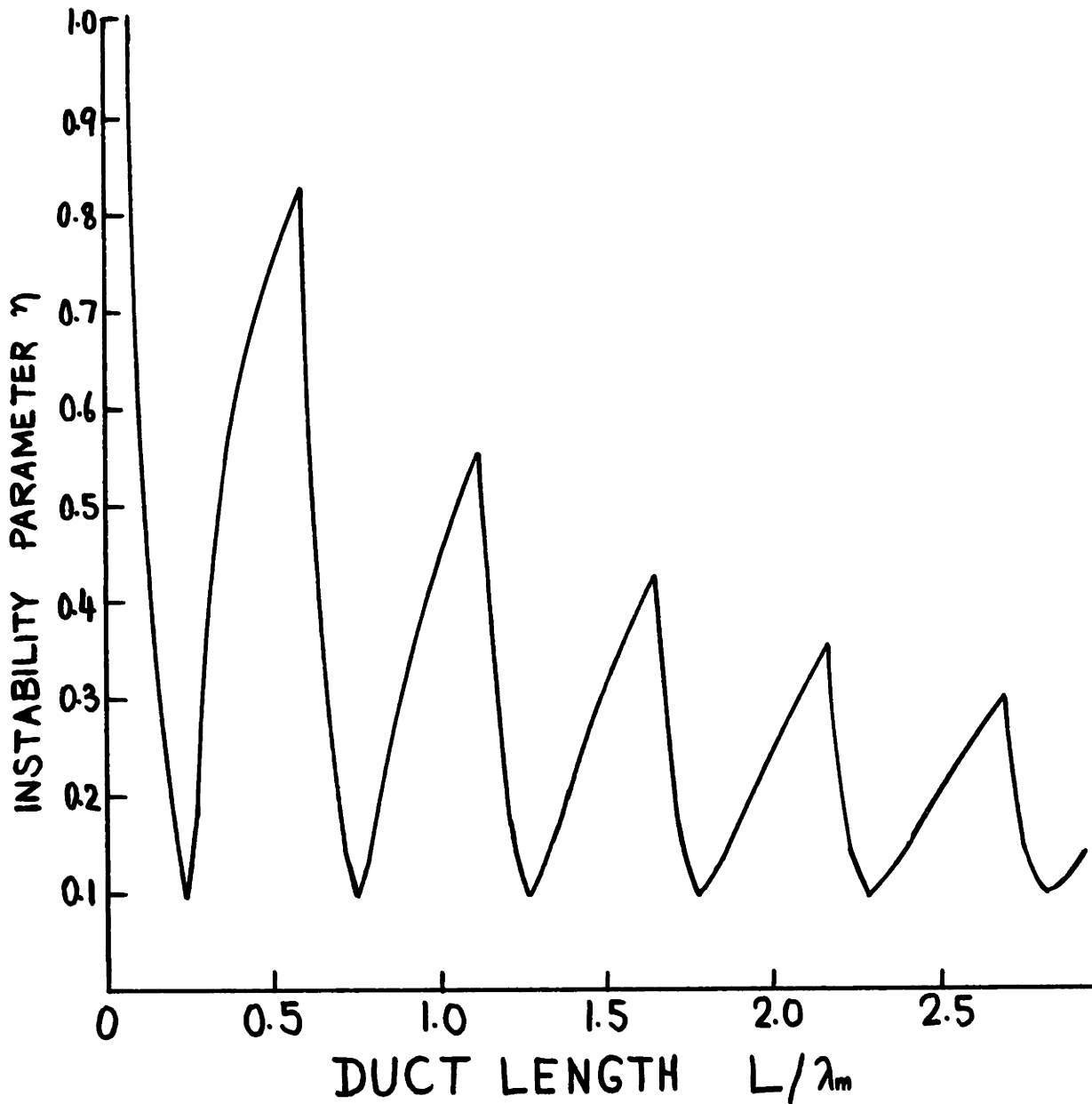


Fig. 4. Analytically determined neutrally stable region. Mechanical Q of the valve = 20, duct termination resistance $\theta_+ = 0.1$. System is stable if the operating point is below the contour and unstable in the region above. The wavelength in the fluid corresponding to the natural frequency of the valve (without flow) is λ_m .

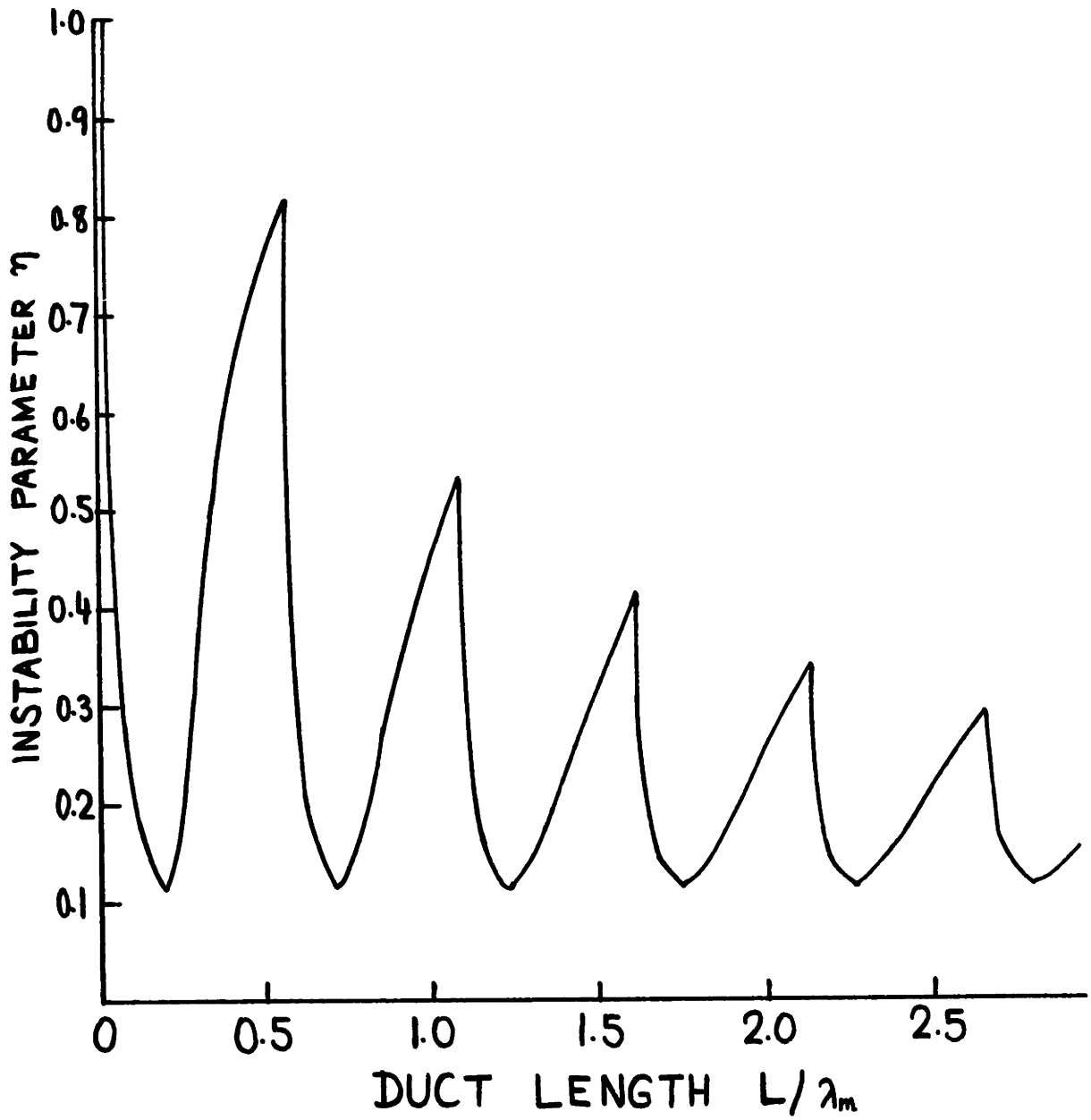


Fig. 5. Stability contour for $Q = 20$, $\theta_t = 0.4$.

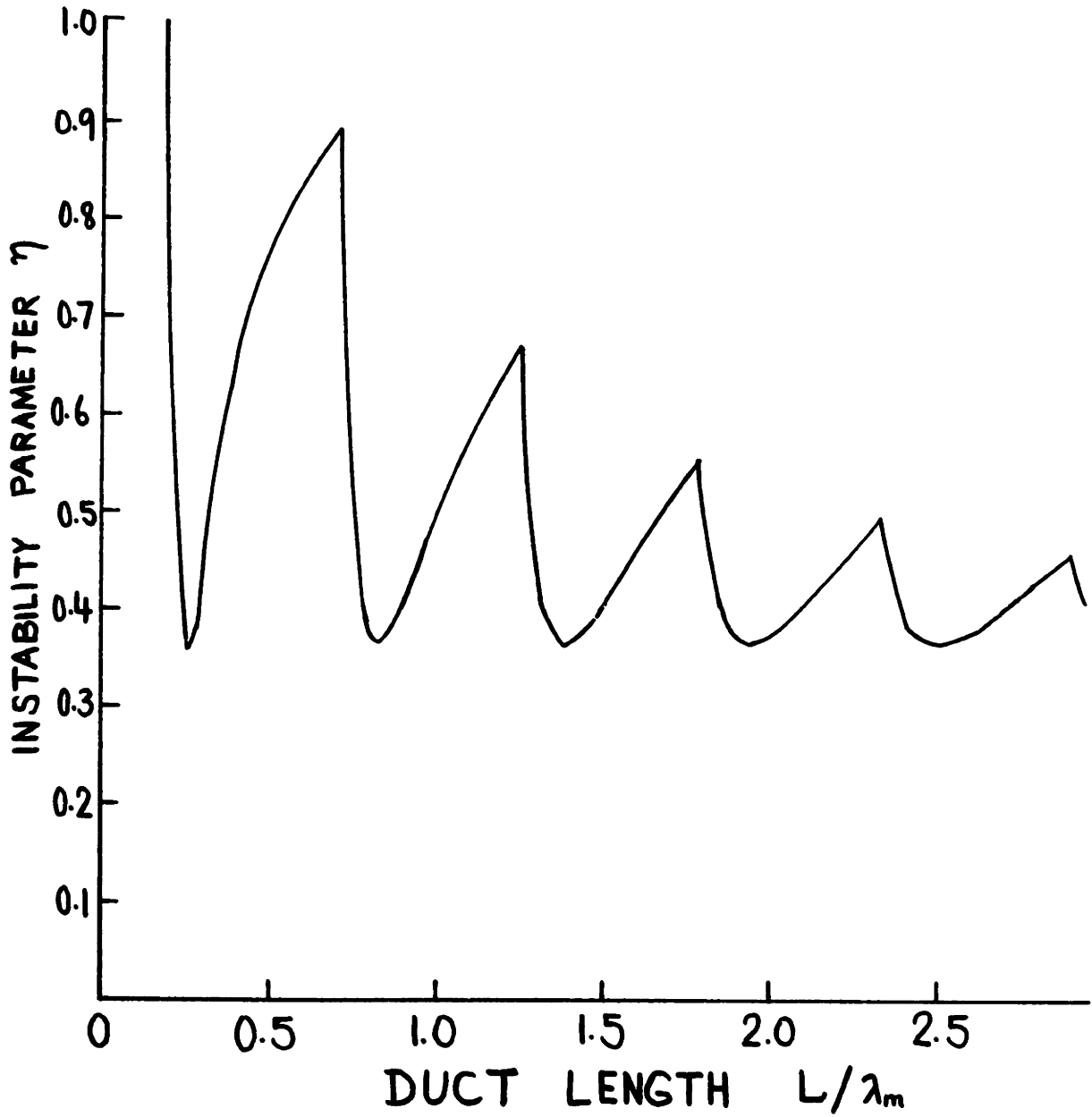


Fig. 6. Stability contour for $Q = 5$, $\theta_t = 0.1$.

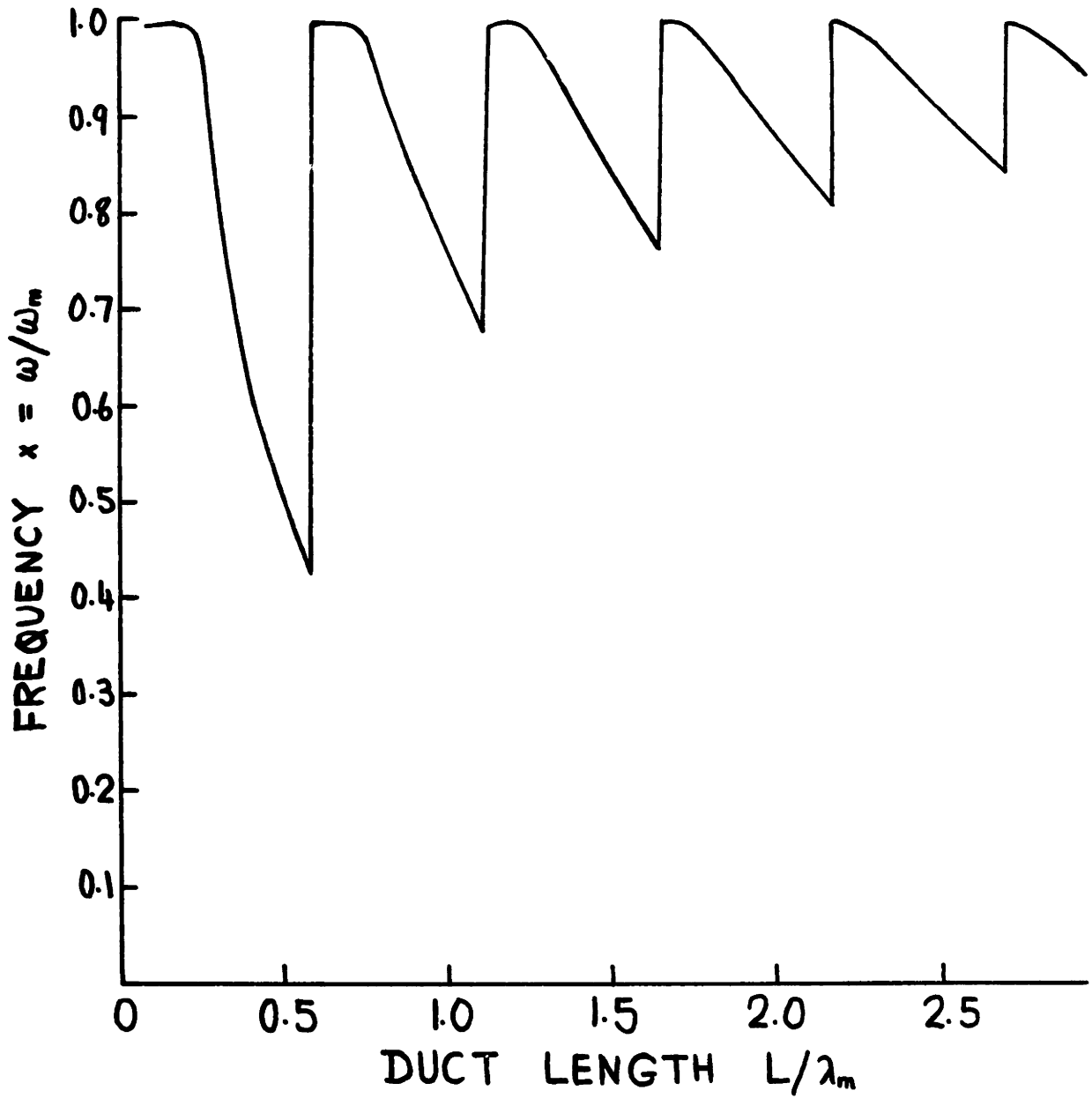


Fig. 7. Theoretically predicted angular frequency of oscillation of the valve on the verge of instability as a function of duct length L for $Q = 20$ and $\theta_t = 0.1$.

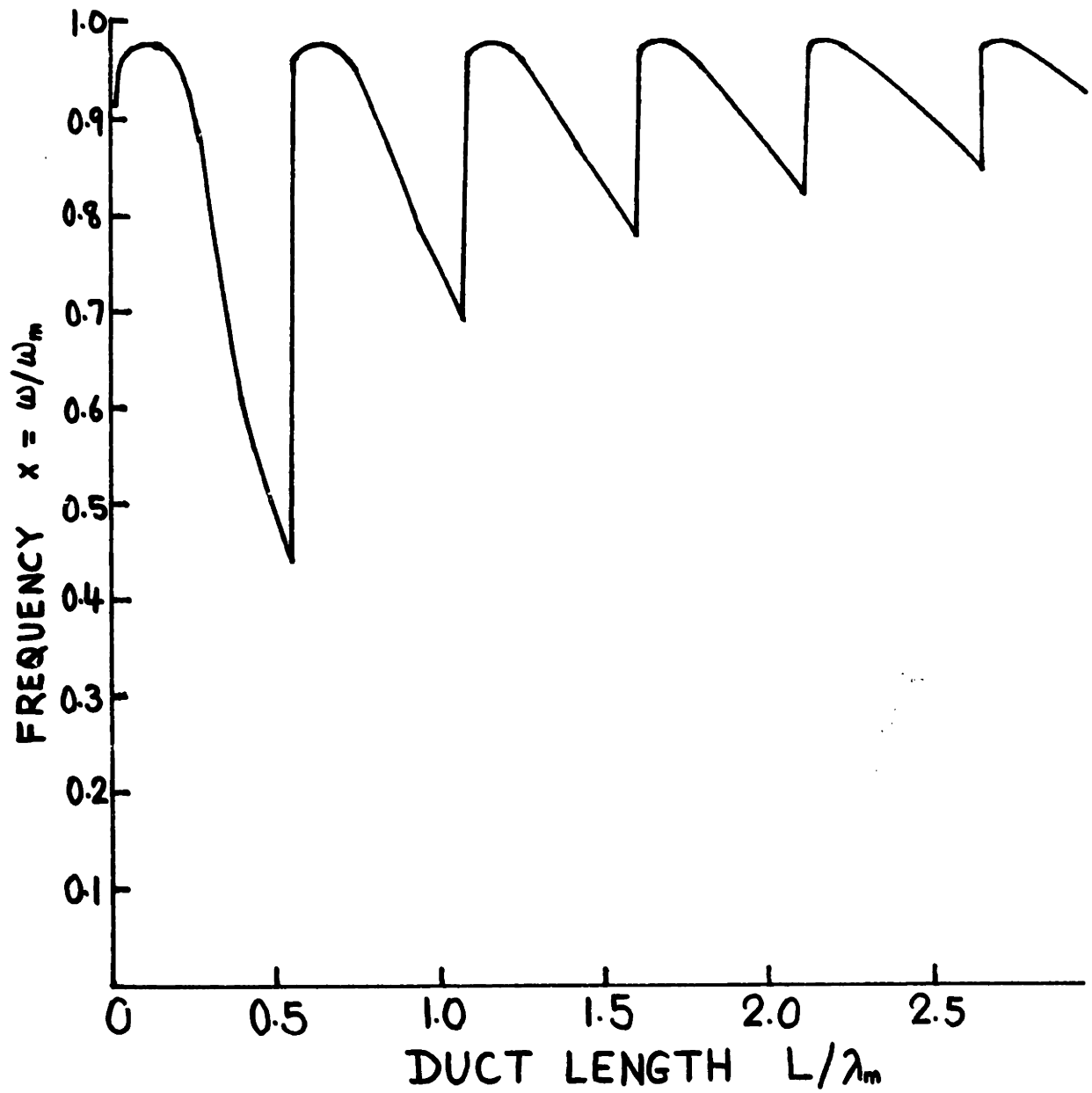


Fig. 8. Oscillation frequency at the stability boundary for $Q = 20$ and $\theta_t = 0.4$.

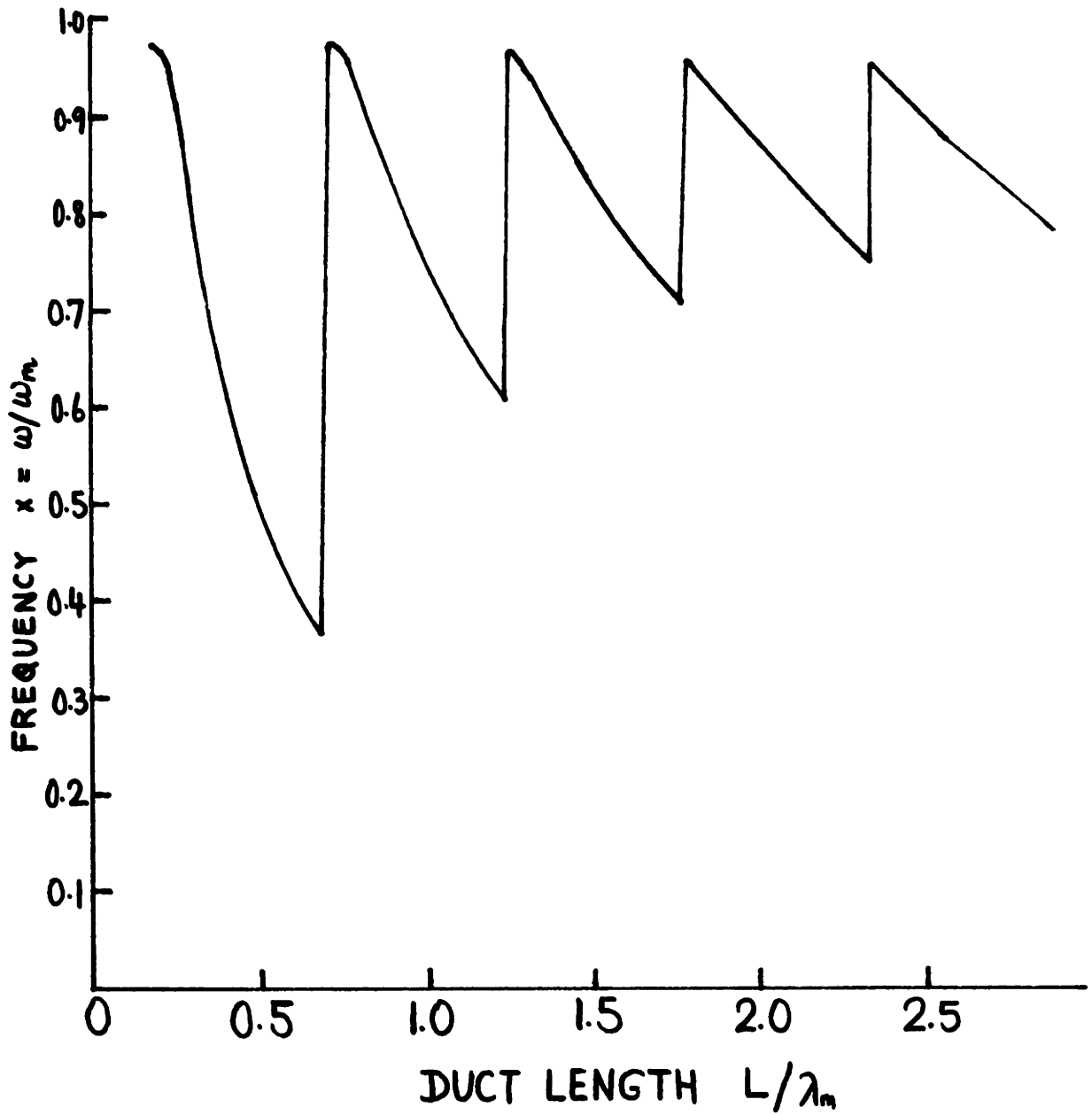


Fig. 9. Oscillation frequency for $Q = 5$ and $\theta_t = 0.1$.

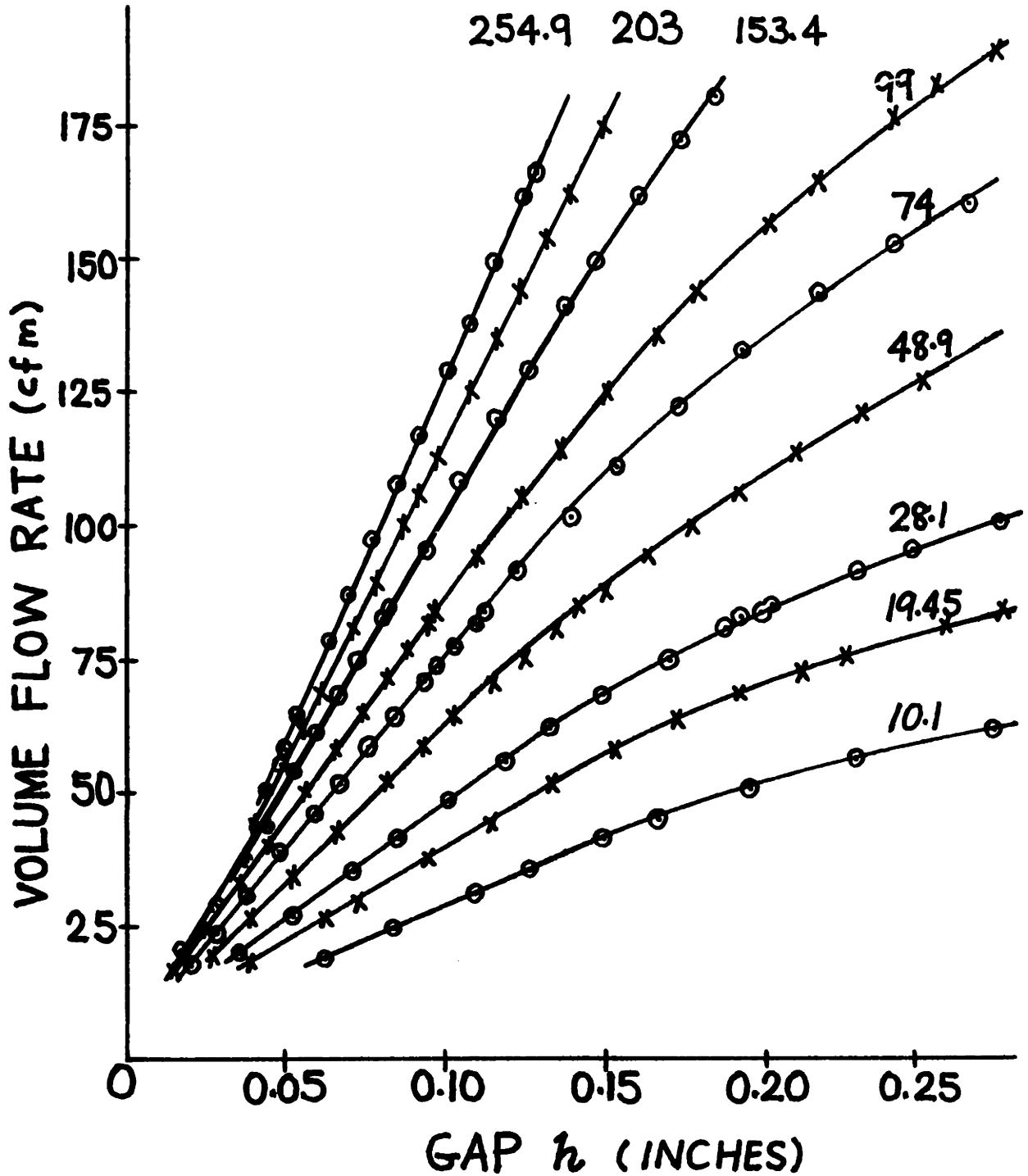


Fig. 10a. Volume flow rate vs. the equilibrium separation distance h between the end of the duct and the valve. Each curve is for the pressure drop $\Delta p = p_1 - p_2$ maintained constant and equal to the value (in millimeters of mercury) shown on the curve.

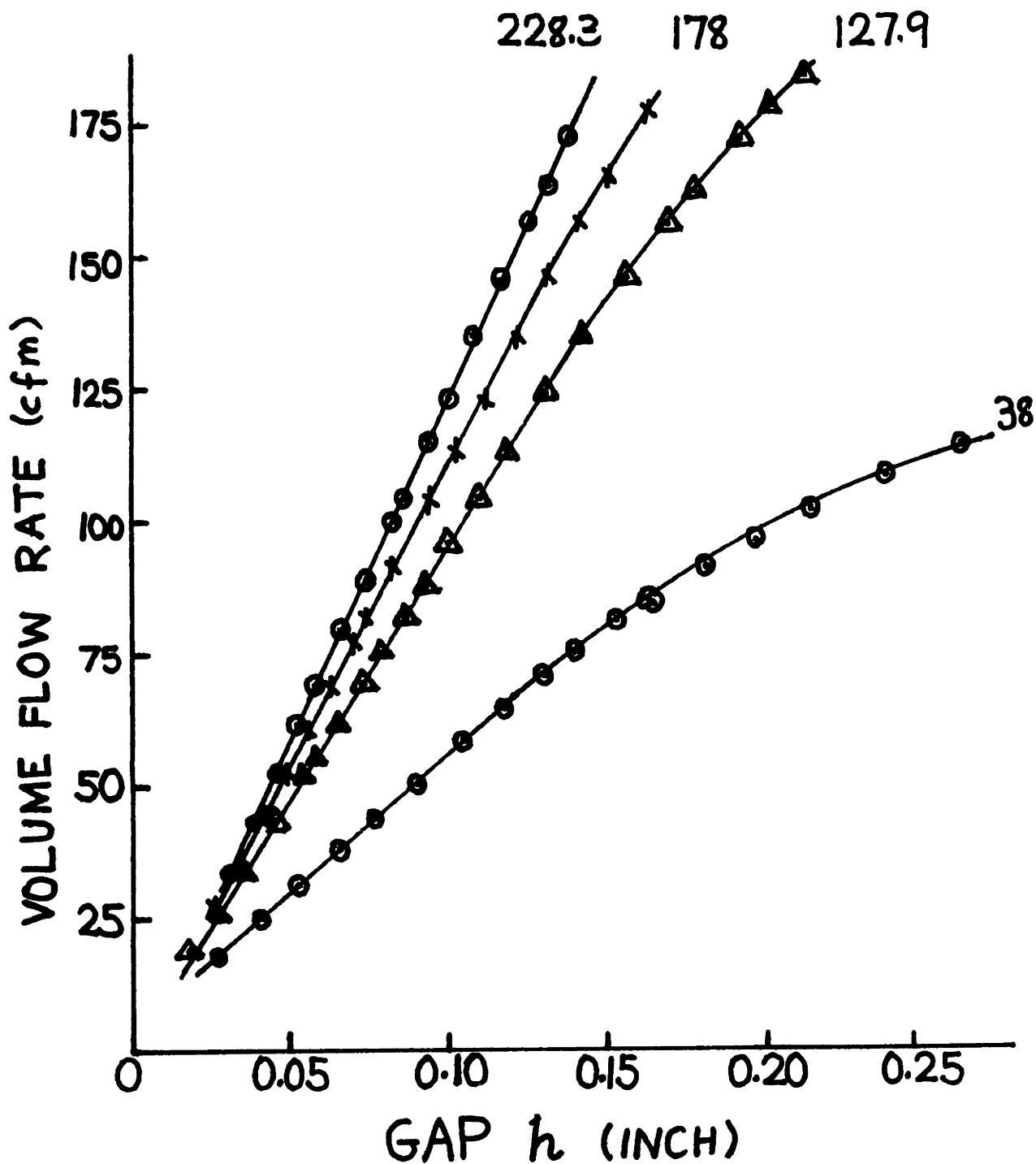


Fig. 10b. Volume flow rate vs. the equilibrium separation distance h between the end of the duct and the valve. Each curve is for the pressure drop $\Delta p = p_1 - p_2$ maintained constant and equal to the value (in millimeters of mercury) shown on the curve.

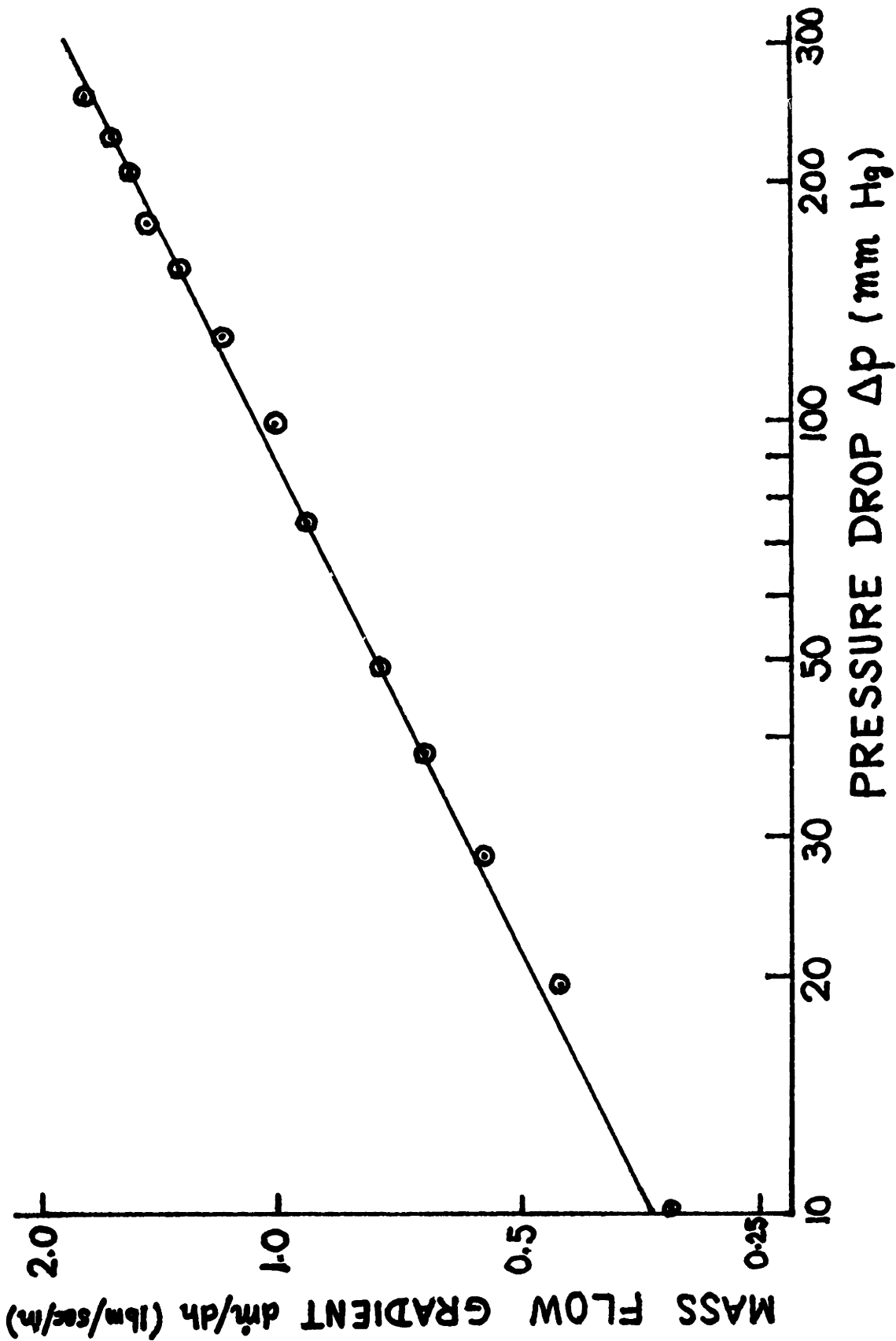


Fig. 11. The mass flow characteristics of the valve shown in Fig. 10 are linear for small h . Mass flow gradient $\frac{dm}{dh}$ as a function of Δp measured in mms of mercury. The line through the points is proportional to $\sqrt{\Delta p}$.

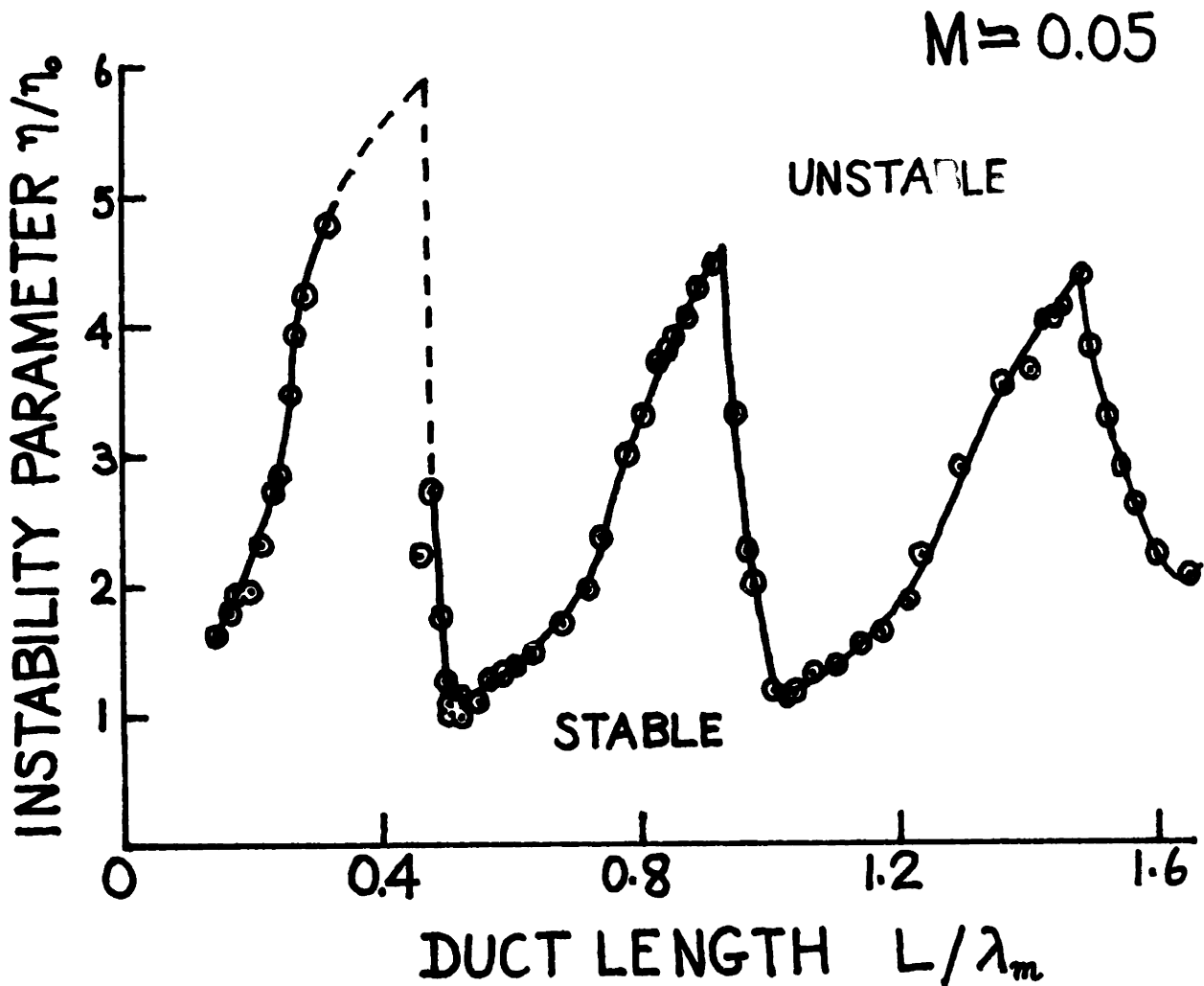


Fig. 12a. Experimentally determined neutral stability curve normalized with respect to the minimum value η_0 . At the minimum point $\eta/\eta_0=1$, measured $\Delta p=6.25$ mms of mercury. The flow rate through the pipe is maintained constant, Duct Mach number $M \approx 0.05$. Note that (estimated) η is less than 1 for all points.

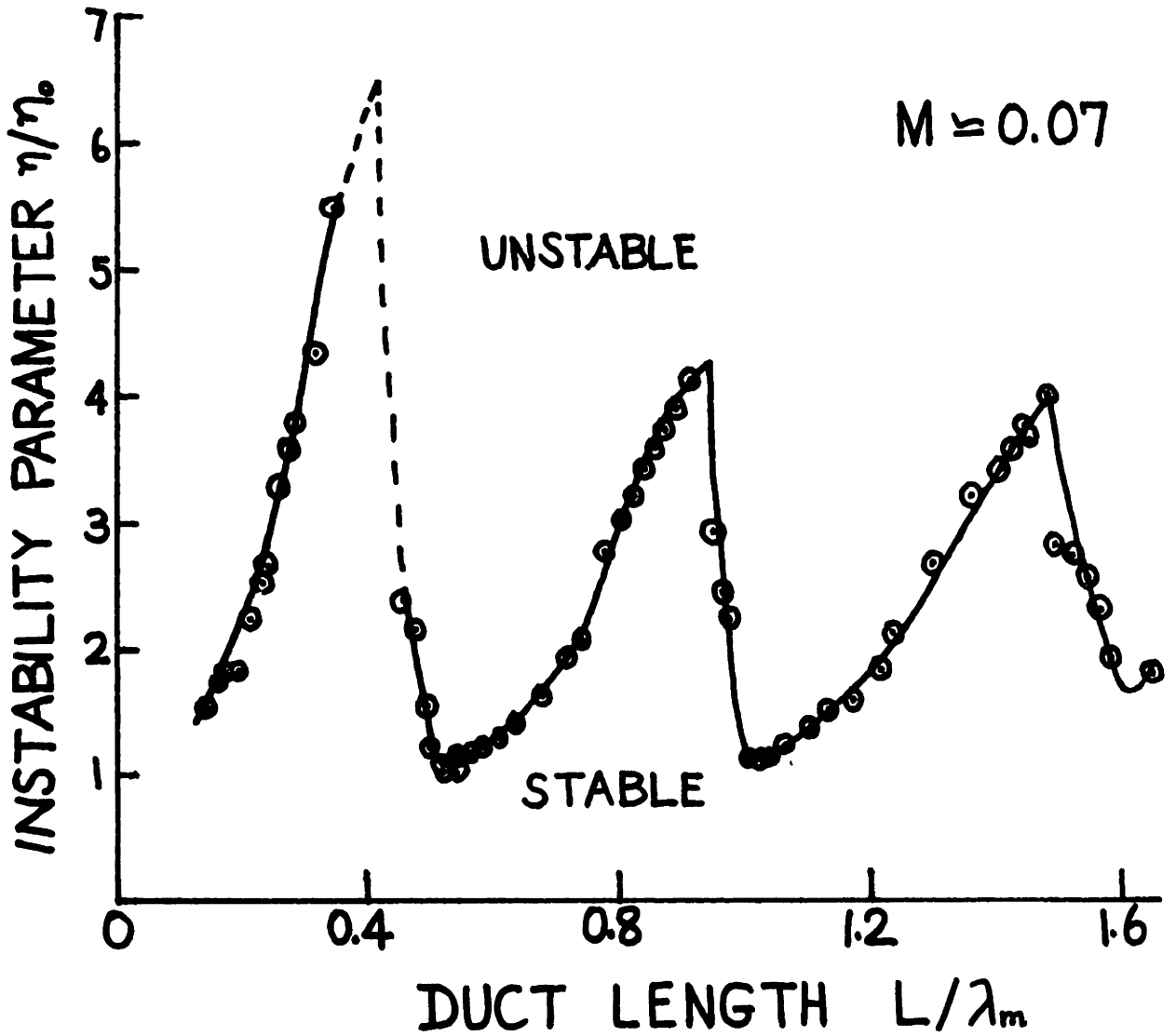


Fig. 12b. Experimental neutral stability curve. At the minimum point, measured $\Delta p = 9.1$ mms of mercury. $M \approx 0.07$.

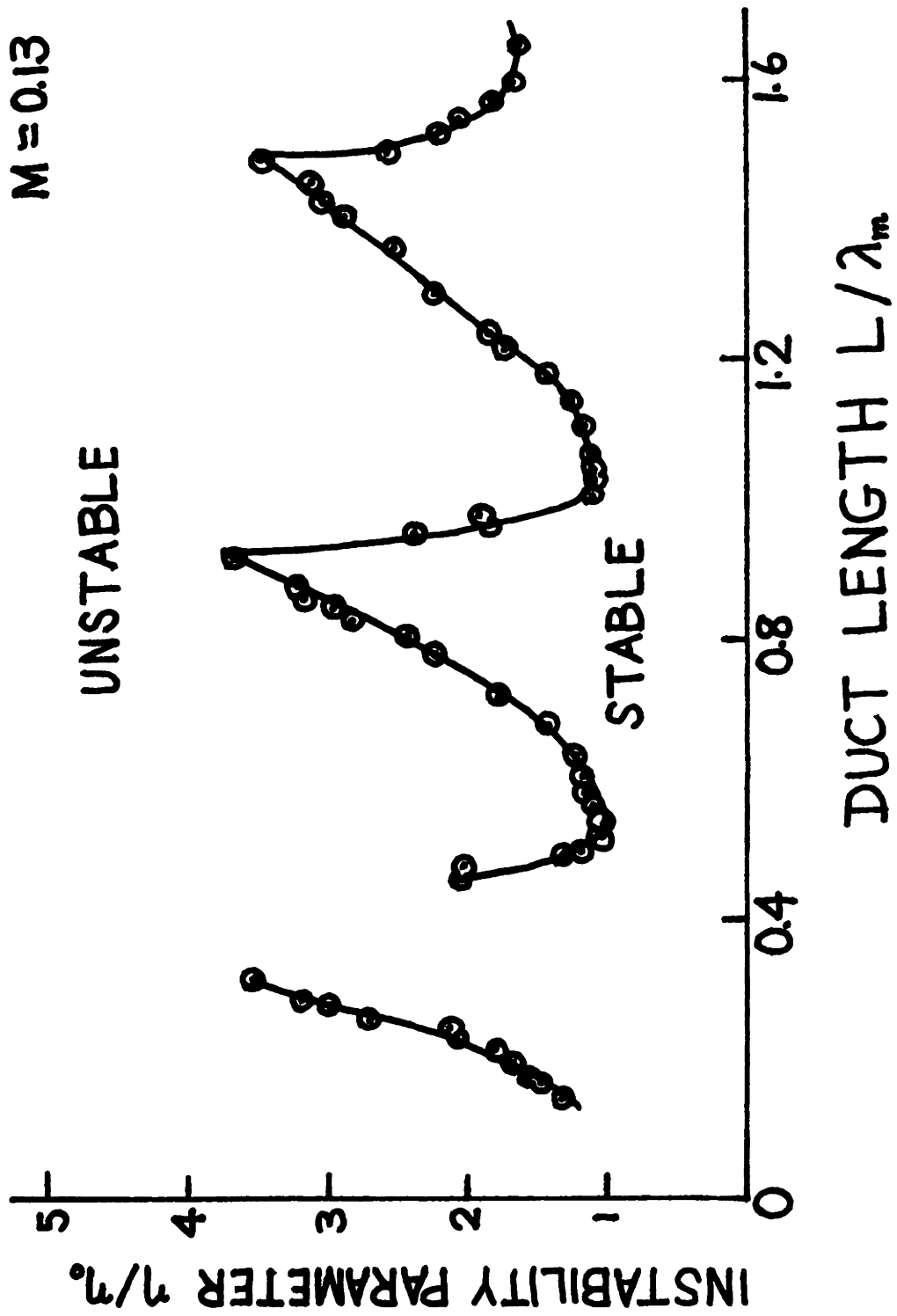


Fig. 12c. Experimental neutral stability curve. At the minimum point, measured $\Delta p = 24.4$ mms of mercury. $M \approx 0.13$. All experimental points (except a few near $\eta = \eta_0$) lie in the linear range of \dot{m} vs h characteristic.

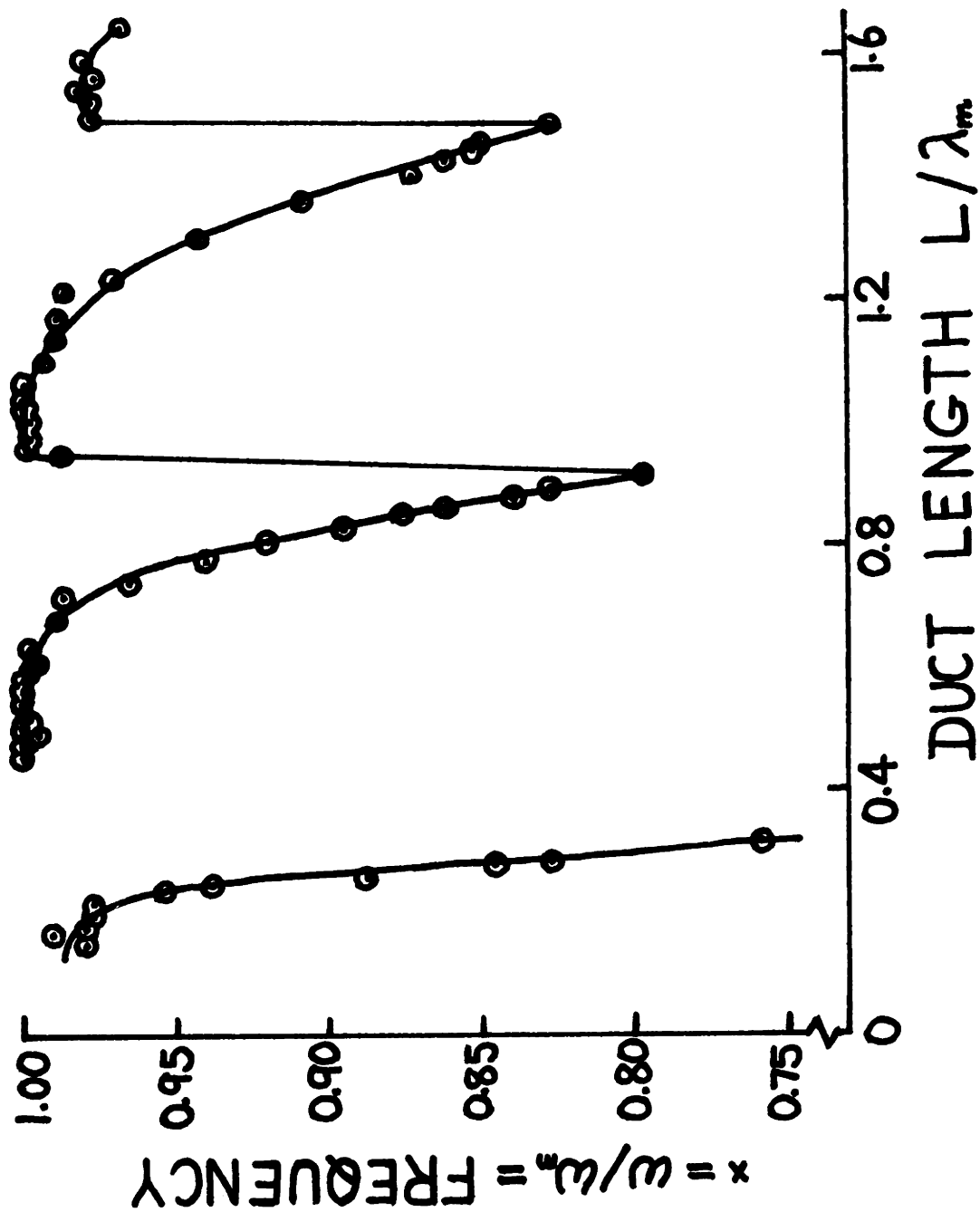


Fig. 13a. Experimentally measured frequency of oscillation for the neutrally stable valve. Natural frequency $\omega_m = 435$ Hz. Duct Mach number $M \approx 0.05$.

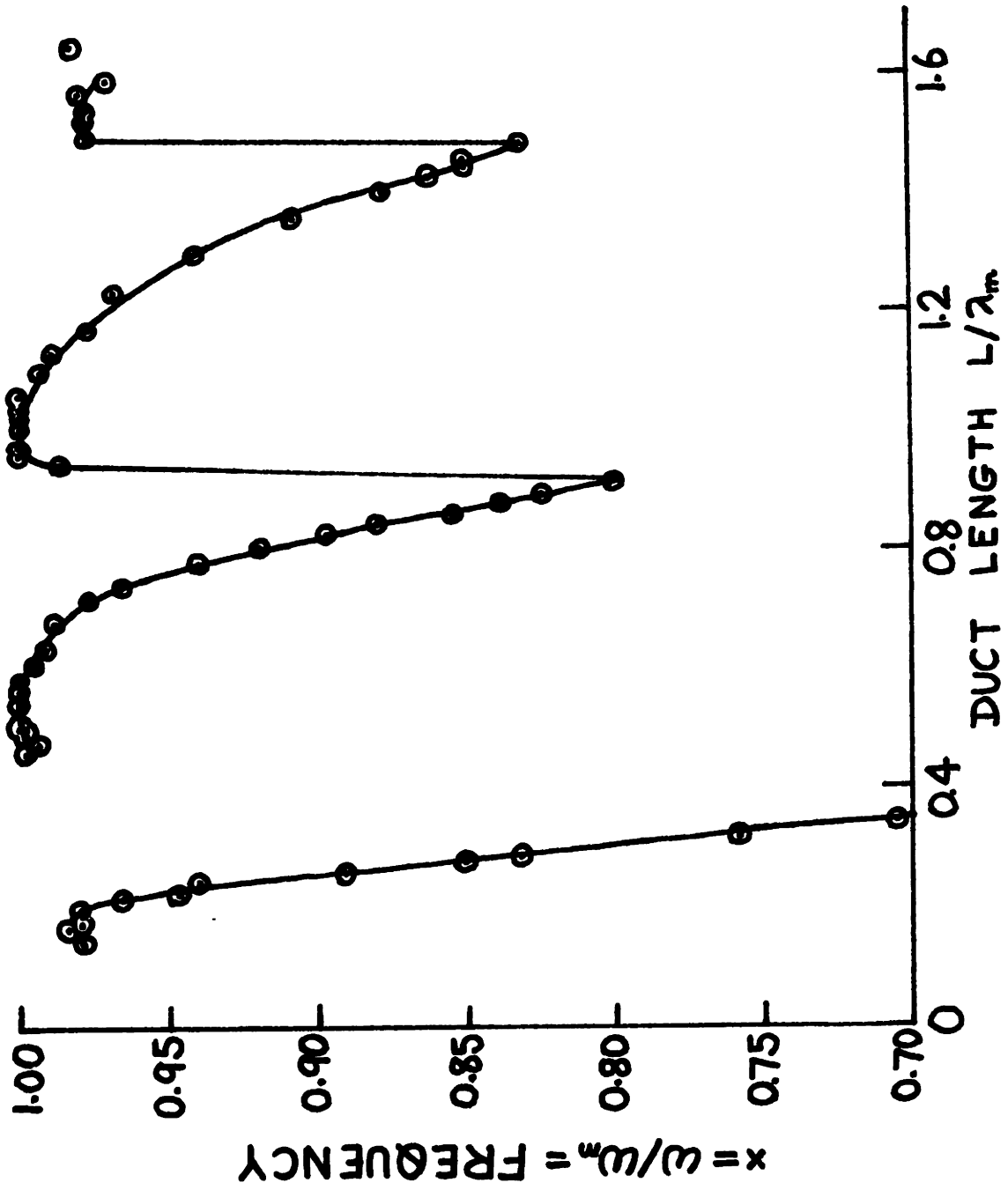


Fig. 13b. Experimentally measured frequency of oscillation. $M \approx 0.07$.

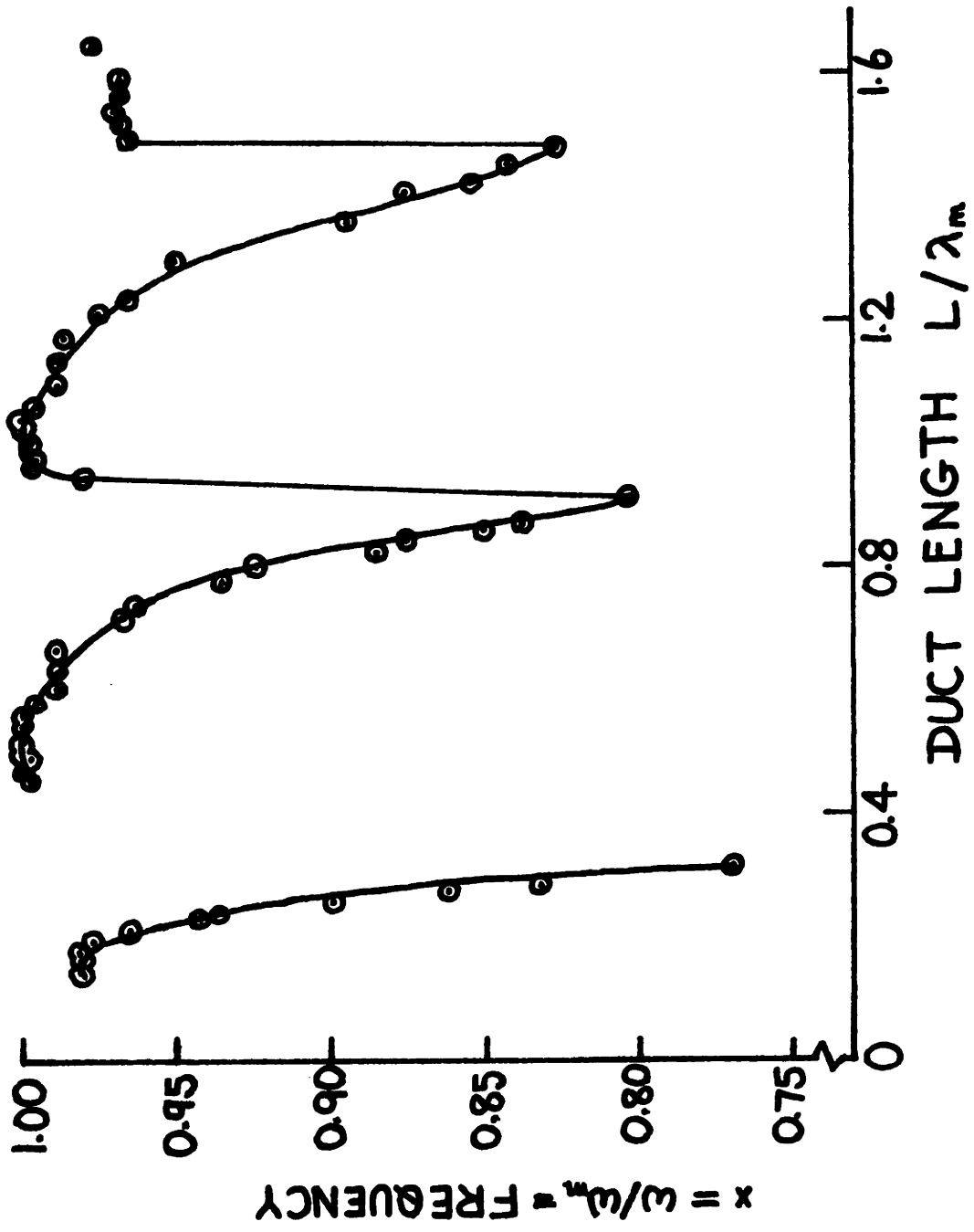


Fig. 13c. Experimentally measured frequency of oscillation, $M \approx 0.13$.

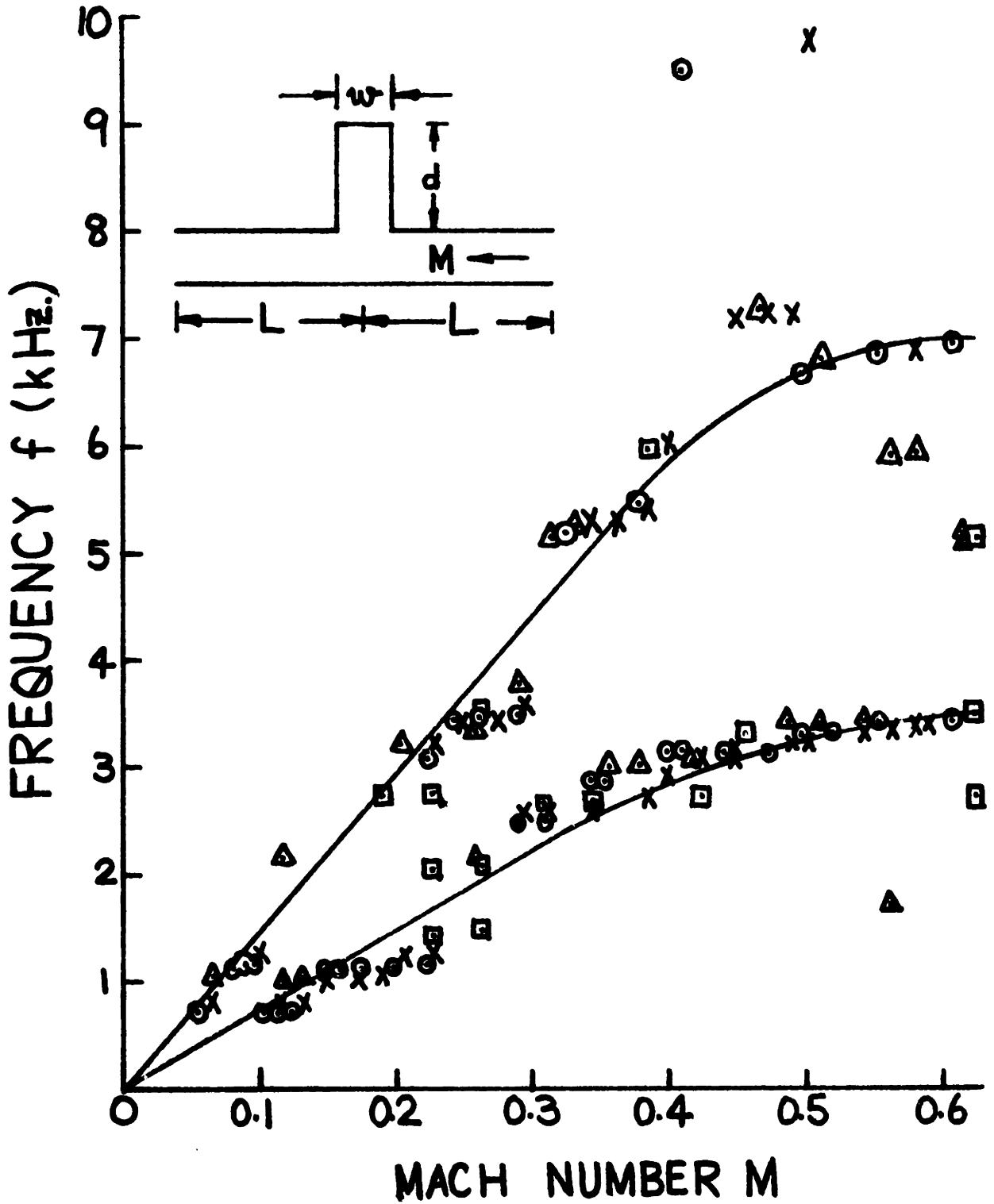


Fig. 14. The screech frequency f as a function of the flow Mach number M in the duct for a side branch resonator. Cavity depth $d = 3$ inches, width $w = 3/4$ inch, duct has $3/4$ inch \times $3/4$ inch rectangular cross-section. \square $L=7.6$ cms, $\Delta L=15.2$ cms, $\circ L=27.3$ cms, $\times L=60.7$ cms.

Fig.15. Nonlinear coupling between the cavity modes. Peaks in the spectrum marked f_1 , f_3 , f_5 are resonances corresponding to cavity depth being one quarter, three quarter and five quarter wavelengths respectively. $L_1 \approx 27.3$ cms, $L_2 \approx 121.6$ cms, $M \approx 0.21$, $w \approx 3/4$ inch, $d = 3$ inches. Duct cross-section is $3/4$ inch x $3/4$ inch. Coupling is evident as peaks f_{3+1} , f_{3-1} , etc; which are respectively the sum and difference of f_3 and f_1 .

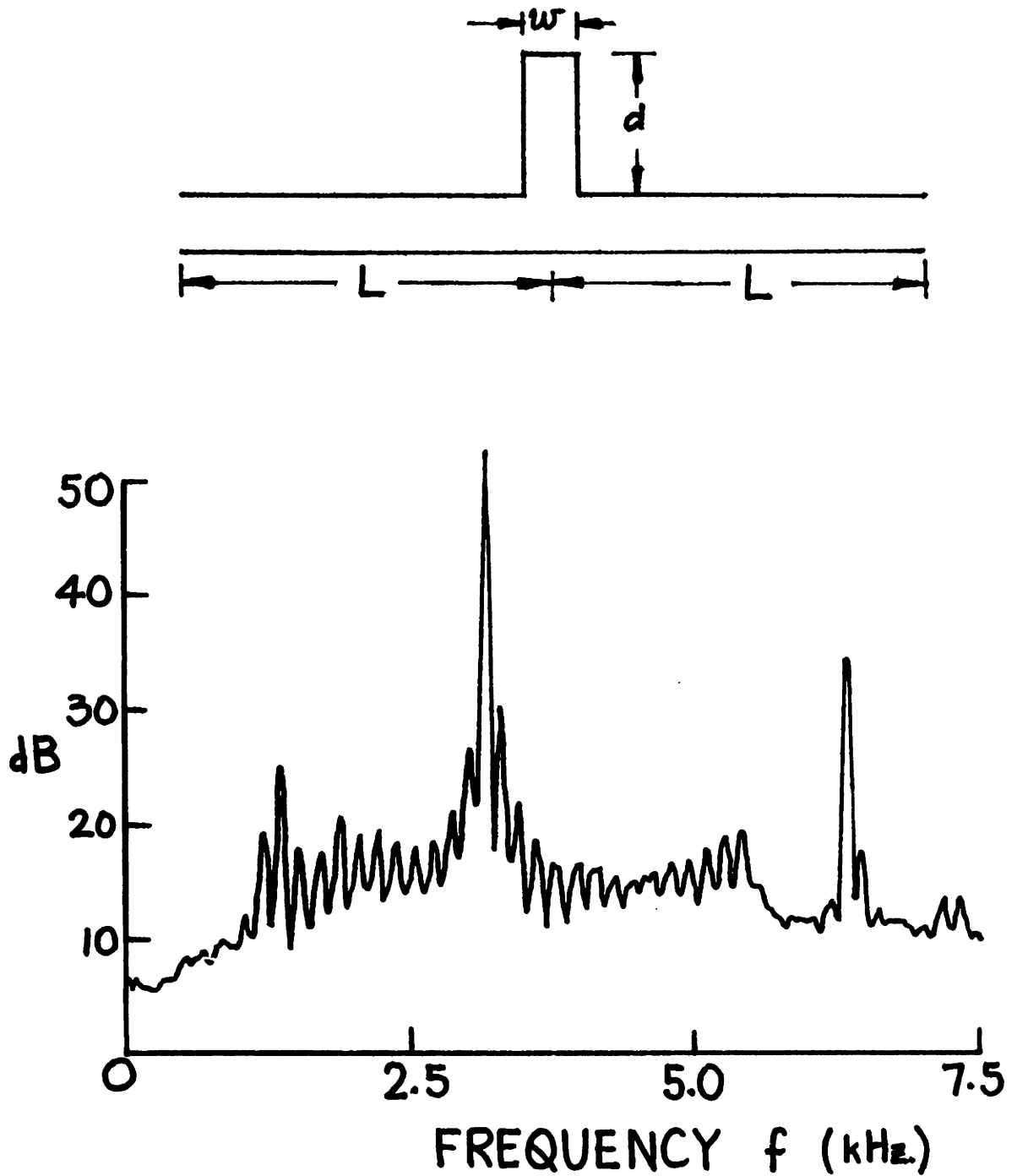


Fig. 16. Nonlinear coupling between the axial modes of the duct and the cavity resonances. $d = 3$ inches, $w = 3/4$ inch, duct cross-section = $3/4$ inch x $3/4$ inch, $L \approx 3$ feet, $M \approx 0.21$. Cavity mode f_c is at 3150 Hz, the "satellites" due to the coupling are at $f_c \pm 180$ Hz; 180 Hz being the axial duct mode corresponding to wavelength = $2L$.

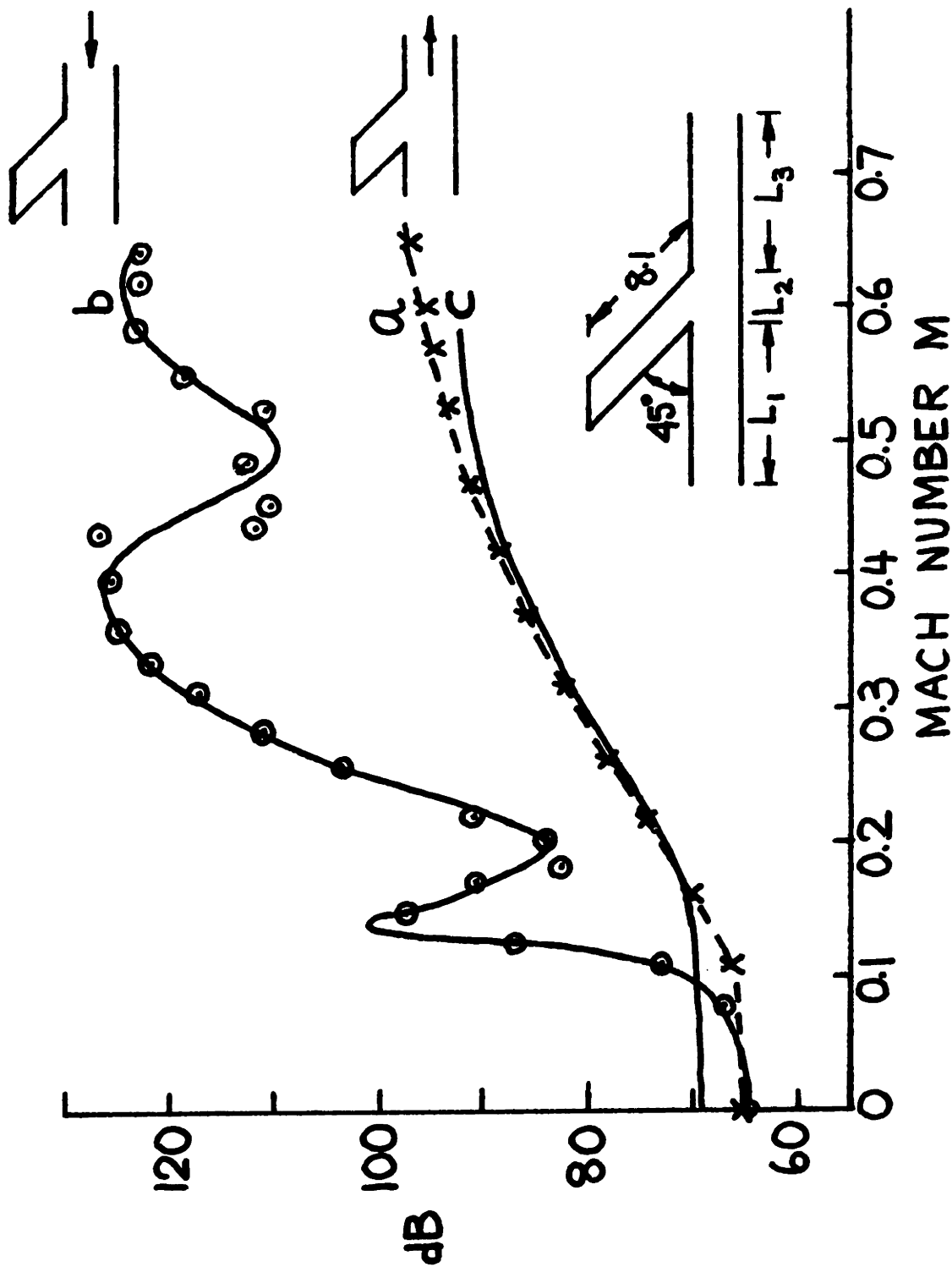


Fig. 17. Sound pressure level as a function of duct Mach number for an inclined cavity. When inclined as shown in (a), the cavity is as quiet as a pipe without the cavity, (c). When inclined the other way (b), it whistles violently. $L_1 \approx 13.0$ cms., $L_2 \approx 2.7$ cms., $L_3 \approx 14.6$ cms.

REFERENCES

1. T. Maeda, "Studies on the Dynamic Characteristics of a Poppet Valve", Bulletin of the Japan Society of Mechanical Engineers, Vol. 13, pp 281-297 (1970).
2. S. Y. Lee and J. F. Blackburn, "Contributions to Hydraulic Control, Transient Flow Forces and Valve Instability", Transactions Am. Soc. of Mech. Engrs., Vol 74, pp 1013-1016 (1952).
3. F. W. Ainsworth, "The Effect of Oil-Column Resonance on Hydraulic Valve Squeal", Trans. Am. Soc. of Mech Engrs., Vol. 78, pp 773-778 (1956).
4. F. D. Ezekiel, "The Effect of Conduit Dynamics on Control Valve Stability", Trans. Am. Soc. of Mech. Engrs, Vol. 80, pp 904-908 (1958). Also see Sc. D. Thesis, Mech. Engg. Dept. MIT (1955).
5. N. Tominari, Preprints for Automatic Control Symposium, (1960-12).
6. T. Saito, Journal Japan Soc. of Mech. Engrs., Vol. 64, pp 1681 (1961); Vol. 18, pp 40 (1952); Vol. 21, pp 374 (1955).
7. J. E. Funk, "Poppet Valve Stability", Trans. Am. Soc. of Mech. Engrs., Series D (Journal of Basic Engg.), Vol 86, pp 207-212 (1964).
8. T. Ito, T. Muto, K. Suzuki and K. Tsukahara, "Study on the Self-Sustained Oscillation of a Piston-Type Valving System",

- Bull. Japan Soc. of Mech. Engrs., Vol. 10, pp 793-807 (1967).
9. T. Ito, T. Muto and T. Shinoda, "Study on the Self-Sustained Oscillation of a Piston-Type Valving System", Bull of Jap. Soc. of Mech. Engrs., Vol 11, pp 487-495 (1968); T. Ito et al, Trans. Jap. Soc. of Mech. Engrs., Vol 33, pp 51-61 (1967); Vol. 33, pp. 62-70 (1967); Vol. 33, pp 1401-1410 (1967).
 10. K. Kasai, "On the Stability of a Poppet Valve with an Elastic Support", Bull. Jap. Soc. of Mech. Engrs., Vol 11, pp 1068-1083 (1968); Bull. Jap. Soc. of Mech. Engrs., Vol 12, pp 1091-1098 (1969).
 11. T. Ichikawa and K. Nakamura, Trans. Jap. Soc. of Mech. Engrs., Vol. 34, pp 91-99 (1968).
 12. D. E. Wandling and B. L. Johnson, "Hydraulic Poppet Valve Stability", Soc. of Automotive Engrs, SAE Paper 720792, 12 pages (1972).
 13. T. A. Wilson and G. S. Beavers, "Operating Modes of the Clarinet", Journal Acous. Soc. of Am., Vol 56, pp 653-658 (1974).
 14. J. Backus, "Small Vibration Theory of the Clarinet", J. Acous. Soc. of Am., Vol 35, pp 305-313 (1963).
 15. A. O. St. Hilaire, T. A. Wilson and G. S. Beavers, "Aero-dynamic Excitation of the Harmonium Reed", J. Fluid Mech., Vol 49, pp 803-816 (1971).
 16. C. Ahrens and D. Ronneberger, "Acoustic Attenuation in Rigid and Rough Tubes with Turbulent Air Flow", Acustica, 25,

- 150-157 (1971). Also, D. Ronneberger and W. Schilz, "Sound Propagation in Streaming Air within Tubes having Changes of Cross-Section and Flow Losses," *Acustica*, Vol 17, pp 168-175 (1966).
17. Uno Ingard and V. K. Singhal, "Sound Attenuation in Turbulent Pipe Flow", *J. Acous. Soc. of Am*, Vol 55, pp 535-538 (1974).
18. Uno Ingard and Vijay K. Singhal, "Effect of Flow on the Acoustic Resonances of an Open-Ended Duct", *J. Acous. Soc. of Am.*, Vol 58, pp 788-793 (1975).
19. F. Mechel, W. Schilz and J. Dietz, "Akustische Impedanz einer Luftdurchströmten Öffnung, " *Acustica*, Vol. 15, pp 199-206 (1965).
20. D. Ronneberger, "Experimental Investigations about the Acoustic Reflection Coefficient of Discontinuous Changes of Cross-Sections in Tubes with Air Flow", *Acustica*, Vol 19, pp 222-235 (1967/68).
21. Uno Ingard and V. K. Singhal, "Upstream and Downstream Sound Radiation into a Moving Fluid", *J. Acous. Soc. of Am.*, Vol 54, pp 1343-1346 (1973).
22. Uno Ingard and V. K. Singhal, "Emission of Higher-Order Acoustic Modes into a Moving Fluid in a Duct", *J. Acous. Soc. of Am.*, Vol 56, pp 805-808 (1974).
23. L. F. East, "Aerodynamically Induced Resonance in Rectangular Cavities", *J. Sound and Vibration*, Vol 3, pp 277-287 (1966).

24. H. H. Heller, D. G. Holmes and E. E. Covert, "Flow Induced Pressure Oscillations in Shallow Cavities", J. Sound and Vibration, Vol 18, pp 545-553 (1971).
25. E. E. Covert, "An Approximate Calculation of the Onset Velocity of Cavity Oscillations", AIAA Journal, Vol 8, pp 2189-2194 (1970).
26. D. Ronneberger, "The Acoustical Impedance of Holes in the Wall of Flow Ducts", J. of Sound and Vibration, Vol 24, pp 133-150 (1972).
27. A. J. Bilanin and E. E. Covert, "Estimation of Possible Excitation Frequencies for Shallow Rectangular Cavities", AIAA Journal, Vol 11, pp 347-352 (1973).
28. V. K. Singhal and Uno Ingard, "Acoustical Characteristics of a Side Branch Resonator in a Duct with Flow", paper BB1 presented at the 88th meeting of the Acoustical Society of America, St. Louis, Missouri, 4-8 November 1974.
29. V. K. Singhal, "Flow Noise and Self-Excitation of Pipes" paper presented at the 89th meeting of the Acoustical Society of America, Austin, Texas, 7-11 April 1975.
30. P. M. Morse and K. Uno Ingard, Theoretical Acoustics (McGraw-Hill, New York, 1968), pp 472.

BIOGRAPHICAL NOTE

The author was born in India in 1948 and spent his formative years in New Delhi. He was placed second in the class of 21000 students taking the Higher Secondary Examination of the Delhi Board of Education in 1964 and obtained distinctions in Mathematics, Physics and Chemistry. He was offered merit scholarship by the Indian Institute of Technology, National scholarship by the Ministry of Education of the Government of India and the 'Science Talent' scholarship by the University Grants Commission. He graduated in 1969 with distinction from the Indian Institute of Technology in New Delhi with a Bachelor of Technology degree in Mechanical Engineering and he specialized in thermal sciences. He was placed second in the graduating class of 210 students. After refusing scholarships from the Indian Institutes of Management in Calcutta and Ahemdabad, he came to the United States for graduate education in Mechanical and Aeronautical Engineering. He served as a teaching assistant at the University of Minnesota from 1969 to 1970 for courses in mechanical vibrations, fluid mechanics and gas dynamics. Next year he was promoted to a teaching associate and served as an instructor for laboratory courses in aeronautical engineering department. In 1971 after getting M.S. in fluid mechanics from Minnesota, he came to the Massachusetts Institute of Technology as a research assistant. He

also spent a summer in Sweden at Chalmers Institute of Technology working on hydrodynamics of liquid crystals. At MIT he has worked on acoustical characteristics of ducts with flow, flow excited instabilities, screeching of orifices and side branch cavities, coupling between orifice or cavity modes with the modes of the duct, sound transmission through converging-diverging nozzles, testing acoustical absorption characteristics of materials, jet noise and instability of vortex sheets.

He has traveled extensively in the United States, Canada, Western Europe and India. He enjoys music, ballet, modern dance, badminton, tennis, skating and swimming.

His research interests are in fluid mechanics, heat transfer, aeroacoustics, automatic control systems and industrial noise control.

His publications include the following:

1. "Studies of Duct Liners and the Interaction of Sound and Flow in Ducts" (with Uno Ingard and A. G. Galaitsis), in Proceedings of the Interagency Symposium on University Research in Transportation Noise, Stanford University, Stanford, California, March 28-30, 1973 (G. Banerian and K. Karamcheti, editors), Vol. II, pp. 430-440.
2. "Upstream and Downstream Sound Radiation into a Moving Fluid" (with Uno Ingard), JASA, 54, 1343-1346, Nov. 1973.
3. "Sound Attenuation in Turbulent Pipe Flow" (with Uno Ingard),

- JASA, 55, 535-538, March 1974.
4. "Emission of Higher Order Acoustic Modes into a Moving Fluid in a Duct" (with U. Ingard), JASA, 56, 805-808, 1974.
 5. "The Viscosities of Nematic and Smectic-A Liquid Crystals by Inelastic Light Scattering" (with D. H. McQueen), J. Phys. D: Appl. Phys. 7, 1983-1987, 1974.
 6. "Effect of Flow on the Acoustic Resonances of an Open-Ended Duct", (with U. Ingard), JASA, 58, 788-793, 1975.
 7. "Studies of Sound Absorption Materials and the Attenuation of Sound in Ducts" (with U. Ingard et al.), in Proceedings of the Second Interagency Symposium on University Research in Transportation Noise, North Carolina State University, Raleigh, North Carolina, June 5-7, 1974 (G. Banerian and W. F. Reiter, editors), Vol. II, pp. 816.
 8. "Acoustically Stimulated Karman Vortex Shedding in a Tube" (with U. Ingard), Research Laboratory of Electronics, M.I.T., Cambridge, Mass., Q. P. R. 114, July 15, 1974, pp. 96-98.
 9. "Reflection of Sound from a Side-Branch Cavity in a Duct in the Presence of Flow" (with U. Ingard), R. L. E., M.I.T., Cambridge, Ma., Q. P. R. 114, July 15, 1974 pp 95-96. Also "Acoustical Characteristics of a Side-Branch Resonator in a Duct with Flow" (with U. Ingard), Paper presented at the 88th meeting of ASA, St. Louis, Missouri, Nov. 4-8, 1974.
 10. "Flow Noise and Self-Excitation of Pipes", Paper presented

at the 89th meeting of ASA, Austin, Texas, April 7-11, 1975.

11. "Flow Excitation and Nonlinear Coupling of Acoustic Modes of a Side Branch Cavity in a Duct" (with U. Ingard), to be published in JASA, 1976.